promotor:	dr. G.J. Fleer, hoogleraar op persoonlijke gronden werkzaam bij de vakgroep Fysische en Kolloïdchemie
co-promotor:	dr. ir. F.A.M. Leermakers, universitair docent bij de vakgroep Fysische en Kolloïdchemie

polymer adsorption theory

universal aspects and intricacies

C.C. van der Linden

polymer adsorption theory

universal aspects and intricacies

Proefschrift
ter verkrijging van de graad van doctor
in de landbouw- en milieuwetenschappen
op gezag van de rector magnificus,
dr. C.M. Karssen,
in het openbaar te verdedigen
op vrijdag 20 oktober 1995
des namiddags te vier uur in de Aula
van de Landbouwuniversiteit te Wageningen

CIP-DATA KONINKLIJKE BIBLIOTHEEK, DEN HAAG

Linden, C.C. van der

Polymer adsorption theory: universal aspects and
intricacies / C.C. van der Linden.- [S.l : s.n.]. - III.
Thesis Landbouwuniversiteit Wageningen. - With ref. -
With summary in Dutch
ISBN 90-5485-420-0
Subject headings: heterogeneous surfaces / comb polymers

Dit proefschrift is tot stand gekomen met steun van de Stichting Scheikundig Onderzoek in Nederland (SON) met een subsidie van de Nederlandse Organisatie voor Wetenschappelijk onderzoek (NWO).

CONTENTS

INTRODUCTION

Polymers and colloids

A polymer is a molecule consisting of many (πολύς) parts (μέρος). The word polymer was introduced in 1833 by the Swedish chemist Berzelius [1]. At that time, the first analyses of the molecular formula of organic compounds were established and Berzelius was trying to make a classification of closely related molecules. Molecules having the same overall molecular formula but different physical properties were defined to be isomers (ἴσος = equal), metamers were molecules that reorganize into other isomers spontaneously (μετά indicating a change), and polymers were molecules that have the same relative, but different absolute amount of atoms, and differ in physical properties. The material he used as an example for his polymer definition was "Weinöl", the oily substance obtained after steam destillation of cognac preparation residues and used as a perfume additive. It was analyzed to be C_4H_8, a fourfold of a substance ("ölbildendes Gas") that was thought to be CH_2. Later, it turned out that "Weinöl" consists mainly of ethyl- and amyl esters of lower fatty acids, which is far from C_4H_8 [2]. Nevertheless, the idea of multiples of groups of atoms is still in use, although contrary to Berzelius' ideas the current definition states that the physical properties of polymers do not vary much with the number of parts [3].

In 1861, Thomas Graham [4] performed diffusion experiments on a large variety of systems: solutions of polymers like starch, gelatin and gum-arabic, natural dispersions like blood and milk, and dispersions of silica and metal oxide particles in water (so-called sols). He found that all of these systems contained particles which moved very slowly in solution, and were unable to pass a semi-permeable membrane like parchment paper or animal mucus. As all of his systems can be treated to form a more or less sticky and gelly-like phase, *e.g.* by heating, by adding acid or by evaporating water, and as glue itself appeared to be of its type, he called those systems colloids, from the Greek κόλλα (glue) and -ειδής (-like). Later, the word colloid was used in a broader sense: any system containing relatively large (more than 1 nanometer) entities [5,6]. These "entities" need not be solid; they can also be liquid, as in an emulsion, or gaseous, as in a foam. Especially for these latter systems the term "glue-like" does not seem very appropriate, but the word colloid is still widely used.

Graham already wondered if the typical behaviour of a "colloid molecule" could be ascribed to a "grouping together of a number of smaller crystalloid molecules, and whether the basis of colloidality may not really be this composite character of the molecule." The question arising from this proposition was the nature of the association force. Colloid scientists rejected the idea of covalent chemical bonds, leading to giant molecules; their main interest was in inorganic sols and soap solutions where the low molecular weight of the constituent parts was established beyond doubt. The polymer scientists were divided into two groups: the people studying biopolymers like cellulose, starch and rubber, and the organic chemists who more or less inadvertently polymerized substances like ethylene glycol and styrene. They were not aware of one another's results, and although several people at the end of the 19th century measured large molecular weights, the "macromolecular theory" was not accepted widely. Only around 1930, almost a century after Berzelius' definition, Staudinger established that polymers were molecules of high molecular weight containing multiples of repeating units [7]. He coined the word "eucolloids" (proper colloids) for polymers as polymer solutions are most typically glue-like of all colloids. Since then, polymer science developed rapidly: determining the nature of the repeating units in biopolymers, synthesizing new polymers and, alas, turning its back to the colloid scientists who had impeded its progress for so long.

Polymers in solution

The simplest polymer that can be imagined is a linear polymer. It is basically a long chain of beads, where each bead is called the repeating unit or polymer segment. If all segments have the same chemical composition, the polymer is called a homopolymer (ὁμός = equal). Most polymers are more or less flexible, and in solution they tend to coil up (Fig. 1). There are many ways in which the chain can fold, and this leads to the high conformational entropy that is typical for polymers. If there are only a few molecules in a large amount of solvent the coils will not overlap, not even when they are close together. This is because two individual coils have more ways of arranging themselves internally than one big coil consisting of two chains, as the chains cannot intersect.

The gigantic number of ways in which a flexible polymer in dilute solution can be arranged is a major problem in any attempt to model it. A start can be made by the so-called random walk, in which a conformation of a polymer chain is approximated by a sequence of steps. The step length is fixed, but

the direction in which the step is taken is completely random, and independent of all previous steps. This approach is analogous to the random-flight model used in describing the trajectory of a randomly diffusing particle (Brownian motion). As the average displacement of a particle in a given amount of time is zero, it is customary to use the root-mean-square displacement (basically the standard deviation) as a characteristic parameter. In a similar way, the average size of a polymer coil is generally denoted by its radius of gyration, R_g.

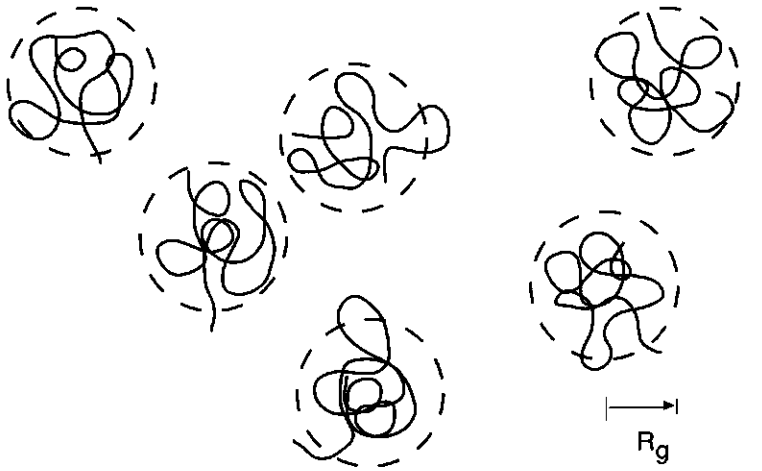

Figure 1. A dilute solution of polymer molecules: non-overlapping polymer coils, each with a radius of gyration R_g.

For a random walk the radius of gyration turns out to be proportional to the square root of the number N of steps taken, so that $R_g \propto N^{1/2}$. However, Flory [8] has shown that in a good solvent, where the interaction between polymer segments and solvent molecules is not too unfavourable, the radius of gyration scales with N (here identified as the number of polymer segments) as $R_g \propto N^{3/5}$. The difference is due to the so-called excluded volume effect: the random-walk model permits the backfolding of a chain onto itself, whereas in reality two segments cannot hold the same position at the same time. This causes the coils to swell. Nevertheless, it turns out to be possible to find random walk statistics in a dilute polymer solution: if the interaction between polymer and solvent is sufficiently unfavourable, the polymers shrink. At a specific point, called the Θ-point, the contraction of the coil due to the attractive interactions exactly cancels the expansion due to the excluded

volume effect. Beyond the Θ-point, where the solvent is very poor, the polymers are in a collapsed state, and $R_g \propto N^{1/3}$.

Upon increasing the concentration of polymer, the point is reached where the total volume of the coils equals the volume of the container. This is called the overlap concentration. If we take as the volume of one coil a sphere with radius R_g, then the overlap concentration c^* can be found to scale as $N / (R_g)^3$ or, using the Flory result, as $N^{-4/5}$. Beyond this point, the coils cannot help but overlap. The solution then resembles a network, with average mesh size ξ (Fig. 2). This mesh size can be viewed upon as a correlation length: on length scales larger than ξ a polymer segment cannot distinguish any more to which polymer chain it is connected. The solution is semi-dilute. The overall shape of the network does not change if one of the polymer chains were to be cut in half, so that the chain length is not a predominant length scale in a semi-dilute solution. Therefore, in a semi-dilute solution the chain length can conveniently be left out of the description of the system.

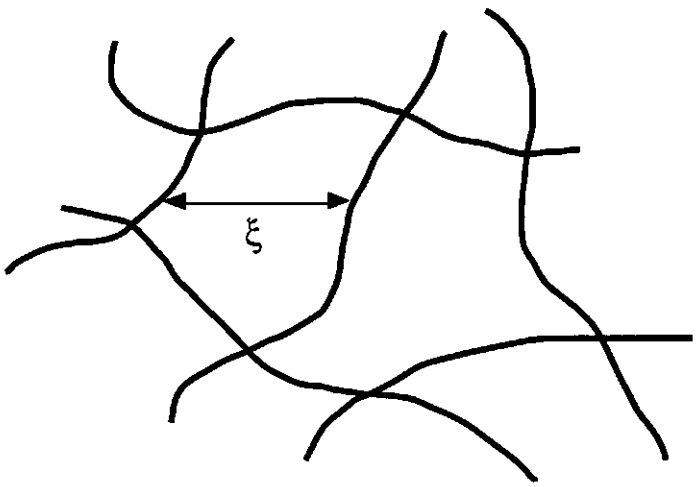

Figure 2. A semi-dilute polymer solution with average mesh size ξ.

In semi-dilute solutions, the correlation length does not depend on the chain length, but it does depend on the concentration: the more polymer, the more the network is squeezed. In other words, the correlation length in a semi-dilute solution ξ^{sd} decreases with increasing concentration. In order to find

the concentration dependence of the correlation length, we can write it as a power law [9] as:

$$\xi^{sd} \cong \xi^{d}\left(\frac{c}{c^*}\right)^{x} \qquad (1)$$

where ξ^d is the correlation length in a dilute solution, c is the concentration and c^* the overlap concentration. Next, we adjust the exponent x such that the outcome is independent of the chain length N, using for ξ^d the Flory radius of gyration. This leads to $x = -3/4$, or $\xi^{sd} \propto c^{-3/4}$.
If we increase the polymer concentration even further to the point where hardly any solvent is present any more, we have a polymer melt. In a polymer melt all interactions are efficiently screened out, and the system behaves ideally, *i.e.*, the polymers follow random-walk statistics.

Polymer adsorption

We have seen that long, flexible polymers in solution are colloids (or, in Staudinger's terms, eucolloids). More precisely, solid particles in a fluid substance are called sols. If the solid particles consist of polymers that do not dissolve readily, the sol is called a latex, after the milky fluid that comes out of a rubber tree *(Hevea brasiliensis).* The difference between the polymer molecules in the core of the latex particles and fully dissolved ones is the freedom of movement: the latter change conformations continuously whereas the latex molecules are in a glassy or even crystalline state. When we add a flexible, soluble polymer to a latex (or another kind of sol) there are two possibilities: adsorption or depletion. If the dissolved polymer has a more favourable energetic interaction with the particles than with the solvent, it may adjust its conformations and stick to the particle surface. This phenomenon is called adsorption. Adsorption limits the number of ways a polymer can arrange itself (and hence, its entropy) considerably, so the energetic interaction of the polymer with the surface (the adsorption energy) has to be large enough to compensate this entropy loss. The point where the adsorption energy is just large enough to yield adsorption is called the critical adsorption energy. For smaller adsorption energies, the polymer will stay away from the surface, leading to a zone where no polymer is present. This region is called the depletion zone, and the polymer is said to be depleted from the surface. Both adsorption and depletion can have a dramatic effect on the stability of a sol or emulsion [10]: depending on circumstances it can either lead to stabilisation (protecting the sol from

creaming, settling or phase separating), or to flocculation (the formation of large flocs). Control of the stability is vital in all applications where colloids are used: in cheese making, in water purification or in ore dressing the system is meant to flocculate, whereas in milk any phase separation is undesirable. In paint it is sometimes convenient to bring the system at the verge of flocculation, as the half-formed flocs are easily broken when poured or stirred, but strong enough to prevent settling of the pigment particles. From the above examples it can be seen that with polymer adsorption and depletion, polymer science has found its place back into colloid science: colloid scientists need polymers that comply to all the specifications they need, and polymer scientist know what those polymers should look like.

Theories, approximations and their problems

A simple general strategy for the design of a polymer adsorption theory is the following: calculate all possible conformations of polymers at the surface and in solution, count all interactions, derive the free energy of the system, and minimize it. For stability, also the effect of bringing particles together has to be taken into account. This procedure would yield all the information needed to predict the behaviour of polymers near interfaces. Unfortunately, this method is in general unfeasible as the number of conformations is too large. Therefore, approximations and model assumptions have to be made. In the theories used in this thesis, several approximations are used:

Markov chain

We have already encountered one popular approximation in the random-walk model. The basic assumption here is that all segments are only influenced by the position of the segment immediately preceding them. This ensures chain connectivity, but cannot prevent backfolding. A series of events where the next state only depends on the current state is called a Markov chain.

lattice

Another tool which facilitates the counting of conformations is the use of a lattice. Here, every polymer segment occupies a lattice site. Often, the size of a polymer segment is chosen to be the size of a solvent molecule (Fig. 3). This can be problematic if there are more than two components in the system, or if the dimension of a lattice site is used for the calculation of measurable quantities.

Basically, the use of a lattice only means the discretization of space, and for a fluid it is often not a severe approximation [11]. In some cases it is possible to prove that a lattice theory yields the same results as a continuous theory provided the lattice spacing is taken to approach zero. Problems can arise if the system contains rigid structures that do not fit in the lattice (*e.g.* tilted crystallites) or if a sharp interface (*i.e.*, an interface with a thickness of the order of the lattice constant) is formed between different components. In the latter case, thermodynamic quantities like free energy or surface tension are extremely sensitive to the exact position of the interface and the kind of lattice used. Fortunately, it is sometimes possible to detect and correct for these so-called lattice artefacts [12].

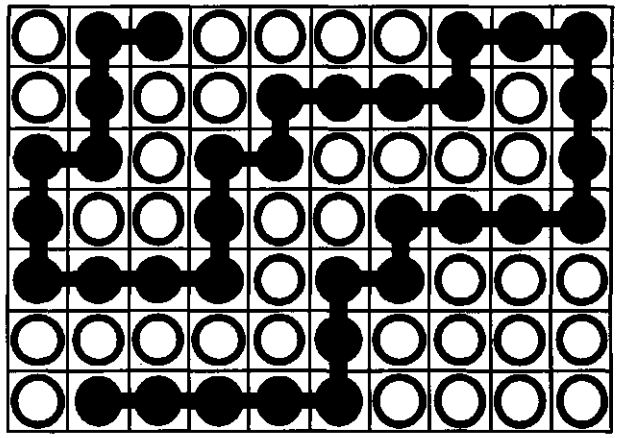

Figure 3. A small polymer molecule in a lattice: the open circles denote the solvent molecules, the closed circles the polymer segments.

random mixing (Bragg-Williams) and mean field

A famous theory using a lattice as depicted in Fig. 3 is the Flory-Huggins theory [8]. It has proven to be very successful in describing the thermodynamics of polymer solutions, predicting qualitatively the phase separation between unlike polymers and the possibility of fractioning polymers with the same chemical composition, but with different molecular weight. However, the precise behaviour of a polymer solution near the point of incipient phase separation (for infinitely long chains a "critical point") is far from experimental findings. Mean-field theories (as the F-H theory) are infamous for their incorrect predictions of systems near a critical point. This discrepancy derives from the neglect of correlations. Some idea of

correlations can be obtained if we look at the dilute solution in Fig. 1. We could try to calculate the probability of inserting another polymer molecule in such a way that none of the segments of the molecule to be inserted will overlap with any segment of the polymers already present. Such a procedure could, *e.g.*, be used in the calculation of the chemical potential of the polymer. If the total volume fraction of polymer segments is denoted as φ, then the probability that any single segment can be inserted properly is $1-\varphi$. But we can immediately see that it will make a huge difference where exactly the first segment is placed: if it is located outside the dashed spheres indicating the radii of gyration, then the whole polymer molecule will probably fit in easily, but if the first segment is placed within the radius of gyration of another polymer molecule, the other segments stand a very good chance of hitting one of the segments already there. So, for all the other segments of the polymer to be inserted $1-\varphi$, the average value for the excluded volume, is a very bad approximation for the probability that they will fit in. The method would be correct if the polymer segments were not connected but distributed in the solution at random. Therefore, this approximation is called the random mixing approximation. It is also known under the name Bragg-Williams approximation. The idea to tag one molecule and let the role of all other molecules be to form an average external field that acts on this tagged molecule is the basis of a mean-field approximation. The use of a Bragg-Williams approximation implies the use of a mean-field approximation, but not the other way around: it is very well possible to improve on the Bragg-Williams approximation, *e.g.*, by using a so-called quasi-chemical approach, where correlations between nearest neighbours are taken into account, but still using a mean-field approximation [11].

energetic interactions

So far, we have mainly been concerned with entropic (excluded volume) interactions. As soon as we consider good or bad solvents, energetic aspects enter the discussion. Energetics are generally modelled by assuming a specific equation for the energy as a function of the interparticle distance and sometimes also of the orientation between particles (segments, molecules or even voids). Next, a cut-off has to be defined: it is impossible to calculate the influence of a particle upon the rest of the universe, but one can start with the energetic interaction of a particle with its immediate surroundings. In a lattice, this is especially convenient as the nearest

neighbours and the distance between them are well-defined. In this case, it is enough to simply define a contact energy.

ground state dominance

The random walk model for a polymer molecule is analogous to the random-flight model for a single Brownian particle. This analogy can also be used in polymer adsorption theories as a popular chain connectivity equation resembles a diffusion equation or even the Schrödinger equation used in quantum mechanics [13]. This method is called the diffusion equation approach. However, a major difference between a diffusing particle and a polymer molecule is the fact that a polymer molecule has two chain ends whereas the diffusing particle does not have a specific "start" or "finish". A polymer segment located near one of the ends will in general behave differently from a middle segment, as the ends have more freedom of motion. In many diffusion equation theories, the importance of the chain ends is neglected. Basically, the polymers are taken to be infinitely long. A term often used in this respect is ground state dominance, jargon stolen from quantum mechanics.

scaling

Instead of starting out with all possible conformations of a polymer molecule and then simplifying the matter with approximations, it is also possible to coarsen the system by using "blobs" having a diameter equal to the correlation length [9]. In this way, no details on a scale smaller than the correlation length can be obtained, but important physical laws can be derived without intricate mathematical methods.

equilibrium

An important remark that has to be made here is that in deriving a minimum in the free energy, one assumes that the system is in equilibrium. As stated before, polymers move very slowly in solution, so that in dense polymer systems it is very well possible that equilibrium is never obtained.

Outline of this thesis

This thesis is based on the theory for polymer adsorption by Scheutjens and Fleer [14], which is an equilibrium lattice theory using Markov chain statistics and a Bragg-Williams approximation. In the first two chapters, some of the approximations are tested: chapter 1 concentrates on the problems of the mean-field approximation in the case of adsorption from a dilute solution by

analyzing volume fraction profiles with scaling arguments. In chapter 2, adsorption from a semi-dilute solution is considered. The results are compared with an analytical, continuous (*i.e.*, no lattice) model using a ground-state approximation. The Markov chain statistics are extended in chapter 3. This extension enables the modelling of polymers having parts that are not completely flexible. Partial stiffness yields entropical prejudice for adsorption, just as branching of the polymer chain does, a subject which is touched in chapter 4, which deals with the adsorption of comb-shaped polymers, also called graft polymers. Finally, in chapter 5 the effects of surface heterogeneity are calculated.

References

[1] J. J. Berzelius, *Jahres-Bericht über die Fortschritte der physischen Wissenschaften* **12** (1833) 63.

[2] E. Gildemeister and F. Hoffmann, "Die ätherischen Öle" 3rd. Ed. (1928) Verlag der Schimmel & Co. A.G., Miltitz, Leipzig.

[3] IUPAC commission on macromolecular nomenclature, "Basic definitions of terms relating to polymers 1974" *Pure Appl. Chem.* **40** (1974) 479.

[4] T. Graham, "Liquid diffusion applied to analysis" *Trans. Roy. Soc. (London)* **151** (1861) 183.

[5] W. Ostwald, "Die Welt der vernachlässigten Dimensionen. Eine Einführung in die moderne Kolloidchemie mit besonderer Berücksichtigung ihrer Anwendungen" 7th and 8th Ed. (1922) Verlag von Theodor Steinkopff, Dresden.

[6] H. Staudinger, "Organische Kolloidchemie" (1940) F. Vieweg & Sohn, Braunschweig.

[7] H. Staudinger, "Über hochpolymere Verbindungen, 26. Mitteil.: Über die organischen Kolloide" *Ber. Dtsch. chem. Ges.* **62** (1929) 2893.

[8] P. J. Flory, "Principles of polymer chemistry" (1953) Cornell University Press, Ithaca, NY.

[9] P.-G. de Gennes, "Scaling concepts in polymer physics" (1979) Cornell University Press, Ithaca, NY.

[10] D. H. Napper, "Polymeric stabilization of colloidal dispersions" (1983) Academic Press, London.

[11] N. A. M. Besseling, "Statistical thermodynamics of fluids with orientation-dependent interactions. Applications to water in homogeneous and heterogeneous systems" Thesis Wageningen Agricultural University (1993).

[12] P. A. Barneveld, J. M. H. M. Scheutjens and J. Lyklema, "Bending moduli and spontaneous curvature. 1. Bilayers and monolayers of pure and mixed nonionic surfactants" *Langmuir* **8** (1992) 3122.

[13] S. F. Edwards, "The statistical mechanics of polymers with excluded volume" *Proc. Phys. Soc.* **85** (1965) 613.

[14] J. M. H. M. Scheutjens and G. J. Fleer, "Statistical theory of the adsorption of interacting chain molecules. 1. Partition function, segment density distribution, and adsorption isotherms" *J. Phys. Chem.* **83** (1979) 1619.

CHAPTER I

On the self-similar structure of adsorbed polymer layers: the dependence of the density profile on molecular weight and solution concentration

It is shown that the self-consistent-field theory to describe polymer adsorption on solid-liquid interfaces [J.M.H.M. Scheutjens, G.J. Fleer, *J.Phys.Chem.* **83** (1979)1619] behaves, for long chains and high adsorption affinities, qualitatively as predicted by scaling theory [P.G. de Gennes, *Macromolecules* **14** (1981) 1637]: a proximal regime of a single lattice layer is followed by a remarkable self-similar region in the semi-dilute (central) part of the profile which crosses over to an exponential decay in the distal regime. For finite bulk volume fraction ϕ^b we find the expected mean field dependence $\varphi(z) \sim z^{-2}$ for infinite chain length N, but in general the power law is more complex and depends on both φ^b and N: $\varphi(z) \sim z^{-\alpha}$, where $\alpha = -2 + \text{const } (\ln \varphi^b) / N^{0.5}$. The distal regime is exponential: $\varphi(z) = \beta \exp(\gamma z)$, where γ has a similar dependence on $\ln \varphi^b$ and N, and β is a function of α and γ. From our mean field analysis we propose that the De Gennes scaling picture of the adsorbed polymer layer is only correct for infinitely long chains. When φ^b is low and the chain length not extremely large, the exponent in the self-similar profile deviates strongly from the mean field value –2, and, analogously, is expected to deviate from the scaling prediction 4/3.

Introduction

Over the last two decades many theories to describe the equilibrium behaviour of homopolymers adsorbed from solutions onto a solid interface have been developed. Among them two schools have emerged and lived more or less side by side. The first school, pioneered by de Gennes [1,2], applies the so-called scaling approach. It is characterised by a maximum of physics in as few computations as possible. The second one uses the Self-Consistent-Field (SCF) theory proposed by Scheutjens and coworkers [3,4]. This computationally more laborious approach provides a large number of detailed predictions, which sometimes prevents one from grasping the main physics. The aim of this chapter is to show that under most conditions the SCF density profiles in the polymer layer next to a surface are characterised by three regimes, like in scaling. These three regimes were first defined by De Gennes: a proximal regime dominated by polymer-surface contacts, a central regime with a self-similar behaviour, and an exponential profile in the distal regime. The two approaches give different predictions for the relevant scaling powers in good solvents. In short, De Gennes predicts a power law regime independent of the bulk volume fraction φ^b and of chain length N: $\varphi(z) \sim z^{-4/3}$, whereas as we will prove, the SCF approach predicts in the limit of infinitely long chains a profile of the form $\varphi(z) \sim z^{-2}$ in the semi-dilute part of the profile. Up to now no scaling analysis of the SCF results has been published, but as we will show below some very interesting conclusions can be deduced from it. We hope that our observations will be useful for understanding the scaling behaviour of polymer layers in general.

Theory

scaling theory

De Gennes recognises three regimes in the equilibrium adsorbed layer profile:

1. Proximal regime. The density profile near the wall is dominated by segment-surface contacts, making the behaviour of the polymers near the wall very system specific.

2. Central regime. The arguments leading to the correct scaling start from the correlation length in semi-dilute polymer solutions $\xi(\varphi) \sim \varphi^{-3/4}$. Next, a generalized correlation length $\xi(z) \sim (\varphi(z))^{-3/4}$ in the adsorption profile is defined which should be proportional to z (so $\xi(z) \sim z$) because there is no other length scale in the polymer layer. Combining these observations leads directly to the well known universal self-similar structure: $\varphi(z) \sim (\xi(z))^{-4/3}$ or

$$\varphi(z) \sim z^{-4/3} \qquad (1)$$

In other words, the local correlation length in the profile is simply the distance to the wall; the "blobs" or mesh sizes near the wall grow linearly with z outwards.

3. Distal regime. The outer part of the profile for $\varphi(z)$ smaller than the overlap concentration $\varphi^* \sim N^{-4/5}$ falls off exponentially:

$$(\varphi(z) - \varphi^b) \sim \varphi^b \exp(-z/\xi^b) \qquad (2)$$

where the superscript b refers to the bulk solution.

self-consistent-field theory

The SCF density profile follows from the (mean field) lattice partition function for the system. We will briefly review the main approximations included in the formalism. In lattice sites equally sized chain segments and solvent molecules are positioned. The lattice is composed of flat layers numbered z=1,..., M. On one side (z=0) an impenetrable wall limits the configurational space of the molecules, whereas on the other side of the system, at layer z = M, a reflecting boundary minimizes any effects of the finite size of the system. The parameter M should be large enough to ensure that the bulk values are reached. A local mean-field approximation in the lattice layer allows an easy evaluation of the local potentials

$$u_i(z)/kT = u'(z) + \chi_{ij}(\langle\varphi_j(z)\rangle - \varphi_j^b) - \delta(1,z)\,\chi_s \qquad (3)$$

for both types of molecule i and j in the system (solvent or polymer). In equation (3) three contributions can be distinguished. The first term, u'(z), is a Lagrange parameter which ensures that each lattice layer is completely filled. The second term, which contains the familiar Flory-Huggins interaction parameter χ, accounts for the polymer-solvent interaction and the third term, containing the Silberberg χ_s parameter, reflects the energetic effect of displacing a polymer segment by a solvent molecule on the surface (thus, by definition, $\chi_s = 0$ for the solvent).

Next, the Boltzmann factor $G_i(z) = \exp(-u_i(z)/kT)$ (also called the free segment distribution function) is defined for both the polymer segments and the solvent molecules. The recurrence relations

$$G_i(z,s|1) = \langle G_i(z,s-1|1)\rangle\, G_i(z) \qquad (4a)$$

$$G_i(z,s|N) = \langle G_i(z,s+1|N)\rangle\, G_i(z) \qquad (4b)$$

ensure chain connectivity for segment s in layer z. In this way, both the chain end distribution functions $G_i(z,s|1)$ (starting from the first segment) and $G_i(z,s|N)$ (starting from the other end) are related to the free segment distribution functions $G_i(z) = G_i(z,1|1) = G_i(z,N|N)$. The angular brackets in equations (2) and (3) indicate an average over three layers z–1, z and z+1 according to a (lattice type dependent) *a priori* step probability to go from z to z–1, to do a step within a layer, and to step from z to z+1, respectively. Equation (3) implies a first-order Markov approximation. The combination of the two chain end distribution functions gives the segment density profiles:

$$\varphi_i(z,s) = (\varphi_i^b/N_i)\, G_i(z,s|1)G_i(z,s|N)/G_i(z) \qquad (5)$$

The division by the free segment distribution function $G_i(z)$ is needed to correct for double counting of segment s and φ_i^b/N_i is the proper normalisation. A stationary point, also called self-consistent profile, is found by solving numerically the coupled implicit equations 3-5 with the boundary condition that in each layer the total volume fraction $\sum_i \varphi_i(z) = 1$. The summation over all segments of the chain molecule leads to the overall polymer segment density profile: $\varphi_i(z) = \sum_s \varphi_i(z,s)$.

Methods

The results presented in this chapter are computed by the standard SCF approach first published in 1979 by Scheutjens and Fleer [3]. The computer programme optimized for long chain molecules was written by Scheutjens [5]. Unless stated otherwise we used a cubic lattice, a Flory-Huggins χ parameter set equal to zero (good solvent), and a Silberberg χ_s parameter equal to 1. This value is above the critical value χ_{sc} which represents the transition from depletion to adsorption. The self-consistency of the segment density profile with the segment potential profile was achieved numerically. In all cases the precision of the results is at least 7 significant digits.

Results

In this section we will present a scaling analysis of the SCF profiles. These are mainly calculated with $\chi_s = 1$, where we find clear scaling behaviour. However, as the situation changes considerably on lowering the adsorption

affinity, a small paragraph is devoted to values of χ_s nearer to the critical value.

high χ_s

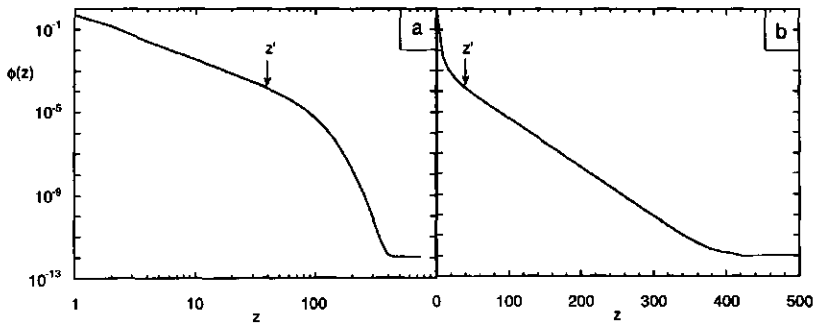

Figure 1. Volume fraction profile for a system with N = 50000 and $\varphi^b = 10^{-12}$, $\chi = 0$, $\chi_s = 1$, cubic lattice. Fig.1a: log-log plot, Fig 1b: log-lin plot. The transition point z' between central and distal regime is indicated by an arrow.

Figure 1 is a typical illustration of the various regimes found in the SCF adsorption profile. The self-similar regime shows up as a straight line in the log-log representation (in this case extending from layer number 2 up to about layer number 50), whereas the exponential part of the profile gives a linear behaviour on a log-lin plot (layers 30 - 350). The transition between the self-similar and exponential regime takes place somewhere between layers 30 and 50 at z'. Detailed calculation, as given below, yields z'=39. This value is indicated in Fig. 1 by an arrow. The volume fraction in the first layer deviates from the straight line in the log-log plot (Fig 1a). Thus, the proximal regime can in this case be identified as being the very first layer adjacent to the interface.

Contrary to the prediction of De Gennes' theory, however, the scaling powers found in plots like Figs 1a and b are dependent on bulk volume fraction φ^b and chain length N.

It has been well recognised that the SCF scheme given by Scheutjens *et al* is equivalent to the 'diffusion equation' approach pioneered by Edwards [6] and used in detail by, for instance, Jones and Richmond [7] and Ploehn *et al* [8,9] in the context of polymer adsorption. In the SCF approach Cohen Stuart already predicted that the following power law behaviour is expected for the semi-dilute part of the density profile [10]:

$$\varphi(z) \sim z^{-2} \tag{6}$$

The power –2 can be related to the correlation length first given by Edwards for mean field chains in the semi-dilute regime [11]: $\xi(\varphi) \sim \varphi^{-1/2}$. Demanding $\xi(z)$ to scale with z as in scaling theory yields the equation above. Eq. (6) should indeed be the natural limit for infinite chain length in a mean field theory. We will show in an appendix that the Ploehn approach, which uses the same field equation, also provides this power law for long chains. We now take a more general form for the central regime:

$$\varphi(z) \sim z^{\alpha} \qquad (1 < z \leq z') \tag{7}$$

where the "cross-over" distance z' will be defined more precisely below. The exponent α is taken to be of the general form

$$\alpha = -2 + f(N, \varphi^b) \tag{8}$$

where f should vanish for infinite chain length.

In the distal regime, the profile falls off exponentially:

$$\varphi(z) \sim \beta\, e^{\gamma z} \qquad (z' \leq z \leq X\, R_g) \tag{9}$$

where X is of order unity and R_g is the radius of gyration of the chain.
In order for the exponent to be dimensionless, we need $\gamma \sim (\xi^b)^{-1}$, where $\xi^b \sim R_g$ is the length scale in the dilute regime. In a mean field theory $R_g \sim N^{0.5}$ (ideal chains). We rewrite eq. (2) so that $\ln \varphi^b$ enters the exponent:

$$\gamma \sim \ln \varphi^b \,/\, N^{0.5} \tag{10}$$

When $\varphi(z) = \varphi^b$ the distal regime ends and crosses over to the bulk. This discontinuity occurs at very low volume fractions and is not a serious problem.

The requirement that at z' the profile should be continuous leads to

$$z' = \alpha/\gamma \tag{11}$$

and to

$$\beta \sim (\alpha/\gamma)^{\alpha}\, e^{-\alpha} \qquad (12)$$

For extremely low bulk volume fractions we expect the power law regime to vanish and thus z' to be of order unity for all N. This suggests f and γ to have a similar chain length and bulk volume fraction dependence:

$$f \sim \ln \varphi^b \; / \; N^{0.5} \qquad (13)$$

Note that both f and γ are 0 for infinite chain length at finite φ^b.
Using the lattice calculations by varying chain lengths and bulk volume fractions, we found from plots like Fig. 1 the exponents α and γ in the central and distal regime, respectively, as a function of the chain length. Results are plotted in Figs 2a and b, where the abscissa scale is $N^{-0.5}$ as suggested by eqs (10) and (13).

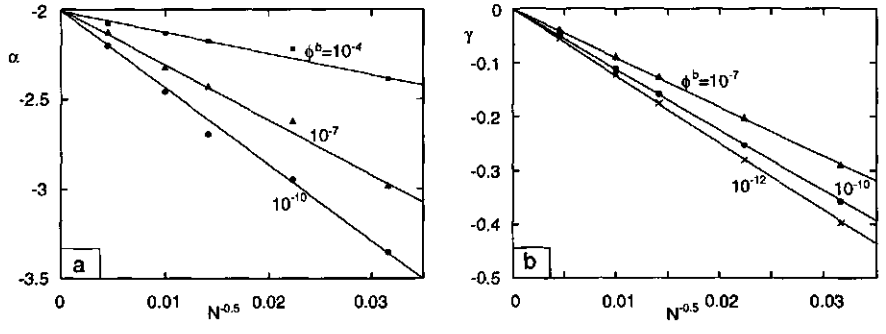

Figure 2. The power law exponent α in the central regime (a) and the slope γ as found in plots like Fig. 1b in the distal regime (b) as a function of $N^{-0.5}$. The values of the bulk volume fraction are: squares 10^{-4}, triangles $\varphi^b = 10^{-7}$, circles $\varphi^b = 10^{-10}$, stars 10^{-12}. Athermal solvent ($\chi = 0$), $\chi_S = 1$.

It can be seen that indeed these exponents are linear in $N^{-0.5}$. The scatter in Fig. 2a is due to the small number of layers that form the central regime, especially for short chains. At given N, α and γ are found to increase proportionally with $\ln \varphi^b$, which is also in agreement with eqs (10) and (13). Hence, we can now specify the numerical coefficients in the parameters α and γ:

$$\alpha = -2 + 1.87\ (\ln \varphi^b\ )/\ N^{0.5} \qquad (14)$$

and

$$\gamma = (\ -4.45 + 0.3\ \ln \varphi^b)\ /\ N^{0.5} \qquad (15)$$

Equations (14) and (15) are found for a cubic lattice. Changing the lattice will only alter the numerical coefficients. Together with eqs (7), (9) and (12) and replacing all the proportionality signs with equality signs, they present analytical expressions for the SCF profiles for $\chi_s = 1$ and $\chi = 0$.

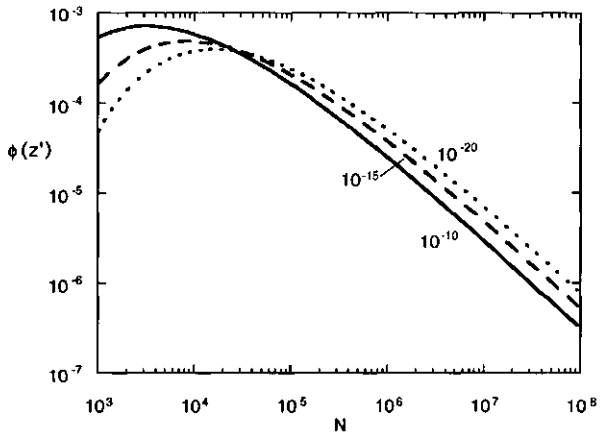

Figure 3. Cross-over volume fraction as a function of chain length, as calculated using Eqs 7, 11, 14 and 15. Full curve: $\varphi^b = 10^{-10}$, dashed curve: $\varphi^b = 10^{-15}$, dotted curve: $\varphi^b = 10^{-20}$.

Combining eqs. (7), (11), (14) and (15) we can calculate $\varphi(z')$, the volume fraction at which cross-over from semi-dilute to dilute behaviour takes place, as a function of chain length N. Using the analytical expressions it is possible to predict $\varphi(z')$ for higher chain lengths than by using the original numerical procedure. The result is shown in Fig. 3. We see that the curves exhibit a maximum at a certain chain length referred to as N', which is higher for lower solution concentrations. For $N < N'$ the power law regime is too narrow to be physically relevant. Working out the numerical values, we find that $N' \approx 0.4\ (\ln \varphi^b)^2$. Scaling behaviour, of the type $\varphi(z') \sim N^{-x}$ is only found for N well above N'. Scaling theory [1] states that the cross-over from semi-dilute to dilute regime will take place at the overlap concentration $\varphi^* \sim N^{-4/5}$. For mean-field chains the cross-over concentration $\varphi^* \sim N^{-1}$. De Gennes

identified the transition from the central to distal regime in the adsorption profile as the overlap concentration [2]. As can be seen from Fig. 3, we find the proper mean field scaling $\varphi(z') \sim N^{-1}$ only for very high chain length ($N > 10^7$). Note, that there is also a dependence of $\varphi(z')$ on $\ln \varphi^b$.

χ_s near χ_{sc}

The scaling theory for polymer adsorption by De Gennes is restricted to the so called weak coupling limit. In our lattice approach this would imply that $\chi_s < 1$. All results given above are for $\chi_s = 1$. In Figure 4 we collect some density profiles for long chains ($N = 50000$) and $\varphi^b = 10^{-12}$ with varying adsorption affinities.

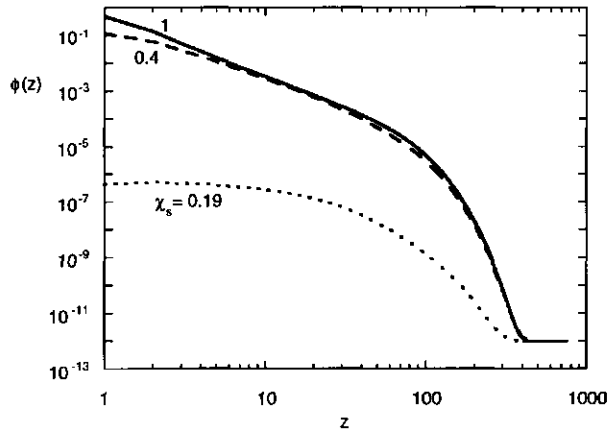

Figure 4. Volume fraction profiles for systems with $N = 50000$ and $\varphi^b = 10^{-12}$, $\chi = 0$, cubic lattice. Full curve: $\chi_s = 1$, dashed curve: $\chi_s = 0.4$, dotted curve: $\chi_s = 0.19$.

We first discuss the difference found between $\chi_s = 1$ (full curve) and $\chi_s = 0.4$ (dashed curve). In contrast to $\chi_s = 1$, the central regime for $\chi_s = 0.4$ does not show a clear power law behaviour. The proximal regime is larger than one layer, and the profile is less steep. This behaviour has been predicted by de Gennes and Pincus in an analysis of the proximal exponent [12]. The cross-over to the central regime is smooth. In this case, for a full analysis computations for much larger chain lengths are needed to unravel the possible chain length and φ^b dependence of the proximal part of the profile. The dotted curve in Fig. 4 is for $\chi_s = 0.19$, close to the critical value of 0.182 for a cubic lattice. In this case the De Gennes and Pincus picture is not valid any longer. We even find a maximum in the segment density profile at layer $z = 2$. A similar maximum was found by Roe [13] in 1966 for an isolated

polymer chain near a weakly adsorbing wall. There is no power law region nor an exponential regime. It should be noted that near χ_{sc} and for low φ^b, the surface densities are too low to justify a local mean field approximation.
For $\chi_s > 1$, the profile is almost equal to the profile with $\chi_s = 1$ (not shown). The only differences are in the occupancies in the first two layers, which increases with increasing adsorption energy (although always $\varphi(1) < 1$). The slopes in the central and distal regimes are not affected at all.
We summarize that scaling behaviour is only found for high values of the adsorption energy parameter χ_s. This is in contrast to De Gennes' conjecture that it should be valid for weak adsorption.

theta solvent

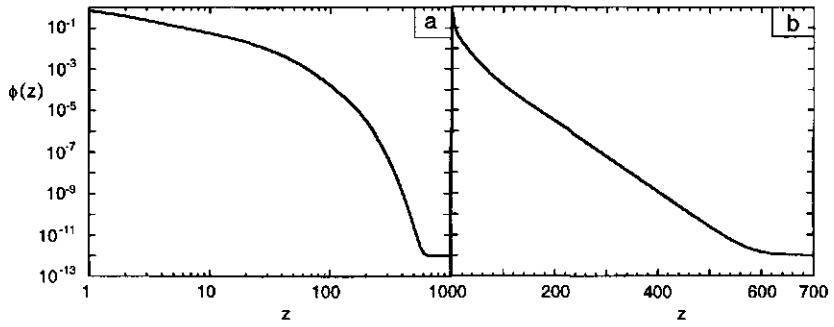

Figure 5. Volume fraction profile for a system with N = 100,000 and $\varphi^b = 10^{-12}$, $\chi = 0.5$ (Θ solvent), $\chi_s = 1$, cubic lattice. Figure 5a: log-log plot, Figure 5b: log-lin plot.

In Figure 5 similar plots as in Figure 1 are constructed, but for a Θ-solvent ($\chi = 0.5$). It can be seen that although the distal and the central regimes are definitely present, they do not adjoin: the central regime seems to end already at z = 20, whereas the distal regime does not start before z = 100. In other words: there seems to be an additional regime in this case in between the central and the distal regime. It starts before the overlap concentration φ^* ($\approx N^{-0.5}$ in a Θ-solvent) is reached and extends well into the dilute regime.
In analogy to the good solvent case, we expect the exponent in the power law regime to scale as (–1 + correction). Although the exponent is definitely higher than in the good solvent case (about –1.24 in Fig. 5) its chain length and bulk volume fraction dependence is difficult to obtain due to the small extent of the central regime. In a Θ-solvent a mean-field approximation is thought to be exact: the excluded volume is compensated by the

unfavourable energetic interaction of the polymer with the solvent. On the other hand, if we increase the chain length of the polymer in a Θ-solvent, we are approaching a critical point, where again a mean-field approximation is inappropriate. The longer the polymer, the more it will tend to phase separate. The surface can then act as a condensation nucleus for the incipient phase separation, leading to very thick and eventually to macroscopic adsorbed layers.

Discussion

From the results summarized in eqs 13 and 14 we can check that the density profiles fall off to the bulk values always at shorter distances than about 3 R_g, and for most practical cases shorter than 2 R_g, *i.e.*, the chain diameter. In the SCF model, decreasing φ^b has two opposite effects on the profile: the distal regime becomes wider because it takes longer to reach φ^b, but both $|\alpha|$ and $|\gamma|$ are larger which strongly reduces the layer thickness. Only for infinite chain length the corrections vanish. In that case the distal regime is effectively not present and the De Gennes scaling $\varphi(z) \sim z^{-4/3}$ is expected to be exact.

The –4/3 power arises from the correlation length in the semi-dilute regime which has been shown to be correct [14]. The SCF approach shows, for good solvents, the wrong limiting behaviour because it neglects correlations. The SCF theory predicts a clear chain length and bulk concentration dependence on the segment density profile. For high χ_s and N, eqs 13 and 14 define the profiles for good solvents. It is tempting to suggest that the exact result $\varphi(z) \sim z^{-4/3}$ should be generalized for finite chain length and concentration effects, in a similar way as given in eqs 13 and 14.

Integrating the volume fraction profile in the power law regime (*i.e.* from z=1 to z') yields a good estimate of the excess amount of polymer adsorbed Γ. For long chains $\Gamma \sim 1 + \ln \varphi^b / N^{0.5}$, so that, for infinite N, Γ reaches a limiting value. This limit is similar to the De Gennes result.

Conclusions

We have found analytical expressions for the volume fraction profiles of homopolymers adsorbing on a solid interface from a good solvent and for relatively high χ_s values. The results indicate that the scaling picture of De Gennes is qualitatively correct. However, our suggestion is that the "universal" density profile $\varphi(z) = z^{-4/3}$ should be corrected for effects of a finite chain length and a finite bulk solution concentration.

References

[1] P.-G. de Gennes, "Scaling concepts in polymer physics" (1979) Cornell University Press, Ithaca, N.Y.

[2] P.-G. de Gennes, "Polymer solutions near an interface. 1. Adsorption and depletion layers" *Macromolecules* **14** (1981) 1637.

[3] J. M. H. M. Scheutjens and G. J. Fleer, "Statistical theory of the adsorption of interacting chain molecules. 1. Partition function, segment density distribution, and adsorption isotherms" *J. Phys. Chem.* **83** (1979) 1619.

[4] O. A. Evers, J. M. H. M. Scheutjens and G. J. Fleer, "Statistical thermodynamics of block copolymer adsorption. 1. Formulation of the model and results for the adsorbed layer structure" *Macromolecules* **23** (1990) 5221.

[5] J. M. H. M. Scheutjens, *polad.sim* , 9b. copies available on request.

[6] S. F. Edwards, "The statistical mechanics of polymers with excluded volume" *Proc. Phys. Soc. London* **85** (1965) 613.

[7] I. S. Jones and P. Richmond, "Effects of excluded volume on the conformation of adsorbed polymers" *J. Chem. Soc., Faraday Trans. II* **73** (1977) 1062.

[8] H. J. Ploehn, W. B. Russel and C. K. Hall, "Self-consistent field model of polymer adsorption: generalized formulation and ground-state solution" *Macromolecules* **21** (1988) 1075.

[9] H. J. Ploehn and W. B. Russel, "Self-consistent field model of polymer adsorption: matched asymptotic expansion describing tails" *Macromolecules* **22** (1989) 266.

[10] M. A. Cohen Stuart, in *Future directions in polymer colloids* (1987) F. M. S. El-Aasser, Ed.; NATO Advanced Study Institute Series, vol. **E138**. Dordrecht, the Netherlands.

[11] S. F. Edwards, "The theory of polymer solutions at intermediate concentration" *Proc. Phys. Soc.* **88** (1966) 265.

[12] P.-G. de Gennes and P. Pincus, "Scaling theory of polymer adsorption: proximal exponent" *J. Phys. Lett.* **44** (1983) 241.

[13] R. J. Roe, "Conformation of an isolated polymer molecule at an interface. 3. Distributions of segment densities near the interface and of other shape parameters" *J. Chem. Phys.* **44** (1966) 4264.

[14] M. Daoud, J. P. Cotton, B. Farnoux, G. Jannink, G. Sarma, H. Benoit, R. Duplessix, C. Picot and P.-G. de Gennes, "Solutions of flexible polymers. Neutron experiments and interpretation" *Macromolecules* **8** (1975) 804.

Appendix: Ploehn theory

Ploehn *et al* [8,9] developed a continuous Self-Consistent Field model using a ground state approximation. Their expression for the volume fraction profile is

$$\varphi(z) = \frac{4\lambda_0 c_i \exp(-\sqrt{24\lambda_0}z)}{\left(c_i - \frac{v}{2}\exp(-\sqrt{24\lambda_0}z)\right)^2 - \frac{2}{3}\lambda_0 w \exp(-2\sqrt{24\lambda_0}z)} \qquad \text{(A1)}$$

where

$$c_i = \frac{1}{\varphi(0)}\left\{2\sqrt{\lambda_0}\left[\lambda_0 + \frac{v}{2}\varphi(0) + \frac{w}{6}\varphi^2(0)\right]^{0.5} + \frac{v}{2}\varphi(0) + 2\lambda_0\right\} \qquad \text{(A2)}$$

and v and w are excluded volume parameters. For long chains, λ_0 is a small number, as exp (λ_0 N) is of order 1. Neglecting terms in λ_0, (A2) reduces to

$$c_i = \frac{v}{2} \qquad \text{(A3)}$$

Substituting (A3) in (A1) and again neglecting terms of order λ_0 yields

$$\varphi(z) = \frac{4\lambda_0}{v\left(-1+\cosh\left(\sqrt{24\lambda_0}z\right)\right)} \qquad \text{(A4)}$$

By expanding the cosh term, the unity term in the denominator cancels, as well as λ_0 ,so that indeed for long chains $\varphi(z) \sim z^{-2}$.

Analogously, for a theta solvent v = 0 so that

$$c_i^2 = \frac{2}{3}w\lambda_0 \qquad \text{(A5)}$$

This leads to a sinh term in the denominator:

$$\varphi(z) = \frac{\sqrt{\frac{6\lambda_0}{w}}}{\sinh(\sqrt{24\lambda_0}z)} \qquad \text{(A6)}$$

Expanding the sinh, keeping only the lowest order in z, we find $\varphi(z) \sim z^{-1}$.

CHAPTER II

Adsorption from semi-dilute solution

Polymer adsorption from semi-dilute solutions under good solvency conditions is studied by comparing the numerical mean-field theory for polymer adsorption by Scheutjens and Fleer with the analytical mean-field approach of Johner *et al.* It is found that the overall volume fraction profile is independent of polymer chain length and it can be described by a simple explicit equation containing only the bulk correlation length and the adsorption strength. For low adsorption energies and high bulk concentrations, the ground-state approximation neglecting segment number dependence can be successfully applied to extract the adsorbed profile and the distribution of the end segments within the adsorbed profile. However, for high adsorption energies and lower bulk concentrations the correspondence of the analytical theory with the numerical theory is less satisfactorily, which is attributed to the greater importance of tails in this case. The universality in the overall volume fraction profile implies that polydisperse samples can be used to measure the adsorption profile in the semi-dilute case. Yet, in these polydisperse systems the individual profiles for the molecules of different chain lengths show that other length scales are still present in the adsorption problem, which is caused by preferential adsorption phenomena.

Introduction

In 1893, Van der Waals [1] proposed that the volume fraction profile of an interfacial system can be obtained by writing the free energy as a functional of the local volume fraction and the square of its first derivative, and then minimising this free energy under variation of the volume fraction. The "square gradient term" turned out to be necessary for obtaining a finite interfacial tension. Only after Cahn and Hilliard [2] used this approach in the 50's, the procedure has become popular. For polymer adsorption it has been applied by, *e.g.*, Helfand [3,4], Jones and Richmond [5], De Gennes [6] and Johner *et al.* [7,8]. All these polymer theories use the assumption that in a long polymer chain all individual segments have the same distribution. This is the so-called ground-state approximation, which is correct for infinitely long polymers or for ring polymers. In the case of adsorption from a dilute solution it is known to be incorrect: the segments located near one of the chain ends are in general further away from the surface in long dangling tails [9]. The distribution of the segments depends strongly on the chain length. On the other hand, it is also well-known that in a semi-dilute solution, where the polymer concentration is so high that the chains overlap, the polymer chain length is irrelevant for the description of the system. This controversy makes the semi-dilute regime particularly interesting to re-investigate the ground-state approximation. To this end, we rewrite the free energy expression in the polymer adsorption theory by Scheutjens and Fleer [10] as a free energy functional using the method outlined in ref. [11], and arrive at Johner's analytical equations. This enables us to appreciate not only the effects of the ground state approximation, but also to check the possible errors of a lattice model.

Theory

SF-theory - general equations

The theory of Scheutjens and Fleer is a lattice theory: each polymer segment or solvent molecule is assumed to occupy exactly one lattice site. We use a simple cubic lattice, in which each lattice site has six neighbours. The lattice constant is chosen to be unity for simplicity. Upon adsorption, a volume fraction profile $\{\varphi(z)\}$ develops perpendicular to the surface. All inhomogeneities parallel to the surface are neglected. The surface is located at $z = 0$, adsorption takes place at $z = 1$, the layer adjacent to the surface, and the bulk solution is far away from the surface at $z = M$, where M is a large number. Two kinds of molecules are distinguished: the solvent, indicated with subscript o, and the polymer, with subscript p. The

dimensionless potential energy $u_i(z)$ that a segment of molecule type i (where i is either o or p) feels in layer z is written as:

$$u_p(z) = \chi\left(\langle\varphi_o(z)\rangle - \varphi_o^b\right) - \chi_s\delta(1,z) + u'(z)/kT \quad (1a)$$

$$u_o(z) = \chi\left(\langle\varphi_p(z)\rangle - \varphi_p^b\right) + u'(z)/kT \quad (1b)$$

Here, u'(z) is the "space-filling potential", essentially a Lagrange parameter to ensure that the lattice is completely filled, χ is the Flory-Huggins interaction parameter [12], and $\langle\varphi_i(z)\rangle$ is a neighbour average of the volume fraction $\varphi_i(z)$, in a cubic lattice defined as

$$\langle\varphi_i(z)\rangle = (\varphi_i(z-1) + 4\varphi_i(z) + \varphi_i(z+1))/6 \quad (2)$$

The quantity φ_i^b is the bulk volume fraction of i (polymer or solvent), χ_s is the Silberberg adsorption energy parameter for the polymer/solvent pair on the surface, the Kronecker delta $\delta(1,z)$ equals 1 if z = 1, and 0 otherwise and kT is the thermal energy. Free, unconnected segments, like the solvent molecules o, are distributed in the system according to Boltzmann's law:

$$\varphi_o(z) = \varphi_o^b e^{-u_o(z)} \quad (3)$$

The exponential factor in eq. (3) is called free segment weighting factor $G_i(z)$ for a segment of molecule type i:

$$G_i(z) = e^{-u_i(z)} \quad (4)$$

In the remainder of this text, we drop the subscript p as we will focus on the distribution of the polymer. Thus, the polymer volume fraction in layer z is simply $\varphi(z)$. In placing polymers in a lattice, we have to keep in mind that the segments are connected: if segment number s is in layer z, segment s+1 has to be either in layer z–1, or in layer z, or in layer z+1. The statistical weight of a segment number s of the polymer to be in layer z, given that the first segment is free to distribute according to eq. (4), is called the end segment distribution function (e.d.f.) $G(z,s\,|\,1)$. Analogously, we can define the e.d.f. starting from the other end N, $G(z,s\,|\,N)$, where N denotes the polymer chain length. The e.d.f. of segment s can be obtained from the e.d.f. of the preceding one according to a recurrence relation:

$$G(z,s\,|\,1) = G(z)\langle G(z,s-1\,|\,1)\rangle \tag{5a}$$
$$G(z,s\,|\,N) = G(z)\langle G(z,s+1\,|\,N)\rangle \tag{5b}$$

where the angular brackets denote a weighted average over the neighbouring lattice layers, similar as in eq. (2). The end points do not have a preceding segment, so their e.d.f.'s are simply equal to the corresponding free segment weighting factor: G(z,N|N) = G(z,1|1) = G(z). Combining the two ends and summing over all segments, we arrive at the volume fraction profile of the polymer:

$$\varphi(z) = \frac{\varphi^b}{N}\sum_s \frac{G(z,s\,|\,1)G(z,s\,|\,N)}{G(z)} \tag{6}$$

The division by G(z) is necessary to correct for the double counting of segment s, and φ^b/N is the proper normalisation. Equation (6) is known as the composition law: it relates the volume fraction profile $\{\varphi(z)\}$ to the potential profile $\{u(z)\}$. Equation (1) relates the potential profile to the volume fraction profile. The set of coupled equations is solved numerically under the constraint that the whole lattice is filled, *i.e.* $\sum_i \varphi_i(z) = 1$ for any z. The result is the self-consistent solution.

a free energy functional for polymer adsorption

In order to write the SF-theory for a homopolymer in monomeric solvent as a free energy functional, we need to split up the excess (Helmholtz) free energy $\Delta A = A - A^*$ with respect to a homogeneous bulk solution in two terms: a "local" excess free energy $\Delta A^{loc}[\varphi(z)]$, depending only on the local concentration, and a "non-local" excess free energy $\Delta A^{nloc}[\varphi_z]$, depending on the concentration gradient $\varphi_z \equiv \partial\varphi/\partial z$ in z. The local excess free energy $\Delta A^{loc}[\varphi(z)]$ has two contributions: the adsorption free energy, which is only relevant at the surface, and the mixing free energy, corresponding to transferring a solution with concentration φ^b to a homogeneous solution with concentration $\varphi(z)$. The latter can be found by defining an "excess chemical potential" $\Delta\mu_i(z)$ of component i, giving the difference in chemical potential between an imaginary homogeneous solution with concentration $\varphi_i(z)$ and the real chemical potential in the bulk solution:

$$\Delta\mu_i(z) \equiv \mu[\varphi_i(z)] - \mu[\varphi_i^b] \tag{7}$$

Note that this notation is only a matter of definition: in the gradient the chemical potential is obviously constant throughout the solution. Since transferring n polymer molecules would replace N*n solvent molecules, the excess free energy of transfer in the whole system volume V equals

$$\sum_i n_i \Delta\mu_i / V = (1-\varphi)\Delta\mu_o + \varphi\Delta\mu_p / N \qquad (8)$$

In the simple case of a homopolymer in a monomeric solvent, we can use Flory's equation for the chemical potential [12], leading to:

$$\sum_i n_i \Delta\mu_i(z) / V = (1-\varphi(z)) \ln\frac{1-\varphi(z)}{1-\varphi^b} + \frac{\varphi(z)}{N}\ln\frac{\varphi(z)}{\varphi^b} + \left(1-\frac{1}{N}\right)\left(\varphi(z)-\varphi^b\right) - \chi\left(\varphi(z)-\varphi^b\right)^2 \qquad (9)$$

Neglecting terms in 1/N (long chains), expanding the logarithms up to second order in the volume fraction, and substituting $\chi = (1-v)/2$, eq. (9) reduces to

$$\sum_i n_i \Delta\mu_i(z) / V \approx \frac{v}{2}\left(\varphi(z)-\varphi^b\right)^2 \qquad (10)$$

for v > 0 (good solvent). The parameter v is called the excluded volume parameter. Adsorption on a flat wall located at z = 0 leads to an energy gain $\chi_s\varphi(1)$ but also to an entropy loss. For a long chain, the entropy loss per adsorbing segment in a cubic lattice equals ln(6/5), the critical adsorption energy. Defining γ, which is a measure for the adsorption free energy per segment, as

$$\gamma = -6\left(\chi_s - \ln\frac{6}{5}\right) \qquad (11)$$

we arrive at

$$\frac{\Delta A^{loc}}{VkT} \approx \frac{v}{2}\left(\varphi(z)-\varphi^b\right)^2 - \frac{\gamma}{6}\varphi(z)\delta(z,1) \qquad (12)$$

The non-local term derives from the neighbour averages in eqs (1) and (5). It is shown in refs. [11,13] that in the ground-state approximation it can be written as:

$$\frac{\Delta A^{nloc}}{VkT} = \frac{1}{6}\left(\chi + \frac{1}{4\varphi}\right)\left(\frac{\partial\varphi}{\partial z}\right)^2 \tag{13}$$

For a good solvent, where χ is small, the energetic term in eq. (13) can be neglected.
Combining eqs (12) and (13) and summing over all lattice layers, we find for the excess free energy:

$$\frac{A - A^*}{VkT} = \sum_z \left(\frac{1}{24\varphi}\left(\frac{\partial\varphi}{\partial z}\right)^2 + \frac{v}{2}\left(\varphi(z) - \varphi^b\right)^2 - \frac{\gamma}{6}\varphi(z)\delta(z,1) \right) \tag{14}$$

Replacing the summation for an integral and the Kronecker delta for a Dirac delta function at the surface, we end up with

$$\frac{A - A^*}{VkT} = \int_0^\infty \left\{ \frac{1}{24\varphi}\left(\frac{\partial\varphi}{\partial z}\right)^2 + \frac{v}{2}\left(\varphi - \varphi^b\right)^2 - \frac{\gamma}{6}\varphi\,\delta(z) \right\} dz \tag{15}$$

This is the same equation as used by Johner *et al.* [7,8].

analytical solution for the ground-state approximation
Above we have an expression for the free energy. The next task is to find a volume fraction profile that minimises it. It turns out to be useful to solve this problem using an order parameter ψ, which is related to the volume fraction φ by $\psi^2 = \varphi/\varphi^b$. The distance to the surface can be normalised with respect to the correlation length in the bulk solution ξ^b, using $y = z/\xi^b$. The correlation length in a good solvent for a mean field theory is given by

$$\xi^b = \frac{1}{\sqrt{3v\varphi^b}} \tag{16}$$

Rewriting eq. (15) in these new parameters, we get:

$$\frac{A - A^*}{VkT} = \frac{v(\varphi^b)^2}{2}\int_0^\infty \left\{ \left(\frac{\partial\psi}{\partial y}\right)^2 + \left(\psi^2 - 1\right)^2 - \gamma\xi^b\psi^2\,\delta(y) \right\} dy \tag{17}$$

Minimising the free energy with respect to the order parameter profile $\psi(y)$ gives for the Euler-Lagrange equation (see Appendix 1):

$$2\psi(\psi^2-1)-\gamma\xi^b\psi\delta(y)-\frac{\partial^2\psi}{\partial y^2}=0 \qquad (18)$$

A solution to eq. (18) is

$$\psi(y)=\coth(y+b) \qquad (19)$$

where we have used the boundary condition that far from the surface the gradient is zero. Also, the solution $\psi(y) = \tanh(y+b)$ is discarded because in the case of adsorption the profile should be decreasing. The integration constant b is found from :

$$\sinh(b)\cosh(b)=\frac{1}{\gamma\xi^b} \qquad (20)$$

which can be derived from substituting eq. (19) into eq. (18) and integrating over the surface, taking that the slope within the surface is zero. Returning to the original parameters, we arrive at the following equation for the equilibrium volume fraction profile:

$$\varphi(z)=\varphi^b\coth^2\left(\frac{z}{\xi^b}+b\right) \qquad (21)$$

Note that this is an explicit equation for the volume fraction profile, so it can be used to estimate a potential energy profile $u_p(z)$, with an equation similar to eq. (1). With this approximate potential, segment distributions can again be calculated (which implies the loss of self-consistency) from the Edwards "diffusion" equation [14,15]:

$$\frac{\partial G(z,s\,|\,1)}{\partial s}=\frac{1}{6}\frac{\partial^2 G(z,s\,|\,1)}{\partial z^2}-u(z)G(z,s\,|\,1) \qquad (22)$$

with G(z,s|1) the analytical analogue of the end segment distribution function. This famous equation is equivalent to the time-dependent Schrödinger equation $((\hbar^2/2m)\nabla^2\Psi-E\Psi=(\hbar/i)\partial\psi/\partial t)$ if we take for the e.d.f. the wave function ψ and for the segment number imaginary time.
The equivalence of eq. (22) with the Scheutjens-Fleer recurrence relations (5) can be seen if we write eq. (5a) for segment s+1 instead of s:

$$G(z,s+1|1) = \frac{1}{6} e^{-u_p(z)} \{G(z-1,s|1) + 4G(z,s|1) + G(z+1,s|1)\} \qquad (23)$$

In order to find the continuous limit, we have to scale down the step size from 1 to h (where h < 1). Using a potential energy per h segments $u_h(z) = h\, u_p(z)$ we get:

$$G(z,s+h|1) = \frac{1}{6} e^{-u_h(z)} \{G(z-h,s|1) + 4G(z,s|1) + G(z+h,s|1)\} \qquad (24)$$

All elements in eq. (24) can be expanded in a Taylor series. The exponential function is the easiest:

$$\exp(-u_h(z)) = 1 - u_h(z) + \frac{(u_h(z))^2}{2!} - \cdots \qquad (25)$$

This series converges quickly as $u_h(z)$ is a small number.
The segment-dependence can be expanded as:

$$G(z,s+h|1) = G(z,s|1) + h\frac{\partial G(z,s|1)}{\partial s} + \frac{h^2}{2!}\frac{\partial^2 G(z,s|1)}{\partial s^2} + \cdots \qquad (26)$$

In the sum of G(z–h,s|1) and G(z+h|1) the odd orders of the derivatives cancel:

$$G(z-h,s|1) + G(z+h,s|1) = 2\left(G(z,s|1) + \frac{h^2}{2!}\frac{\partial^2 G(z,s|1)}{\partial z^2} + \frac{h^4}{4!}\frac{\partial^4 G(z,s|1)}{\partial z^4} + \cdots\right) \qquad (27)$$

Thus, when only the lowest orders of the derivatives are used and the term in $u_h(z)\,\partial^2 G/\partial z^2$ is neglected, it turns out that eq. (23) can be seen as the discrete (h=1) analogue of eq. (22). The neglect of higher order derivatives of G(z,s|1) is equivalent to stating that it has to be a slowly varying function of s, and to a lesser extent also of z.
Johner *et al.* [7] solve equation (22) by Laplace transformation. Once the distribution of segments is known, the adsorbed profile $\varphi^a(z)$, defined as the part of the overall profile $\varphi(z)$ containing polymers that touch the surface, can be calculated. If $bR_g/\xi^b > 1$, where b is given by eq. (20) and $R_g = \sqrt{N/6}$

is the radius of gyration, we are in the so-called large loop dominance regime, and the adsorbed volume fraction profile is given by:

$$\varphi^a(z) = 8\varphi(z)\left(i^2\mathrm{erfc}\left(\frac{z}{2R_g}\right) - \frac{1}{2}i^2\mathrm{erfc}\left(\frac{z}{R_g}\right)\right) \tag{28}$$

where i^2erfc is the second repeated integral of the error function [16].
The end segments belonging to adsorbed chains form the profile:

$$\varphi^e(z,N) = \frac{2\varphi^b}{N}\coth\left(\frac{z}{\xi}+b\right)\mathrm{erfc}\left(\frac{z}{2R_g}\right) \tag{29}$$

On the other hand, if $bR_g/\xi^b < 1$, another regime, the surface excess regime, applies. In this case, the adsorbed profiles are [17]:

$$\varphi^a(z) \propto \varphi(z)\left\{i^4\mathrm{erfc}\left(\frac{z}{R_g}\right) + \frac{\coth(b)}{\sqrt{Nv\varphi^b/2}}\left(i^3\mathrm{erfc}\left(\frac{z}{2R_g}\right) - i^3\mathrm{erfc}\left(\frac{z}{R_g}\right)\right)\right\} \tag{30}$$

and for the end segments

$$\varphi^e(z) \propto \coth\left(\frac{z}{\xi}+b\right)\left\{\frac{2}{\sqrt{\pi}}\exp\left(\frac{-z^2}{4R_g}\right) - \mathrm{erfc}\left(\frac{z}{2R_g}\right)\right\} \tag{31}$$

Calculations

We have seen that the equivalence between the analytical theory of Johner *et al* and the numerical self-consistent-field theory of Scheutjens and Fleer (SF) can only be established by making a large number of assumptions and approximations. An easy way to check whether these are valid is to perform calculations using both theories. We discuss such results in the next sections.

volume fraction profiles

In Figure 1 volume fraction profiles for a semi-dilute solution according to both models are given. The numerical SF results for three different chain lengths (squares: 40000, triangles: 10000, crosses: 5000) are shown calculated using the SF theory. There is hardly any difference between the three chain lengths, so that we can conclude that indeed the volume fraction profile is universal. This implies also that all equilibrium thermodynamic

quantities, such as the free energy and the surface tension, are independent of the polymer chain length, in contrast to the situation in dilute solution. Numerical calculation of these quantities show that this is indeed the case. The drawn curve in Fig. 1 was calculated from the analytical equation (21).

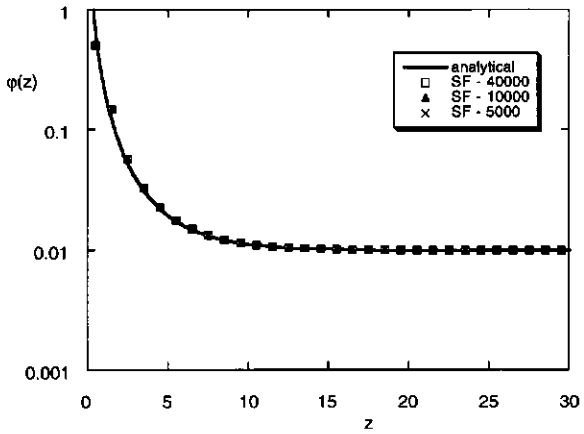

Figure 1. Volume fraction profile for a homopolymer adsorbing from a semi-dilute solution (φ^b = 0.01). Solid curve: analytical profile, given by eq. (21). The points were calculated using the SF theory for three different chain lengths: N = 40000 (squares), N = 10000 (triangles), N = 5000 (crosses). Athermal solvent (χ = 0), adsorption energy parameter χ_s = 1.

Note that we have shifted the SF-profiles half a layer from z to z – 0.5: layer 1 comprises the space between z = 0 and z = 1 and the centre of mass can be thought to be in the middle. The correspondence between the analytical and the numerical theory is excellent. A similar agreement is obtained using different values for the solvency, adsorption strength and bulk volume fraction, as long as the polymer is in a good solvent above the overlap concentration. At very small distances from the surface (z < 0.4), the analytical profile exceeds unity, which is physically unrealistic. We return to this point below.

Next, we look at the deconvolution of the volume fraction profile into adsorbed chains and their end segments. In Figure 2 we show results for the long loop dominance regime (low adsorption energy, high bulk concentration), where the adsorbed amount (comprising all chains that touch the surface) differs greatly from the excess amount and long loops are formed. Again, predictions for the overall profile (circles for the SF-theory, full

curve for the analytical theory) agree nicely, although this is hard to see as the profiles fall off quickly. The adsorbed end segment profile (analytical: dotted, SF: diamonds) is multiplied by N/2 so that all curves can be plotted on the same scale. In this way, the integral under both the curve for all adsorbed segments and the curve for only the adsorbed end segments is equal to the total adsorbed amount. It can be seen that although the correspondence is not as exact as for the overall profile, it is perfectly satisfactorily over a range of at least 2.5 times the radius of gyration. For these high concentrations, the difference between the end segments and the average of all segments is not very large, which explains the success of the ground-state approximation here.

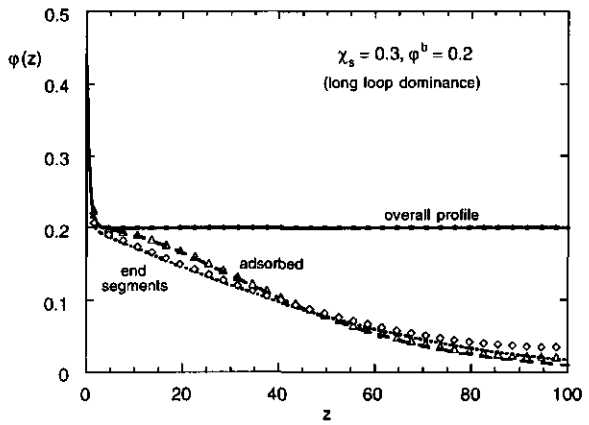

Figure 2. Adsorbed volume fraction profile for a polymer with chain length N = 10000 in an athermal solvent, for the long loops dominance regime: χ_S = 0.3, φ^b = 0.2. The drawn curves are calculated using the analytical theory by Johner *et al* (eq. 21 and 28-31): full curve: overall volume fraction profile, dashed curve: adsorbed volume fraction profile, dotted curve: adsorbed end segment profile. Points are calculated using the SF-theory. Circles: overall profile, triangles: adsorbed profile, diamonds: adsorbed end segments.

This situation changes when we go to the surface excess dominance regime (Figure 3, note the semi-logarithmic scale) with higher adsorption energy and lower bulk concentration (though still within the semi-dilute regime). Here, the end segments have a much stronger preference to be away from the surface. The analytical profiles should be normalised by their total adsorbed amount. This turns out to be a problem in this case, as the volume fraction exceeds 1 close to the surface due to the high value of the adsorption energy parameter. The adsorbed amount is then dominated by

the unphysical region less than a segment radius away from the surface, leading to much too high values. Therefore, we have tried to chose another normalisation, such that the outer part of the profile coincides with the numerical values. For the adsorbed profile, it would have been more convenient to normalise using the overall profile, as close to the surface all segments are adsorbed. However, this procedure would yield around z = 20 an adsorbed volume fraction that is higher than the overall volume fraction. The maximum in the analytical adsorbed profile is due to the tails, which are thus probably not described very well in the analytical approach in this case.

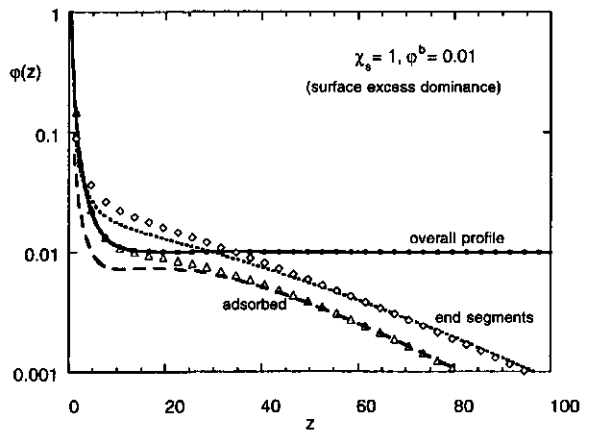

Figure 3. Volume fraction profiles for the surface excess dominance regime $\chi_S = 1.0$, $\varphi^b = 0.01$. Legends equal to those in Figure 2.

excess amount

In the SF theory, the excess amount is defined as $\sum_z(\varphi(z)-\varphi^b)$. In the analytical case a similar quantity can be defined by replacing the summation with an integration. In Fig. 4 we plot the excess amount obtained by integrating the squared cotangent profile from the surface (z = 0) to the bulk (z –> ∞) as a function of the adsorption energy parameter χ_S (dotted curve). The analytical curve increases linearly with the adsorption energy, whereas the SF-curve (solid) levels off at high adsorption strength. The difference is due to the high concentration very close to the surface. In the SF-theory, the volume fraction of the first layer cannot exceed unity, and once it is completely filled, no more polymer can adsorb. Thus, the discretisation using a lattice turns out to be advantageous in this respect. The erroneous behaviour of the analytical theory can be eliminated by starting the

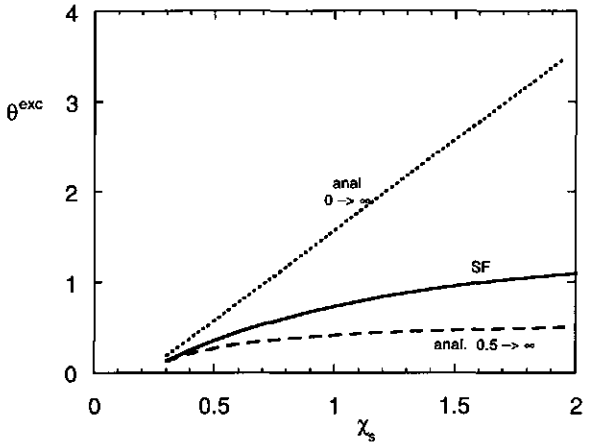

Figure 4. Excess amount as a function of the Silberberg adsorption parameter χ_s, for a polymer chain length N = 10000, an athermal solvent (χ = 0), and a bulk volume fraction φ^b = 0.01. Solid curve: SF- theory, dotted curve: analytical theory with integration from z = 0, dashed curve: analytical theory with integration from z = 0.5.

integration not at z = 0, but at a small distance away from the surface. We have taken z = 0.5, this choice is somewhat arbitrary but at any rate it should be of the order of the thickness of a polymer segment. This leads to the dashed curve in Fig. 4, which indeed shows the proper trend: adsorption increases with increasing adsorption energy and levels off for higher values.

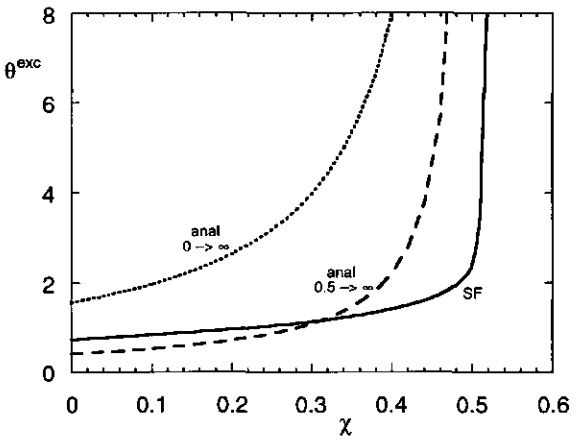

Figure 5. Excess amount as a function of the Flory-Huggins parameter χ. Adsorption energy: χ_s = 1 kT. Other symbols as in Figure 4.

The same trick can be used in varying the solvent quality (Fig. 5). Again, the dotted curve is the one obtained by integrating the overall profile from z = 0 and the dashed curve by integrating from z = 0.5.
The analytical theory was derived for the case of a good solvent: the energetic term in the square gradient (eq. 13) was neglected and only v was used as an excluded volume parameter in the free energy functional (eq. 15). In a Θ-solvent (v = 0 or χ = 0.5) higher order terms in the virial expansion should be taken into account, so the behaviour around the Θ–point is not correct. The neglect of the energetic term in the square gradient is only a problem at high values of χ (more than, say 0.4) and at high concentration, which in this case is only relevant close to the surface. Upon increasing χ, and thus decreasing the solvent quality, the adsorption increases gradually until the point is reached where phase separation takes place in the bulk solution. In the SF-theory, this occurs at the value predicted by the Flory-Huggins theory: χ = 0.51 for N = 10000. The surface then behaves as a condensation nucleus and the excess amount diverges, starting from the surface.

bidisperse polymers

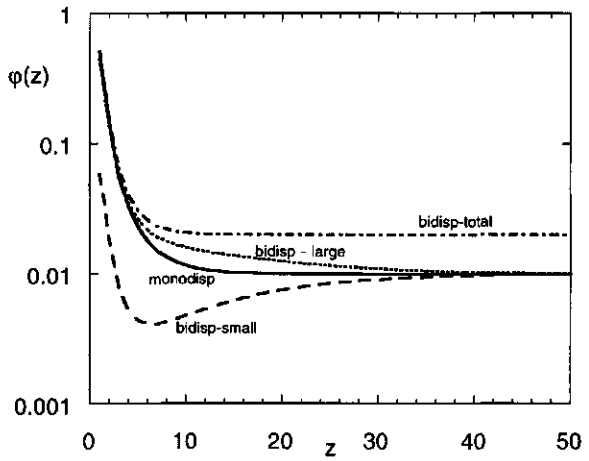

Figure 6. Volume fraction profile for a polymer of 10000 segments (full curve) and for a bidisperse mixture of two polymers having 1000 segments (dashed curve) and 10000 segments (dotted curve). Dashed-dotted: total volume fraction in the bidisperse case. All polymers are in full equilibrium with an athermal solution having a volume fraction of 0.01. Adsorption energy parameter χ_s = 1.0.

Now that we have seen that the volume fraction profile in the semi-dilute regime is universal, the question arises what will happen to a system containing more than one chain length. The adsorption of polydisperse polymers has been calculated before [18,19] and it was shown that at low concentrations, long polymers adsorb preferentially over short ones, whereas the reverse takes place at very high concentrations (several tens of a percent). In these calculations, the bulk volume fractions of all components differ, so that it is hard to compare with the situation we have here, where full equilibrium with an infinite bulk solution is assumed. Therefore, we will take a bidisperse system containing only two chain lengths. Bidisperse polymers have been treated by Sommer and Daoud [20] using a scaling approach, but only at low adsorption energy so that the concentration of the larger polymer cannot exceed the concentration of the smaller one. In our calculations, we have taken a system containing polymers with 1000 and with 10000 segments, both having a solution concentration of 0.01. In Fig. 6 the individual volume fraction profiles are compared with that of a system containing a monodisperse polymer of 10000 segments. The solid curve refers to the monodisperse case, the dashed curve gives the contribution of the small (1000 segments) polymer in the bidisperse case, and the dotted curve the contribution of the large (10000) polymer. As before, we find that the small polymer is depleted from the surface. The longer polymer in the bidisperse mixture adsorbs to a greater extent than the monodisperse polymer due to the increase in chemical potential in the solution: if the contributions of both polymers are added (dashed-dotted curve) the profile is indistinguishable from that of a monodisperse polymer adsorbing from a solution with bulk concentration 0.02. However, the interesting point in Fig. 6 is the fact that in the mixture there is an inhomogeneity in the system over a longer length scale than the one determining the overall profile. In principle, this effect could be measured by specific labelling of either kind of polymer.

Conclusions

We have shown the correspondence between the numerical self-consistent field theory by Scheutjens and Fleer and the analytical theory by Johner *et al.* In the case of adsorption from semi-dilute solution the overall volume fraction profile turns out to be universal, *i.e.* independent of the polymer chain length. Also, the numerical profile is described well by the analytical theory. The analytical deconvolution of the overall profile into adsorbed segments and adsorbed end segments works well in the long loop dominance regime, where the segment number dependence is not very

large, but less well in the surface excess regime. If the solvent quality is poor or the adsorption energy high, the analytical volume fraction profile exceeds 1 close to the surface on length scales smaller than the radius of a polymer segment. For integrated quantities like the excess amount or the adsorbed amount, this leads to values that are unrealistically high. In the case of adsorption of a bidisperse polymer mixture, more than one length scale is found to play a role.

References

[1] J. D. van der Waals, "Thermodynamische theorie der capillariteit in de onderstelling van continue dichtheidsverandering" *Verhand. Kon. Akad. v. Wetensch. (Sect. 1)* **1 (No. 8)** (1893) 1. Translation in German: *Zeit. phys. Chem.* **13** (1894) 657, in French: *Arch. Néerl.* **28** (1895)121, in English: *J. Stat. Phys.* **20** (1979) 197.

[2] J. W. Cahn and J. E. Hilliard, "Free energy of a nonuniform system. 1. Interfacial free energy" *J. Chem. Phys.* **28** (1958) 258.

[3] E. Helfand, "Theory of inhomogeneous polymers: lattice model for polymer-polymer interfaces" *J. Chem. Phys.* **63** (1975) 2192.

[4] E. Helfand and A. M. Sapse, "Theory of unsymmetric polymer-polymer interfaces" *J. Chem. Phys.* **62** (1975) 1327.

[5] I. S. Jones and P. Richmond, "Effects of excluded volume on the conformation of adsorbed polymers" *J. Chem. Soc. Far. II* **73** (1977) 1062.

[6] P.-G. de Gennes, "Scaling concepts in polymer physics" (1979) Cornell University Press, Ithaca, NY.

[7] A. Johner, J.-F. Joanny and M. Rubinstein, "Chain statistics in adsorbed polymer solutions" *Europhys. Lett.* **22** (1993) 591.

[8] J. Bonet Avalos and A. Johner, "Structure of adsorbed polymer layers" *Faraday Disc.* **98** (1994) ?.

[9] J. M. H. M. Scheutjens, G. J. Fleer and M. A. Cohen Stuart, "End effects in polymer adsorption: a tale of tails" *Colloids Surfaces* **21** (1986) 285.

[10] J. M. H. M. Scheutjens and G. J. Fleer, "Statistical theory of the adsorption of interacting chain molecules. 1. Partition function, segment density distribution and adsorption isotherms" *J. Phys. Chem.* **83** (1979) 1619.

[11] G. J. Fleer, M. A. Cohen Stuart, J. M. H. M. Scheutjens, T. Cosgrove and B. Vincent, "Polymers at Interfaces" (1993) Chapman & Hall, London.

[12] P. J. Flory, "Principles of polymer chemistry" (1953) Cornell University Press, Ithaca, N.Y.

[13] E. Helfand and A. M. Sapse, "Theory of the concentrated polymer solution/solvent interface" *J. Polym. Sci. Symp.* **54** (1976) 289.

[14] S. F. Edwards, "The statistical mechanics of polymers with excluded volume" *Proc. Phys. Soc. (London)* **85** (1965) 613.

[15] P.-G. de Gennes, "Some conformation problems for long macromolecules" *Rep. Prog. Phys.* **32** (1969) 187.

[16] M. Abramowitz and I. A. Stegun, "Handbook of mathematical functions" (1964) Dover Publications, Inc., New York.
[17] A. Johner, personal communication.
[18] J. M. H. M. Scheutjens and G. J. Fleer, "Some implications of recent polymer adsorption theory", in *The effect of polymers on dispersion properties* (1982) T. F. Tadros, Ed. Academic Press, London.
[19] S. P. F. M. Roefs, J. M. H. M. Scheutjens and F. A. M. Leermakers, "Adsorption theory for polydisperse polymers" *Macromolecules* **27** (1994) 4810.
[20] J.-U. Sommer and M. Daoud, "Adsorption of long polymers dissolved in a semi-dilute solution of shorter chains" *J. Phys. II (France)* **4** (1994) 2257.

Appendix: Calculus of variations.

We have a quantity J, that is given as an integral:

$$J = \int_{x_1}^{x_2} f(y, y_x, x)dx \qquad (A1)$$

Under the integral sign is a known function $f = f(y, y_x, x)$, where $y_x = dy/dx$. What we are looking for is the function y(x) that minimises J. Thus, we know how f depends on y, y_x and x, and we want to determine how y depends on x. It is not obvious that a solution to this problem exists, but we will assume that it does. The mathematical treatment needed to solve this problem is called variational calculus. We will briefly outline the procedure here, following the line of reasoning of ref. [1]. A more detailed discussion can be found in [2,3,4].

Let y(x) be the admissible solution for which J is a minimum. It passes through the (given) end points $(x_1, y(x_1))$ and $(x_2, y(x_2))$. Admissible functions should be differentiable on the interval $x_1 \le x \le x_2$. Next, we arbitrarily take an admissible function $\eta(x)$ which satisfies the conditions

$$\eta(x_1) = \eta(x_2) = 0 \qquad (A2)$$

We can define a family of functions

$$y(x, \alpha) = y(x, 0) + \alpha\eta(x) \qquad (A3)$$

where y(x,0) is again the solution we are looking for, and all of the functions of the family pass through the end points. The value of the integral J along any member of the family now depends upon the value of α:

$$J(\alpha) = \int_{x_1}^{x_2} f(y(x,\alpha), y_x(x,\alpha), x)dx \tag{A4}$$

In differential calculus, an extreme of a function g(x) can be found by setting the first derivative (dg/dx) equal to zero. The same trick applies in variational calculus: to find the extreme in $J(\alpha)$, which should occur for $\alpha = 0$, the necessary condition is

$$\left[\frac{\partial J(\alpha)}{\partial \alpha}\right]_{\alpha=0} = 0 \tag{A5}$$

Differentiating:

$$\frac{\partial J(\alpha)}{\partial \alpha} = \int_{x_1}^{x_2}\left(\frac{\partial f}{\partial y}\frac{\partial y}{\partial \alpha} + \frac{\partial f}{\partial y_x}\frac{\partial y_x}{\partial \alpha}\right)dx \tag{A6}$$

Note that y and y_x are treated as independent variables.
From (A3):

$$\frac{\partial y(x,\alpha)}{\partial \alpha} = \eta(x) \tag{A7a}$$

and

$$\frac{\partial y_x(x,\alpha)}{\partial \alpha} = \frac{d\eta(x)}{dx} \tag{A7b}$$

Substituting in (A6):

$$\frac{\partial J(\alpha)}{\partial \alpha} = \int_{x_1}^{x_2}\left(\frac{\partial f}{\partial y}\eta(x) + \frac{\partial f}{\partial y_x}\frac{d\eta(x)}{dx}\right)dx \tag{A8}$$

The second term can be integrated by parts, where the integrated part vanishes through (A2). This leads to

$$\frac{\partial J(\alpha)}{\partial \alpha} = \int_{x_1}^{x_2}\left(\frac{\partial f}{\partial y} - \frac{d}{dx}\frac{\partial f}{\partial y_x}\right)\eta(x)dx = 0 \tag{A9}$$

Now α can be set to zero. As $\eta(x)$ is an arbitrary function, it can have the same sign as the expression in brackets. The only way (A9) is satisfied irrespective of the choice of $\eta(x)$ is to have the whole term in brackets to equal zero:

$$\frac{\partial f}{\partial y} - \frac{d}{dx}\frac{\partial f}{\partial y_x} = 0 \qquad \text{(A10)}$$

Equation (A10) is known as the Euler-Lagrange equation. Several other forms of this equations are known, *e.g.*, if f does not depend explicitly on x (*i.e.*, $\partial f / \partial x = 0$) it can be rewritten to

$$\frac{d}{dx}\left(f - y_x \frac{\partial f}{\partial y_x}\right) = 0 \qquad \text{(A11)}$$

which is easily integrated to

$$f - y_x \frac{\partial f}{\partial y_x} = \text{constant} \qquad \text{(A12)}$$

The Euler equation is a necessary condition for any extremal for J: if there is a minimum, it will comply to (A10). The reverse is not necessarily true: a solution to (A10) may not be a minimum for J. For instance, it may be a maximum, or it may be physically unrealistic.

Sometimes, the end points or one of the end points are not explicitly given. In this case, (A2) is not necessarily true. The solutions we had using (A2) are a subclass of the solutions with variable end points. If a curve y(x) gives a minimum for a problem with variable end points, then that curve necessarily also gives a minimum with respect to the more restricted class of curves having the specific end points of y(x). Therefore, the Euler equation, which is a fundamental necessary condition for the occurrence of a minimum, should hold for the problem with variable end points as well. For the variable end points problem, we need extra boundary conditions, which can be obtained by demanding the equality between (A8) and (A9), and thus, the vanishing of the integrated part:

$$\left[\frac{\partial f}{\partial y_x}\eta(x)\right]_{x_1}^{x_2} = 0 \qquad \text{(A13)}$$

References - appendix

[1] G. Arfken, "Mathematical methods for physicists." 3rd. ed. (1985) Academic Press, London.

[2] G. A. Bliss, "Calculus of variations" (1925) The Mathematical Association of America. The Open Court Publishing Company, La Salle, Illinois.

[3] L. A. Pars, "An introduction to the calculus of variations." (1962) Heinemann Educational Books Ltd., London.

[4] L. E. Elsgolc, "Calculus of variations" (1961) Pergamon Press Ltd., Oxford.

CHAPTER III

Adsorption of semi-flexible polymers

The self-consistent field model for polymer adsorption of Scheutjens and Fleer is extended to the case of semi-flexible chains in a cubic lattice. It is found that the scaling behaviour for adsorption from dilute solution of polymers with the same radius of gyration, but with a varying degree of stiffness, is markedly different. Adsorption from semi-dilute solution gives a universal (chain-length independent) profile, even when bond correlations are taken into account. Adsorbing block copolymers with blocks that differ only in the rigidity of the blocks adsorb with the stiffer block on the surface. This preference has an entropical origin. Such copolymers behave similar to "energetic" block copolymers, where the blocks differ in energetic interaction with the solvent or with the surface. The effects of chain stiffness are of the same order of magnitude as energetic effects.

Introduction

The first theoretical model for polymers was probably the random-walk model by Kuhn [1]. In this model a polymer molecule is taken to consist of randomly jointed segments, *i.e.*, the orientation of each segment is independent of all the others. In practice, the backbone of a polymer molecule is not completely flexible: the segments cannot fold back onto themselves, and usually bond angles are restricted to specific values determined by the hybridization of the constituent atoms. However, this is not necessarily a problem: the chain-length dependence of the radius of gyration of an ideal polymer chain does not change if the bond angles are restricted, provided a number of bonds are combined into one statistical unit, which in turn can rotate independently. Still, it can be necessary to model chain stiffness: the fact that the radius of gyration can be rescaled properly does not imply that other parameters in more complicated systems are not altered. Also, if the polymer is very stiff, the statistical units become so large that for a finite chain length there are too few units to get reliable statistics. This is the "worm-like chain" case [2,3], in which the persistence length P of the chain plays a key role. The persistence length is a measure for the distance over which the polymer chain is stiff. By comparing the adsorption characteristics for polymers differing in flexibility but having the same radius of gyration it is possible to check whether rescaling works also in the case of adsorption.

Most of the research about semi-flexible polymers is devoted to isotropic-nematic transitions, which is important for the field of polymer liquid crystals. An excellent review on these systems is written by Odijk [4]; we will not discuss them here.

Yetiraj *et al.* [5] have recently found that in a polymer blend containing stiff and flexible molecules the stiff molecules segregate to the surface. This is a purely entropic effect: the stiffer polymers lose less entropy when adsorbing than the flexible ones. The theory to be presented below allows for molecules that have rigid and flexible blocks. In a sense these molecules can be considered to be block copolymers, although the blocks do not differ in mixing or adsorption energy. Thus, we can investigate the entropic effects of surface segregation of block copolymers. Usually in block copolymer systems one does not include the effect of the difference in local chain rigidity, although it is often present. One of the goals of this chapter is to investigate the problems encountered in this approach.

Theory

The model is based on the self-consistent-field theory for homopolymer adsorption by Scheutjens and Fleer [6], using extensions for copolymers [7], chain stiffness in a cubic lattice [8], and bond correlations [9]. We use a simple cubic lattice. A polymer molecule consists of N segments, where the diameter of a segment equals the lattice spacing. Layers are chosen parallel to the (flat) surface and numbered z = 0 (the surface), 1 (the layer immediately adjoining the surface) to M (in the bulk solution, far from the surface). The volume fraction of segment number s of molecule i in layer z is $\varphi_i(z,s)$. If molecule i consists of more than one monomer type, we can define $\varphi_{Ai}(z)$ as the contribution of segment type A to the volume fraction of component i in layer z.

interactions

The relative preference of a free monomer of type A to be in layer z with respect to the bulk solution is denoted as $G_A(z)$, the free segment distribution function. It can be related to the potential energy $u_A(z)$ of monomer type A in layer z using a Boltzmann equation:

$$G_A(z) = \exp(-u_A(z)/kT) \tag{1}$$

In this equation T is the absolute temperature and k Boltzmann's constant. The potential energy consists of two contibutions: hard-core and energetic interactions: $u_A(z) = u'(z) + u_A^{int}(z)$. The hard-core contribution u'(z), is calculated numerically by demanding that the lattice is completely filled with solvent molecules and polymer segments *i.e.*, $\sum_{i,s} \varphi_i(z,s) = 1$ for any z. For the energetic interactions, we use a Bragg-Williams or random-mixing approximation:

$$u_A^{int}(z) = \sum_B \chi_{AB}\left(\langle\varphi_B(z)\rangle - \varphi_B^b\right) \tag{2}$$

where φ_B^b stands for the volume fraction of monomer type B in the bulk, χ_{AB} is the Flory-Huggins interaction parameter between A and B, and $\langle\varphi_B(z)\rangle$ is the so-called neighbour-average of B around layer z:

$$\langle\varphi_B(z)\rangle = \sum_{d=-1,0,1} \lambda_d \varphi_B(z+d) \tag{3}$$

where d is one of the three directions in the lattice: from layer z to layer z–1 ("down") d = –1, within layer z ("sidewards") d = 0, or from layer z to layer z+1 ("up") d = 1. For a simple cubic lattice $\lambda_{-1} = \lambda_1 = 1/6$ and $\lambda_0 = 4/6$.
The adsorption energy is included in eq. 2 by taking the surface S as a separate component, with volume fraction $\varphi_S(z) = 1$ for $z < 1$ and $\varphi_S(z) = 0$ for $z \geq 1$. The resulting χ_{AS} relates to the more common Silberberg adsorption energy parameter χ_s [10] as $\chi_{AS} = -\lambda_{-1} \cdot \chi_s$, where all adsorption energies are calculated with respect to the solvent o, *i.e.*, $\chi_{oS} = 0$.

bond correlations

In eq. 2, we have used a random-mixing approximation for the interaction energy. This approximation can also be used while placing the molecules in the system: the probability that a site on which a segment or molecule is to be placed is empty (the vacancy probability) is then equal to the volume fraction of empty sites. However, as we will be calculating the volume fraction per bond direction, it is possible to improve on the calculation of the vacancy probability as follows. Suppose we want to place a bond "up", *i.e.*, from layer z to layer z+1. Then all segments in layer z+1 which are part of a bond between z and z+1 will not block this step. This means that the vacancy probability is greater than one would expect from a pure random mixing approximation, by a factor proportional to $1 - \varphi(z+1 \mid z)$. The last term is the volume fraction of segments having bonds between z and z+1. Introducing $\varphi_i(z,s,d)$ as the volume fraction of segment s of molecule i in layer z with its bond to segment s+1 in direction d, we can write for the weighting factor $g(z + d \mid z)$ for a bond between z+d and z :

$$g(z+d \mid z) = \frac{1 - \sum_j \varphi_{j,d}^{bulk}}{1 - \sum_i \varphi_i(z+d \mid z)} \tag{4}$$

where

$$\varphi_i(z+d \mid z) = \sum_s \left(\varphi_i(z,s,d) + \delta(|d|,1) \cdot \varphi_i(z+d,s,-d)\right) \tag{5}$$

is the volume fraction of bonds that molecule i has in layer z. The Kronecker δ factor $\delta(|d|,1)$ is inserted to ensure that bonds within layer z are not counted twice. The parameter $\varphi_{i,d}^{b}$ is defined as

$$\varphi_{i,d}^{b} = \varphi_i^{b} \frac{N_i - 1}{3N_i} \tag{6}$$

and denotes the relative number of bonds of i in direction d in the bulk solution. The factor 1/3 stems from the use of a cubic lattice: in general each direction contributes a factor 2/Z, where Z is the co-ordination number of the lattice. The use of eq. 4-6 leads to an anisotropy in the polymer statistics. Therefore, it has been called SCAF, for Self-Consistent Anisotropic Field [9]. The self-consistency arises from the fact that the volume fractions of bonds are needed for the calculation of the weighting factors, but also the other way around: the weighting factors are needed for the calculation of the volume fractions of bonds. The SCAF can be seen as a first order improvement on the random-mixing approximation, but it still implements a mean-field approach.

chain stiffness in polymer statistics

In a cubic lattice, two consecutive bonds can have three relative orientations: a straight conformation, where a bond makes an angle of 180° with the preceding one, a perpendicular conformation of 90°, and direct backfolding where the angle is 0°. We denote the energy difference between a straight conformation between the segments s–1, s and s+1 and a perpendicular one as $\Delta U_{sp}(s)$. Typically, $\Delta U_{sp}(s)$ is negative. The weighting factor $\lambda_s(s)$ for a straight conformation is related to the weighting factor $\lambda_p(s)$ for a perpendicular conformation as

$$\lambda_s(s) = \lambda_p(s) \exp\left(-\frac{\Delta U_{sp}(s)}{kT} \right) \tag{7}$$

for $1 < s < N$. We will exclude direct backfolding of two consecutive bonds, so that the weighting factor $\lambda_b(s)$ for backfolding is zero for $1 < s < N$. Everywhere along the chain, we must have

$$\lambda_b(s) + 4\lambda_p(s) + \lambda_s(s) = 1 \tag{8}$$

The end points only have one bond, so that $\lambda_b(s) = \lambda_p(s) = \lambda_s(s) = 1/6$ for $s = 1$ and $s = N$.

Wijmans *et al.* [11] have shown that for a homopolymer (where ΔU_{sp} does not depend on the segment number) with infinite chain length there is a simple relation between the persistence length P, here defined as the number of bonds that are joined together in a Kuhn segment, and the bending energy ΔU_{sp}, namely

$$P = 1 + 0.5\ \exp(-\Delta U_{sp}) \tag{9}$$

The statistical weight of a segment s of polymer i in layer z that will make a step in the direction d, given that the first segment is somewhere in the system, is called the end segment distribution function $G_i(z,s,d\,|\,1)$. As a starting condition we take

$$G_i(z,1,d\,|\,1) = G_A(z) \tag{10}$$

for any d, if s = 1 of molecule i is monomer type A. Connecting the segments in a second order Markov approximation yields:

$$G_i(z,s,-1\,|\,1) = G_i(z,s)\left\{\begin{matrix}\lambda_b(s)\cdot g(z-1\,|\,z)\cdot G_i(z-1,s-1,1\,|\,1)\\ +4\lambda_p(s)\cdot g(z\,|\,z)\cdot G_i(z,s-1,0\,|\,1)\\ +\lambda_s(s)\cdot g(z+1\,|\,z)\cdot G_i(z+1,s-1,-1\,|\,1)\end{matrix}\right\} \tag{11a}$$

$$G_i(z,s,0\,|\,1) = G_i(z,s)\left\{\begin{matrix}\lambda_p(s)\cdot g(z-1\,|\,z)\cdot G_i(z-1,s-1,1\,|\,1)\\ +\left(2\lambda_p(s)+\lambda_s(s)+\lambda_b(s)\right)\cdot g(z\,|\,z)\cdot G_i(z,s-1,0\,|\,1)\\ +\lambda_p(s)\cdot g(z+1\,|\,z)\cdot G_i(z+1,s-1,-1\,|\,1)\end{matrix}\right\} \tag{11b}$$

$$G_i(z,s,1\,|\,1) = G_i(z,s)\left\{\begin{matrix}\lambda_s(s)\cdot g(z-1\,|\,z)\cdot G_i(z-1,s-1,1\,|\,1)\\ +4\lambda_p(s)\cdot g(z\,|\,z)\cdot G_i(z,s-1,0\,|\,1)\\ +\lambda_b(s)\cdot g(z+1\,|\,z)\cdot G_i(z+1,s-1,-1\,|\,1)\end{matrix}\right\} \tag{11c}$$

Starting from the other side of the chain, we have to keep in mind that the bonds are defined from segment s to segment s+1, and the conformations are now between the segments s, s+1, and s+2. This leads to an asymmetry in the end segment distribution functions: $G_i(z,s,d\,|\,N)$ is the statistical weight of segment s of polymer i to have reached layer z coming from the direction

d, with the end segment N somewhere in the system. The starting condition is

$$G_i(z,N,d\,|\,N) = G_A(z) \tag{12}$$

as in (9). The other segments are connected using

$$G_i(z,s,-1|N) = G_i(z,s)\cdot g(z+1|z)\begin{Bmatrix}\lambda_b(s+1)\cdot G_i(z+1,s+1,1|N)\\ +4\lambda_p(s+1)\cdot G_i(z+1,s+1,0|N)\\ +\lambda_s(s+1)\cdot G_i(z+1,s+1,-1|N)\end{Bmatrix} \tag{13a}$$

$$G_i(z,s,0|N) = G_i(z,s)\cdot g(z|z)\begin{Bmatrix}\lambda_p(s+1)\cdot G_i(z,s+1,1|N)\\ +\left(2\lambda_p(s+1)+\lambda_s(s+1)+\lambda_b(s+1)\right)\cdot G_i(z,s+1,0|N)\\ +\lambda_p(s+1)\cdot G_i(z,s+1,-1|N)\end{Bmatrix} \tag{13b}$$

$$G_i(z,s,1|N) = G_i(z,s)\cdot g(z-1|z)\begin{Bmatrix}\lambda_s(s+1)\cdot G_i(z-1,s+1,1|N)\\ +4\lambda_p(s+1)\cdot G_i(z-1,s+1,0|N)\\ +\lambda_b(s+1)\cdot G_i(z-1,s+1,-1|N)\end{Bmatrix} \tag{13c}$$

Finally, two end segment distribution functions can be joined to find the segment density profile:

$$\varphi_i(z,s,d) = C_i\lambda_d\frac{G_i(z,s,d\,|\,N)G_i(z,s,-d\,|\,1)}{G_i(z,s)} \tag{14}$$

where C_i is a normalisation constant. For a polymer in full equilibrium C_i is equal to φ_i^{bulk}/N_i. Equation (14) is called the composition law. It relates volume fractions via chain statistics to (potential) energies. However, the energies depend on the volume fractions (eq. 2 and the space-filling constraint), so that, as with the bond correlations, we have a self-consistent set of equations that has to be solved numerically.

Results

In chapters 1 and 2, we have discussed several general aspects of polymer adsorption. In the case of adsorption from a dilute solution (chapter 1), we found that the volume fraction profile consists of three parts: a proximal regime which for high adsorption energies consists of only one lattice layer, a central regime showing a power law decay $\varphi(z) \propto z^{\alpha}$ with α depending on chain length and bulk volume fraction, and a distal regime far from the surface, where the volume fraction decays exponentially as $\varphi(z) \propto \exp(-\gamma z)$, with γ inversely proportional to the radius of gyration. If the polymer adsorbs from a semi-dilute solution, the profile is independent of chain length. With the theory presented above, we can check whether these scaling results still apply for semi-flexible polymers. Also, as the rigidity is defined to be a local parameter (*i.e.*, it depends on the segment ranking number), it is possible to model block copolymers with blocks having different rigidity. In doing such, we can distinguish between energetic and entropic driving forces for adsorption. Entropic factors are usually neglected, it remains to be seen whether this is justified or not. Unless stated otherwise, we have taken g(z+dlz) to equal 1, *i.e.*, we did not use the SCAF extensions.

critical adsorption energy

We consider the case of a homopolymer adsorbing from a monomeric solvent. Such a polymer is restricted in the number of conformations that it can assume near an impenetrable interface and this entropy loss must be compensated for. If the adsorption energy is not sufficiently negative, the polymer molecules will avoid the interface. This leads to the concept of a critical adsorption energy which is, in contrast to the adsorption energy parameter χ_{AS}, independent of the kind of solvent used. In the limit of infinitely long freely jointed chains on a cubic lattice the critical adsorption energy is $\chi_{AS}^{cr} = 6\ln\frac{5}{6}$.

Birshtein *et al.* [12] have derived that the critical adsorption energy in the limit of infinite chain length becomes a function of the persistence length P. Their result can be written as:

$$\chi_{AS}^{cr} = 6 \cdot \ln\left(\frac{P + \sqrt{P^2 + 4}}{2P + 2}\right) \qquad (15)$$

which indicates that in the limit of rigid rods (P –> ∞) the critical adsorption energy approaches zero as there is no entropy loss. Note that P = 1 in their

model does not exactly give the freely jointed chain result, since direct backfolding is prohibited.

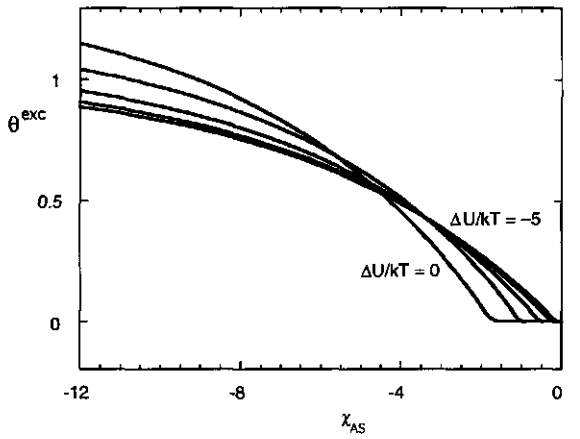

Figure1. Excess amount of a homopolymer with 1000 segments adsorbed from an athermal monomeric solvent, as a function of the adsorption energy χ_{AS}. The energy difference between a straight and a perpendicular bond ΔU_{sp} was varied as 0, –1, –2, –3, –4, –5 kT. The polymer volume fraction in the bulk solution is 10^{-4}.

In order to investigate how the critical adsorption energy of polymer chains of finite chain length, adsorbing from a monomeric solvent, depends on the flexibility of the chain, we have conducted a number of calculations the results of which are presented in Figure 1. In this figure the excess amount θ_i^{exc}, defined as $\theta_i^{exc} = \sum_z \left(\varphi_i(z) - \varphi_i^{bulk}\right)$, is plotted as a function of the adsorption energy for a homopolymer consisting of 1000 segments. We find a shift in the critical adsorption energy to less negative values. This is easily explained by the fact that stiff molecules lose less entropy per segment than fully flexible ones. In Figure 2a we have plotted the critical adsorption energy as a function of the straight-perpendicular energy difference ΔU_{sp}. The critical adsorption point is defined by the surface affinity for which $\theta^{exc} = 0$. In this figure we note that at high absolute values of ΔU_{sp}, the critical adsorption energy becomes almost independent of ΔU_{sp}. In Figure 2b we check the prediction of eq. 15. If the numerical results would be predicted perfectly by eq. 15 then all points should fall on the solid line. We see that the agreement with the analytical theory is excellent. Naturally the long chains follow the predictions of eq. 6 to higher degree of stiffness than the shorter ones.

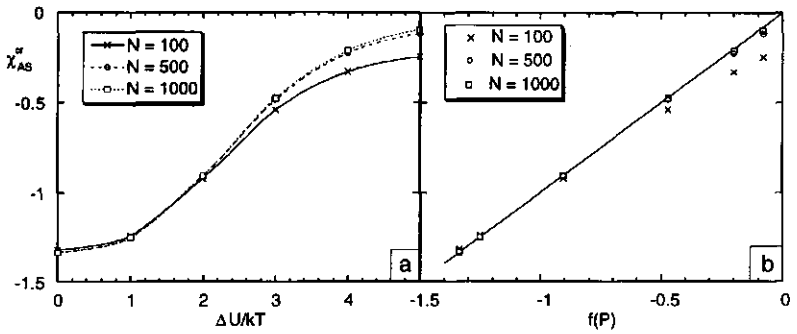

Figure 2a. The critical adsorption energy for three polymers of different chain length, which adsorb from an athermal monomeric solvent as a function of the energy difference ΔU_{sp} between straight and perpendicular bond orientations. Crosses: N = 100, spheres: N = 500 , squares: N = 1000. Athermal solvent, polymer bulk volume fraction $\varphi^b = 10^{-7}$.

Diagram (b): the critical adsorption energy plotted as a function of f(P), where P is the persistence length and $f(P) = 6\ln\left[\left(P+\sqrt{P^2+4}\right)/(2P+2)\right]$. The full line is the prediction by the analytical theory of Birshtein *et al.* (eq. 15). Other parameters as in (a).

rescaling and the persistence length

As already stated before, the radius of gyration of an ideal semi-flexible polymer can be rescaled to a polymer with less segments, but a larger Kuhn length. Fleer *et al.* [13] ventured that this procedure might also be used in the case of polymer adsorption. In practice, the value taken for the ratio between the Kuhn length and the bond length is the so-called characteristic ratio, which is tabulated for a large variety of polymers [14]. In a lattice theory, the Kuhn length is usually taken to equal the lattice spacing for convenience. Thus, in the first-order Markov statistics used in the standard Scheutjens and Fleer scheme we take the persistence length P to be 1, and for the second-order statistics we use eq. (9). As an example, we take a homopolymer containing 5000 segments with ΔU_{sp} /kT = –ln(2), so that P = 2. There are now two ways to rescale this polymer to a fully flexible one with P = 1: by halving the chain length, which should be accompanied by a doubling of the lattice spacing (case I), or by doubling the chain length without changing the lattice spacing (case II). The resulting volume fraction profiles are plotted in Fig. 3: the dashed curve is case number I, the dotted curve case number II. In Fig. 3b where the profiles are plotted on a log-lin scale, we can check that the radius of gyration is indeed scaled back properly as the curves run parallel in the distal regime: as shown in chapter 1 and ref. [15], the

exponent in the distal regime scales with the correlation length in the dilute solution, which equals the radius of gyration. However, the log-log scale in Fig. 3a shows clearly that the behaviour in the central regime differs considerably in both cases. The difference could be due to the fact that resizing the polymer or the lattice spacing changes the conformational entropy of the polymer and it is not obvious whether or not the difference in entropy is the same in the bulk as near the surface. A recent theory by Ploehn [16] allowing for a difference in molecular volume between polymer and solvent seems to indicate that indeed there is a problem here.

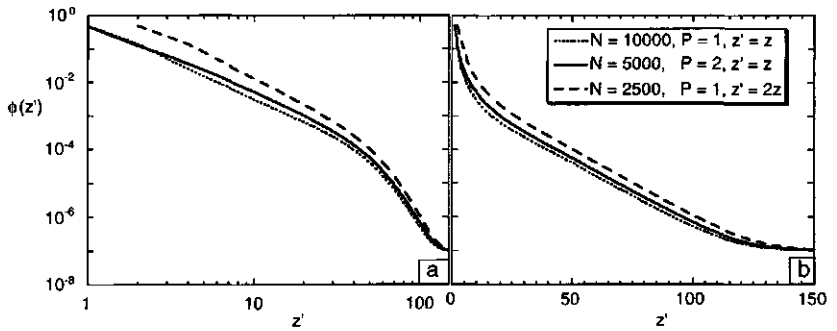

Figure 3. Volume fraction profiles for a homopolymer with (i) chain length 5000 using second-order Markov statistics, no backfolding ($\lambda_b = 0$), and $\Delta U_{sp}/kT = -\ln 2$ (solid curve), (ii) chain length 10000 using first-order Markov statistics (dotted curve), and (iii) chain length 2500 using first-order statistics and plotted against 2z instead of z (dashed curve). Adsorption energy: $\chi_{AS} = -6$, other parameters as in Fig. 2.

We conclude that rescaling does not work in the case of polymer adsorption. Another conclusion that can be drawn from this example is that one cannot expect experimental volume fraction profiles to coincide with calculated ones if the characteristic ratio is used as an input parameter.

influence of bond correlations

In chapter 2 of this thesis, it was shown that the volume fraction profile in the case of a polymer adsorbing from an athermal semi-dilute solution is independent of the chain length. This universality should also be independent of the details of the model used, as it derives from the general idea that in a semi-dilute solution the chain length is not a predominant parameter. With the use of the SCAF, equations for thermodynamic parameters like the partition function, (excess) free energy and chemical potential differ significantly from the ones without the SCAF, even though

both approaches use a mean-field approximation [9]. The SCAF was originally used for chains in a Rotational Isomeric State (RIS) scheme. RIS applies third order Markov statistics, and was devised by Volkenstein [17] to incorporate trans-gauche isomerism in polymer statistics. The cubic lattice scheme is computationally much faster than RIS, enabling the modelling of longer molecules.

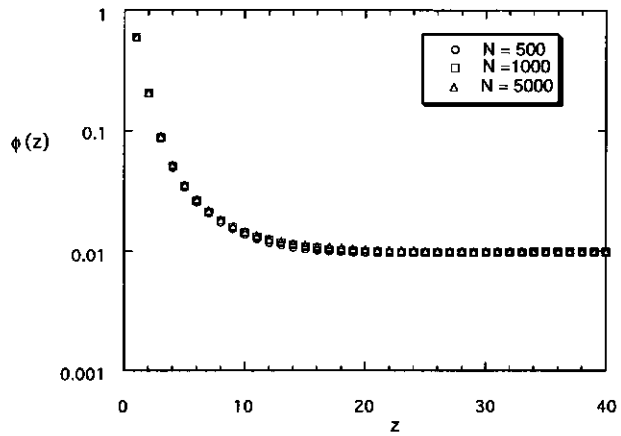

Figure 4. Volume fraction profiles in the semi-dilute regime (φ^b = 0.01) for homopolymers with 500 (circles), 1000 (squares) and 5000 (triangles) segments using second order Markov statistics, no backfolding (λ_b= 0), ΔU_{sp}/ kT = 0, and a SCAF approach.

Figure 4 shows the volume fraction profile for polymers with different chain lengths. It can be seen that again the profile is universal: there is hardly any chain length dependence. It must be noted that these profiles do not coincide with the profiles using only first-order statistics or even only second-order Markov statistics: each model has its own profile, which is universal within that model. Of course, other theoretical models, not using a mean-field approximation, should be applied to test the universality of the profile. Unfortunately, models like Monte Carlo or Molecular Dynamics are not easily used for the long chains needed to find universal behaviour.

stiff-flexible copolymers

In writing down the chain statistics, care was taken to have the bending energies depend on the segment ranking number. This enables us to model a copolymer where the constituent monomers differ in stiffness. In practice, this is often the case: *e.g.,* for polystyrene the characteristic ratio is 2.6 times

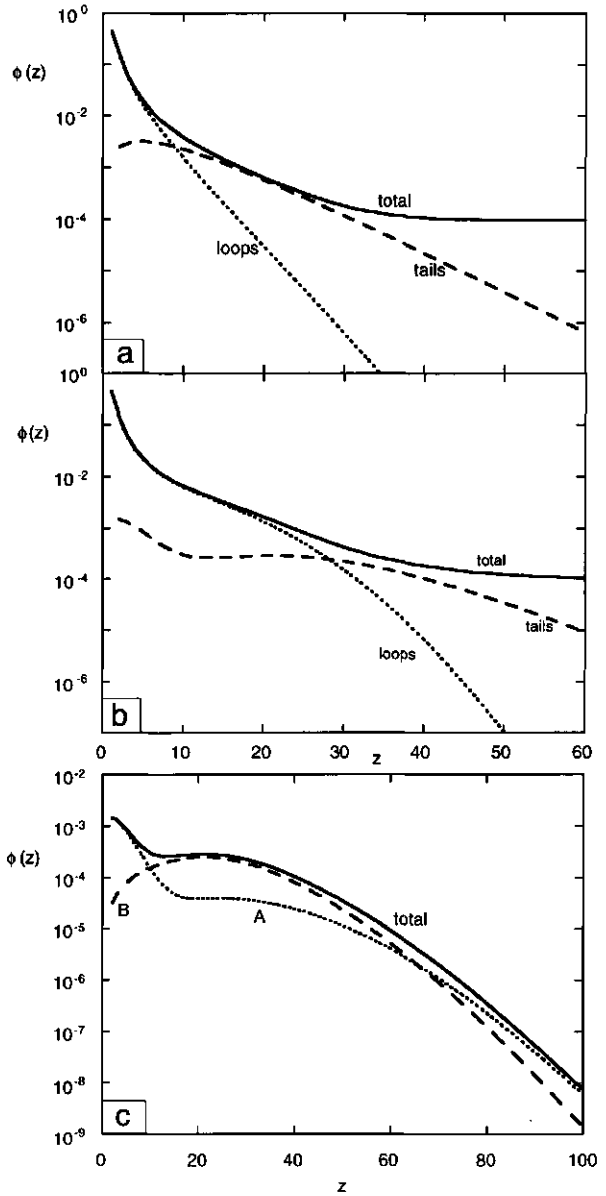

Figure 5. Volume fraction profiles for a polymer with 1001 segments, using second-order Markov statistics. In diagram (a) all segments have the same bending energy difference: $\Delta U_{sp}(s)/kT = -1$, in (b) segments 1 to 100 and segments 900 - 1001 have $\Delta U_{sp}(s)/kT = -1$, the other segments are flexible with $\Delta U_{sp}(s)/kT = 0$. Bulk volume fraction $\varphi^b = 10^{-4}$, adsorption energy: $\chi_{AS} = -6$, athermal solvent. Diagram (c) gives the tail profile from (b) and the contributions to it due to both segment types: dashed curve: B segments, dotted curve: A segments.

as large as for poly(ethylene oxide). This difference in rigidity creates an entropic reason for the stiffer parts to adsorb preferentially over the flexible ones. In order to distinguish the entropic factors from the energetic factors, all Flory-Huggins parameters will be taken equal for all blocks. For a straight or perpendicular local conformation, two bonds are needed. If we have a block copolymer with two segment types A and B, then there are four sequences of segments playing a role: AAA, AAB, ABB and BBB, which all have a different energy. To simplify the calculations, we have taken ΔU_{sp} to depend only on the segment type of the middle segment. Thus, for AAA and AAB the energy difference belonging to the A blocks, and for ABB and BBB the B blocks. This is only a minor simplification for block copolymers, since it affects only the segments next to the joint between two blocks. As an example, we take two polymers with 1001 segments. The first one is denoted A_{1001}, and is a semi-flexible homopolymer: $\Delta U_{sp}/kT = -1$ for all segments. The second one, $A_{100}B_{800}A_{101}$, is a copolymer with 200 stiff ($\Delta U_{sp}/kT = -1$) bonds, 100 on each end, whereas the middle 800 bonds are flexible: $\Delta U_{sp}/kT = 0$. Figure 5 shows the volume fraction profiles, with diagram (a) for the homopolymer and (b) for the copolymer. The volume fractions of the loops and tails of the polymers were calculated using the method outlined in ref. [18]. It turns out that the stiffness disparity in the copolymer leads to long loops, protruding far into the solution. This gives a hydrodynamic layer thickness [19] that is 1.9 times as large as the homopolymer case, whereas the excess amount is only 1.07 times as large. The tail profile shows two maxima. This can be explained using Fig. 5c, where the tail profile is split up into the different segment types. It can be seen that the first maximum is due to the end (A) segments and the second maximum to the middle (B) segments. Furthermore, the periphery of the profile consists again of A segments. This suggests that the polymer behaves like a telechelic polymer as calculated by Wijmans *et al.* [20]. In analogy to their results, we can expect bridge formation and thus flocculation if two surfaces covered with these polymers are brought together.

The idea of telechelic behaviour is further corroborated by Fig. 6 where we plot the relative preference of a segment to be in layer z, defined as $N\varphi(z,s)/\varphi(z)$, for 5 different segments distributed over the molecule: s = 1 corresponds to an end segment, for the copolymer s = 101 is at the joint of two blocks, and s = 201, 301 and 501 relate to various positions in the central B block. Diagram (a) shows the typical homopolymer segment distribution as already shown in ref. [19]: the ends are on average further

from the surface, because the tails protrude far into the solution. On the other hand, the middle segments prefer to be close to the surface. For the block copolymer in (b), this picture changes drastically: the first segment shows two maxima in the preference profile: one in the second layer, corresponding to tail adsorption, and one around layer 50, indicating a stretched conformation. The middle segments are now sticking out into the solution, showing again that large loops are formed. Thus, we have managed to create a system where the polymer tails adsorb preferentially for purely entropic reasons.

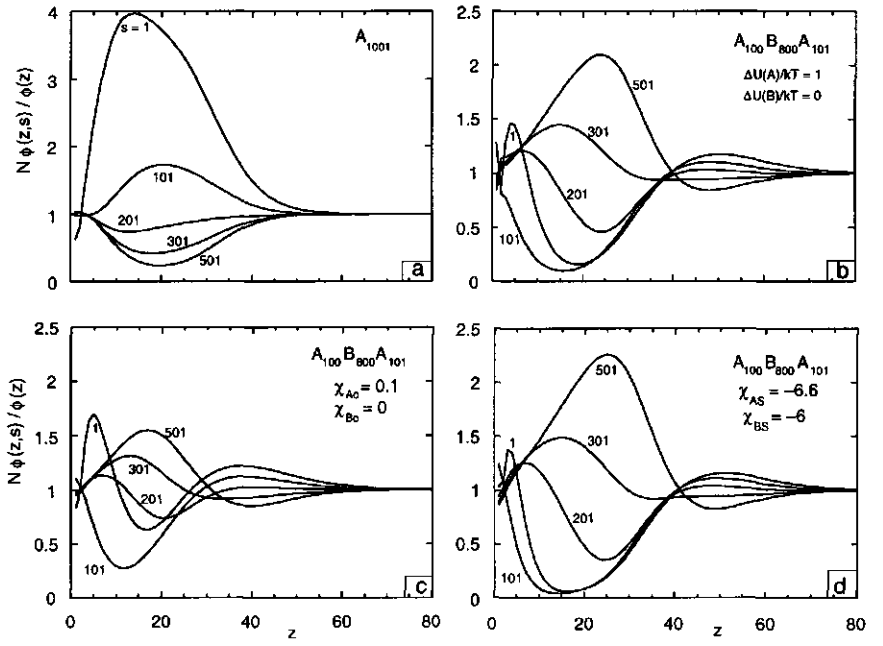

Figure 6. Relative preference profiles for several segments of different polymers. Diagrams (a) and (b) as in Fig. 5, diagrams (c) and (d) refer to flexible copolymers $A_{100}B_{800}A_{100}$ with $\Delta U_{sp}(s)/kT = 0$ for all s. In diagram (c) there is a difference in solvency: $\chi_{Ao} = 0.1$, $\chi_{Bo} = 0$, $\chi_{AS} = \chi_{BS} = -6$. In diagram (d) a difference in adsorption energy: $\chi_{AS} = -6$, $\chi_{BS} = -6$, $\chi_{Ao} = \chi_{Bo} = 0$. Segment numbers are indicated.

For comparison, preference plots are also shown for a fully flexible copolymer where the solvent is slightly worse for the A-blocks ($\chi_{Ao} = 0.1$ and $\chi_{Bo} = 0$, Fig. 6c) and for a flexible copolymer where the A-segments have slightly more adsorption energy than the B-segments ($\chi_{AS} = -6.6$ and $\chi_{BS} = -6$, Fig. 6d). The shape of these plots is the same as Fig. 6b, again

indicating that a difference in rigidity has the same effect as a difference in interaction energy. Also, the effects are of the same order of magnitude. We may conclude that it is not justified to neglect rigidity differences between the blocks of a copolymer.

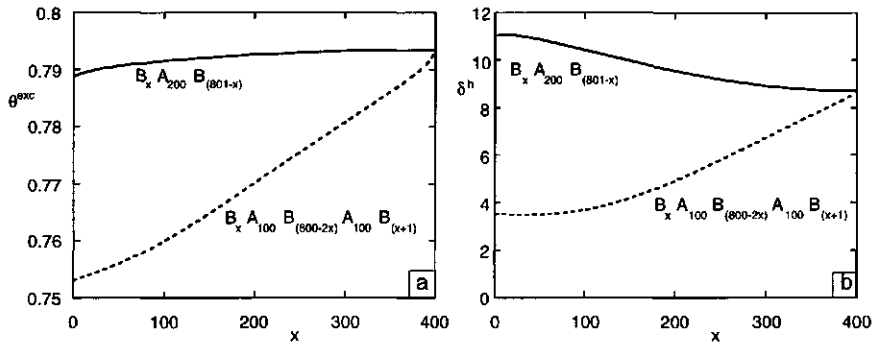

Figure 7. (a) Excess amount and (b) hydrodynamic layer thickness of block copolymers having 200 rigid bonds, associated with the A segments, and 800 flexible bonds at the B segments. Full curve: asymmetric copolymers $B_xA_{200}B_{(801-x)}$, dashed curve: symmetric copolymers $B_xA_{100}B_{(800-2x)}A_{100}B_{(x+1)}$. For x = 400 both cases corres pond to the same molecule. Bulk volume fraction: $\varphi^b = 10^{-7}$, other parameters as in Fig. 5b.

As a last example for stiff-flexible copolymers, we show in Fig. 7 the effect of the relative location of the stiff block. Again, we have 200 stiff bonds with $\Delta U_{sp}/ kT = -1$, and 800 flexible ones, with $\Delta U_{sp}/ kT = 0$. The full curve refers to the case where all the stiff segments are joined in one block, and moved along the molecule. It turns out that the excess amount (Fig. 7a) does not vary much, but the hydrodynamic layer thickness (Fig. 7b) does so considerably. If the adsorbing block is located at the end (x = 0) the adsorbed polymer layer can be regarded as a brush: one tail is sticking out into solution. If the adsorbing block is located in the middle (x = 400) there are two tails, which are necessarily shorter. This leads to the interesting effect that the hydrodynamic layer thickness decreases where the excess amount (which for these low bulk volume fraction equals the adsorbed amount) increases. The dashed curve shows the symmetrical case, in which the stiff segments are split up into two blocks of 100 stiff bonds each. For small x we have the situation of Fig. 6b: the polymer is forced to make long loops and hardly any tails. This leads to a small hydrodynamic layer

thickness, more than three times as low as in the symmetrical case whereas the difference in excess amount is only about 5%. Upon increasing x, tails are being formed. As this is entropically favourable, the adsorption goes up slightly. But initially this does not increase the layer thickness, as the tails grow at the cost of the loops dominating in the outer layers. Only when the tails are sufficiently large, the hydrodynamic layer thickness can go up.

Conclusions

Second-order Markov statistics in a cubic lattice are computationally the simplest way to model chain stiffness. It is possible to model copolymers where parts of the molecule are stiffer than other parts (stiff / flexible copolymers). Using this concept, it is shown that end blocks can adsorb preferentially on the surface for purely entropic reasons if their persistence length is larger than the middle blocks. This effect is of the same order of magnitude as energetic interactions, so that neglecting rigidity differences between blocks seems unjustified. For homopolymers, our model reproduces the predictions of Birshtein *et al.* regarding the dependence of the critical adsorption energy on the rigidity. Although the radius of gyration for a stiff polymer in a dilute solution can be rescaled to a flexible polymer by increasing the step length, this procedure does not work for the adsorption profile of a polymer adsorbing from a dilute solution. In the case of adsorption from a semi-dilute solution, we have shown that incorporating bond correlations does not alter the universality of the volume fraction profile.

References

[1] W. Kuhn, "Über die Gestalt fadenförmiger Moleküle in Lösungen" *Kolloid Z.* **68** (1934) 2.

[2] O. Kratky and G. Porod, "Röntgenuntersuchung gelöster Fadenmoleküle" *Rec. Trav. Chim. Pays-Bas* **68** (1949) 1106.

[3] A. C. Maggs, D. A. Huse and S. Leibler, "Unbinding transitions of semi-flexible polymers" *Europhys. Lett.* **8** (1989) 615.

[4] T. Odijk, "Theory of lyotropic polymer liquid crystals" *Macromolecules* **19** (1986) 2313.

[5] A. Yethiraj, S. Kumar, A. Hariharan and K. S. Schweizer, "Surface segregation in polymer blends due to stiffness disparity" *J. Chem. Phys.* **100** (1994) 4691.

[6] J. M. H. M. Scheutjens and G. J. Fleer, "Statistical theory of the adsorption of interacting chain molecules. 1. Partition function, segment density distribution, and adsorption isotherms" *J. Phys. Chem.* **83** (1979) 1619.

[7] O. A. Evers, J. M. H. M. Scheutjens and G. J. Fleer, "Statistical thermodynamics of block copolymer adsorption. 1. Formulation of the model and results for the adsorbed layer structure" *Macromolecules* **23** (1990) 5221.

[8] F. A. M. Leermakers, J. M. H. M. Scheutjens and R. J. Gaylord, "Modelling the amorphous phase of a melt crystallized, semicrystalline polymer: segment distribution, chain stiffness and deformation" *Polymer* **25** (1984) 1577.

[9] F. A. M. Leermakers and J. M. H. M. Scheutjens, "Statistical thermodynamics of association colloids. 3. The gel to liquid phase transition of lipid bilayer membranes" *J. Chem. Phys.* **89** (1988) 6912.

[10] A. Silberberg, "Adsorption of flexible macromolecules. 4. Effect of solvent-solute interactions, solute concentration, and molecular weight" *J. Chem. Phys.* **48** (1968) 2835.

[11] C. M. Wijmans, F. A. M. Leermakers and G. J. Fleer, "Chain stiffness and bond correlations in polymer brushes" *J. Chem. Phys.* (1994) accepted.

[12] T. M. Birshtein, E. B. Zhulina and A. M. Skvortsov, "Adsorption of polypeptides on solid surfaces. 1. Effect of chain stiffness" *Biopolymers* **18** (1979) 1171.

[13] G. J. Fleer, M. A. Cohen Stuart, J. M. H. M. Scheutjens, T. Cosgrove and B. Vincent, "Polymers at interfaces" (1993) Chapman & Hall, London.

[14] J. Bandrup and E. H. Immergut, "Polymer Handbook" (1989) J. Wiley & Sons, New York.

[15] P.-G. de Gennes, "Polymer solutions near an interface. 1. Adsorption and depletion layers" *Macromolecules* **14** (1981) 1637.

[16] H. J. Ploehn, "Structure of adsorbed polymer layers: molecular volume effects" *Macromolecules* **27** (1994) 1617.

[17] M. V. Volkenstein, "Configurational statistics of polymeric chains" (1963) John Wiley & Sons, Ltd., London.

[18] J. M. H. M. Scheutjens and G. J. Fleer, "Statistical theory of the adsorption of interacting chain molecules. 2. Train, loop, and tail size distribution" *J. Phys. Chem.* **84** (1980) 178.

[19] J. M. H. M. Scheutjens, G. J. Fleer and M. A. Cohen Stuart, "End effects in polymer adsorption: a tale of tails" *Colloids Surfaces* **21** (1986) 285.

[20] C. M. Wijmans, F. A. M. Leermakers and G. J. Fleer, "Multiblock copolymers and colloidal stability" *J. Colloid Interface Sci.* **167** (1994) 124.

CHAPTER IV

Adsorption of comb polymers

The adsorption of comb polymers is studied using a Self-Consistent Field theory. It is found that adsorbed comb polymers form thin layers as compared to linear polymers due to the absence of long dangling tails. The segments in the backbone of the comb adsorb preferentially over the tooth segments, as the end segments of the teeth can gain entropy protruding into the solution. This leads to a brush-like behaviour and a depletion zone adjacent to the adsorbed layer if the teeth are long compared to the backbone spacing. The brush-like behaviour is more pronounced in the case of a comb copolymer with an adsorbing backbone, but non-adsorbing teeth.

Introduction

Scheutjens *et al* [1] have emphasised the role of end segments in polymer adsorption. In the semi-plateau of the isotherm many polymer segments of many molecules compete for adsorption sites. The polymer molecules then prefer to adsorb with their ends protruding in solution to form long tails, and the middle segments form alternating trains (sequences of segments in contact with the surface) and loops. This average conformation is a compromise between gaining as much adsorption energy as possible and at the same time limiting the loss in conformational entropy upon adsorption. The tails are of major importance for colloidal stability, which is one of the main applications of polymer adsorption. Linear polymers can have at most two tails per polymer. For other chain geometries, the number of chain ends is either smaller or larger. For example, ring polymers, which do not have any chain end whatsoever, have been studied by Van Lent *et al* [2]. They found not surprisingly that ring polymer form less extended layers. Chain branching is the other extreme, as it increases the number of chain ends. Often, chain branching can be described by a straightforward extension of existing theories and it can result in interesting new phenomena. Several ways of branching may be distinguished: star polymers, with one central segment and several "arms", star-burst and comb-burst polymers, which are more fractal in nature, randomly branched polymers and comb polymers. This chapter deals with regular comb polymers, consisting of a long backbone with side chains emanating from it in regularly spaced intervals (Figure 1). If the chemical composition of the side chain segments differ from the backbone segments (Fig. 1b) we have a comb copolymer.

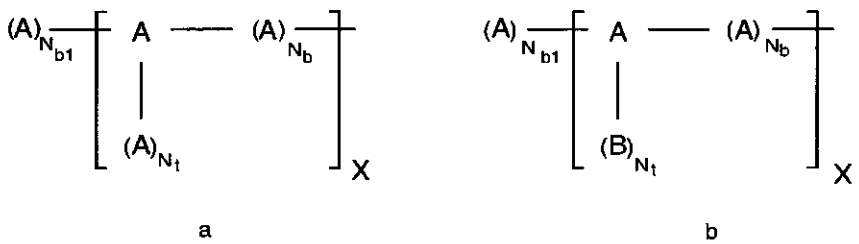

Figure 1. A regular comb homopolymer (a) and a regular comb copolymer (b) with backbone tail length N_{b1}, tooth length N_t, backbone spacing N_b, and polymerisation index X.

The official name for these polymers is graft (co)polymers [3], but in textbooks they are mostly referred to as comb (co)polymers [4,5]. Most of the literature about comb homopolymers deals with the determination of their

extension in solution or in a melt, see *e.g.* ref. [6,7]. Comb copolymers reveal an interesting phase behaviour in the melt [8]. Recently, comb copolymers have attracted attention as possible compatibilisers in polymer blend interfaces [9,10] or in solution as specific solubilisers [11].
The difference in adsorption behaviour between comb and linear polymers was predicted using Monte Carlo techniques by Balazs and Siemasko [12]. They concluded that comb polymers adsorb in dense but thin layers. This has also been found experimentally by Kawaguchi and Takahashi [13]. Balazs and Siemasko found also that the teeth of comb copolymers adsorb preferentially. This is unexpected, as it will cost more entropy than conformations having the backbone on the surface. In this chapter, we will use the theory for polymer adsorption by Scheutjens and Fleer [14,15], as extended to the case of chain branching by Leermakers [16], to explore systematically the parameters governing the adsorption behaviour of comb polymers. It may be expected that if the length of the teeth is small as compared to the length of the backbone the polymer behaves like a linear polymer, whereas typical comb behaviour, if present, will show if the teeth are long and the distance between them (the backbone spacing) short. Our method is more suitable to find general trends than Monte Carlo studies, since long polymer molecules can easily be calculated in a feasible amount of computer time.

Theory

The available space is divided up into lattice layers, parallel to the homogeneous surface. The surface is chosen as the origin of the lattice. The layer number is denoted as z, so that the surface is at z = 0, the layer adjacent to the surface at z = 1, etc. We consider only inhomogeneities perpendicular to the surface. Upon adsorption, a potential energy profile $u_x(z)$ develops, which depends on the volume fraction profiles $\{\varphi_x(z)\}$ of all the segment types x. For this potential energy we write:

$$u_x(z) = u'(z) + kT\left(\sum_y \chi_{xy}\left(\langle\varphi_y(z)\rangle - \varphi_y^b\right) - \chi_{s,x}\delta(z,1)\right) \qquad (1)$$

The first term in eq. (1), u'(z), is a "volume filling potential". It is found iteratively until the lattice is completely filled, *i.e.*, it is calculated from the condition that for all z

$$\sum_x \varphi_x(z) = 1 \qquad (2)$$

The second term corresponds to the energetic interactions of polymer segments with each other or with the solvent. As we will take all Flory-Huggins energy parameters χ_{xy} to be zero, this term vanishes. The last term contains the Silberberg adsorption energy parameter $\chi_{s,x}$, which equals the adsorption energy gain in units kT (Boltzmann's constant times the absolute temperature) if a segment of type x replaces a solvent molecule on the surface. The Kronecker delta $\delta(z,1)$ ensures that adsorption energy is counted only in the first layer. By definition, $\chi_{s,x} = 0$ for the solvent, and for the other segment types it is positive if the adsorption is energetically favourable, *i.e.*, if the adsorption energy is negative.
Next, the free segment weighting factor $G_x(z)$ is defined as the Boltzmann weight connected to the potential energy $u_x(z)$:

$$G_x(z) = \exp(-u_x(z)/kT) \tag{3}$$

Polymer chains are modelled as a series of connected segments, each having the size of one lattice site. In connecting the segments we have to take into account the molecular architecture around the branches. To illustrate the calculation scheme, we will take a simple molecule with only one branch, at $s = s^*$ (Fig. 2).

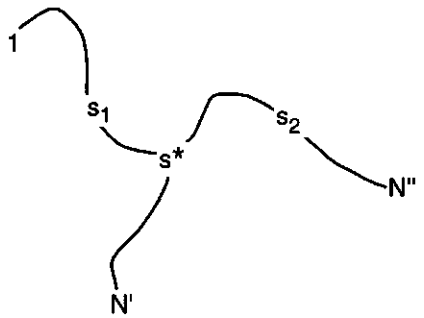

Figure 2: Schematic picture of a polymer with one branch at segment s*

In the SCF formalism of Scheutjens and Fleer a chain end distribution function (e.d.f.) G(z,s|1) is defined. It expresses the combined statistical weight of all possible allowed conformations that the chain fragment from segment 1 to s can assume, under the constraint that s is at a distance z from the surface. This means that the co-ordinate of segment 1 is left unspecified; the segment can assume all positions provided that it does not violate the

connectivity constraints. Thus, for the first segment we can simply use the free segment weighting factor

$$G(z,1|1) = G_x(z) \tag{4}$$

taking that segment 1 is of type x.
Moving along the chain towards the branch point s*, we can express the e.d.f. of a segment s_1 in the e.d.f. of its preceding segment, s_1-1, by realising that if s_1 is in layer z, s_1-1 has to be either in layer z–1, in z or in z+1, with in a cubic lattice an *a priori* probability of resp. 1/6, 4/6 and 1/6. This leads to

$$G(z,s_1|1) = G(z,s_1)\left\{\frac{1}{6}G(z-1,s_1-1|1)+\frac{4}{6}G(z,s_1-1|1)+\frac{1}{6}G(z+1,s_1-1|1)\right\} \tag{5}$$

where $G(z,s_1)$ equals $G_x(z)$ if segment s_1 is of type x. Eq. (5) can be used up to and including the branch point s*. For the subsequent segments, the branch from N' to s* has to be incorporated. The e.d.f. from the end point N', G(z,s|N'), is found analogously to eq. (5). The two branches are connected using

$$G(z,s^*|1,N') = \frac{G(z,s^*|1)G(z,s^*|N')}{G(z,s^*)} \tag{6}$$

where G(z,s*|1,N') is the e.d.f. for segment s* in layer z, given that both segment 1 and segment N' are free to chose their position. For a segment s_2 on the branch from s* to N'', the recurrence relation becomes

$$G(z,s_2|1,N') = G(z,s_2)\left\{\frac{1}{6}G(z-1,s_2-1|1,N')+\frac{4}{6}G(z,s_2-1|1,N')+\frac{1}{6}G(z+1,s_2-1|1,N')\right\} \tag{7}$$

The volume fraction of segment s_2 in layer z can be found by combining eq. (7) with the walk coming from the other free end, N'':

$$\varphi(z,s_2) = \frac{\varphi^b}{N}\frac{G(z,s_2|1,N')G(z,s_2|N'')}{G(z,s_2)} \tag{8}$$

where φ^b is the volume fraction in the bulk and φ^b/N serves as a normalisation constant. For the branch point s*, we have

$$\varphi(z,s^*) = \frac{\varphi^b}{N} \frac{G(z,s^* \mid 1)G(z,s^* \mid N')G(z,s^* \mid N'')}{(G(z,s^*))^2} \tag{9}$$

In this way the volume fraction of all segments in a branched molecule can be found, each time combining all the possible walks from all the end points to the particular segment.

Note that the volume fraction profiles can only be calculated if the potential energy profile is known. However, the potential energy profile depends on the volume fraction profile through eq. (1) and the volume filling constraint (2). The set of coupled equations is solved numerically. Once a solution is found, the adsorption can, for instance, be characterised by the excess amount θ^{exc}, defined as

$$\theta^{exc} = \sum_z \left(\varphi(z) - \varphi^b\right) \tag{10}$$

or using the adsorbed amount θ^{ads}, which is the amount of polymer chains having at least one segment in the first layer [17]. For dilute polymer solutions, the difference between θ^{exc} and θ^{ads} is negligible.

Results and discussion

The comb polymers that will be used can be characterised by four parameters: the tooth length N_t, the backbone spacing N_b, the backbone tail N_{b1} and the number of repeating units X (Fig. 1). The total number of segments N equals $N_{b1} + X\,(1 + N_t + N_b)$. In most cases, the combs are symmetric, *i.e.*, $N_{b1} = N_b$.

Firstly, we will investigate the difference in adsorption behaviour between a comb homopolymer and a linear homopolymer having the same number of segments. Also, the preference of tooth segments for the surface, found by Balazs and Siemasko is checked. The full advantage of the SCF method is exploited when we systematically vary the parameters mentioned above in order to analyse any "typical comb" behaviour if present. As we expect entropic factors to play a role in the adsorption of combs we will look at the situation near the desorption point, where the energetic contributions are of the same order as the entropic ones. Lastly, comb copolymers are considered.

homopolymers

In Fig. 3 adsorption isotherms are shown, where the full curve corresponds to a comb polymer with $N_{b1} = N_b = 5$, $N_t = 25$, and $X = 50$. The dashed curve is for a linear homopolymer with the same number of segments, $N = 1555$.

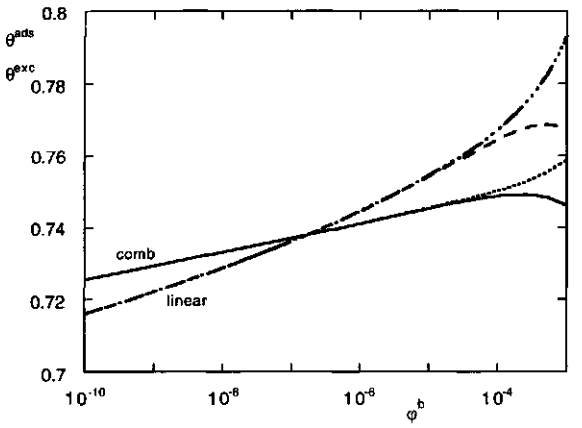

Figure 3. Adsorption isotherm for a comb polymer with $N_{b1} = N_b = 5$, $N_t = 25$, and $X = 50$ (full curve: excess amount; dotted curve: adsorbed amount) and for a homopolymer with $N = 1555$ (*dashed curve: excess amount; dashed-dotted: adsorbed amount*). *Athermal* solvent, adsorption energy parameter $\chi_S = 1$.

At low bulk volume fractions the comb polymer adsorbs to a greater extent than the linear polymer. This is due to the fact that a comb polymer loses less entropy upon adsorption than a linear chain: a comb polymer has more free ends that can stick out into the solution. At higher bulk concentration, the curves cross. If the driving force for adsorption is high enough, more linear polymer adsorbs because it can form longer tails. This can be seen more clearly if we compare the volume fraction profiles in Fig. 4, which are taken at $\varphi^b = 10^{-4}$. The occupation in the first few layers is almost equal, but the linear polymer protrudes much further into the solution. This result agrees with the predictions of Balazs and Siemasko [12] and with the measurements of Kawaguchi and Takahashi [13]: comb polymer form thin layers. The excess amount in Fig. 3 has a maximum for all polymers: as the bulk volume fraction increases the second term in eq. (10) starts to dominate. In the limiting case of a polymer melt ($\varphi^b = 1$), the excess amount is necessarily zero. The adsorbed amount, on the other hand, is a continuously increasing function of the bulk volume fraction.

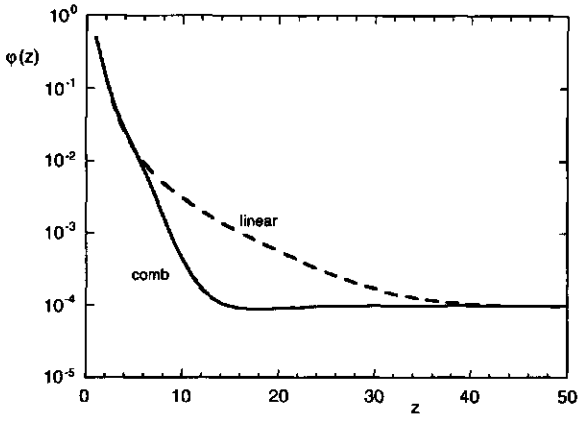

Figure 4. Volume fraction profile from the polymers in Fig. 3 at $\varphi^b = 10^{-4}$.

The distribution of segments within the adsorbed layer of a comb polymer can be illustrated by making a relative preference profile for the constituting segments of the comb (Fig. 5). The relative preference of a segment of type σ in layer z is defined as $\sum_{s=\sigma} N\varphi(z,s)/N_\sigma\varphi(z)$, where N_σ is the number of segments of type σ, and σ can be either a backbone segment, a tooth segment, or a branch point (node). Note that the curve for the backbone in Fig. 5 includes the nodes, as they are part of the backbone. If the relative preference for a particular group of segments in a certain layer exceeds unity, those segments are present more than average in that layer.

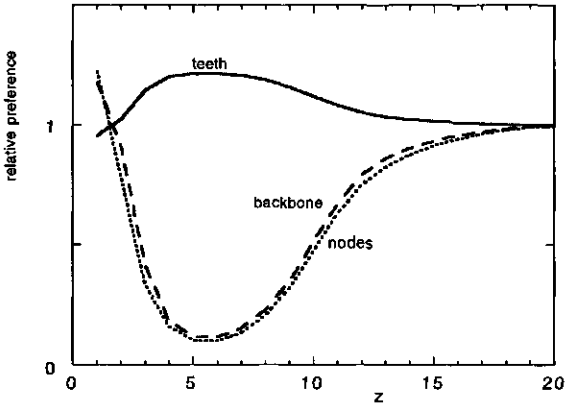

Figure 5. Relative preference profiles for the segments of the comb polymer used in Fig. 3 at $\varphi^b = 10^{-4}$. *Full curve: tooth segments, dashed curve: backbone segments (including nodes), dotted curve: node segments.*

It can be seen that the tooth segments avoid the surface and stick out into the solution, whereas the reverse holds for the backbone segments. Balazs and Siemasko [12] have found the opposite: in their Monte Carlo simulations the tooth segments are closer to the surface than the backbone. This may be due to an underestimation of the time scale for rearrangement of the comb polymer. It can be expected that in the kinetics of the adsorption process the tooth segments will adsorb first and during the subsequent exchange between tooth and backbone segments the surface coverage will hardly change. The constancy of the surface coverage was the stop criterion in the simulations, so that it is very well possible that equilibrium was not reached yet.

The branch points or node segments are even closer to the surface than the rest of the backbone. This is because the nodes have three adjacent adsorbing segments pulling them towards the surface. Note that we permit backfolding of the chain onto itself. If more than one side chain emanates from the node segments and direct backfolding is excluded, for instance using the method outlined in Chapter 3 or the Rotational Isomeric State scheme of ref. [16], the branch points cannot reach the surface anymore because of the excluded volume [18].

We now systematically vary the three parameters controlling the molecular architecture of the combs, starting from the molecule used in Fig. 3. The results are shown in Fig. 6. If the length of the teeth is increased (top diagram) the adsorbed amount increases, but only because the longer tails protrude further into the solution; the occupation in the first few layers (determining most of the adsorbed amount) is almost constant. If the tails get longer than about 40 segments, a depletion zone develops just before the polymer concentration reaches the bulk value. The profile then falls off so steeply that the free polymers in the bulk feel the adsorbed polymer layer as a non-adsorbing wall. The position of the depletion "dip" turns out to be linear in the tail length (Fig. 7). This indicates on a brush-like behaviour, with the backbone adsorbed on the surface and the teeth forming the brush. The lower concentration of polymer in the dip leads to a local decrease in viscosity. Hence, this system could be interesting for lubrication purposes: the adsorbed layer prevents aggregation, whereas the depletion dip facilitates the sliding of particles.

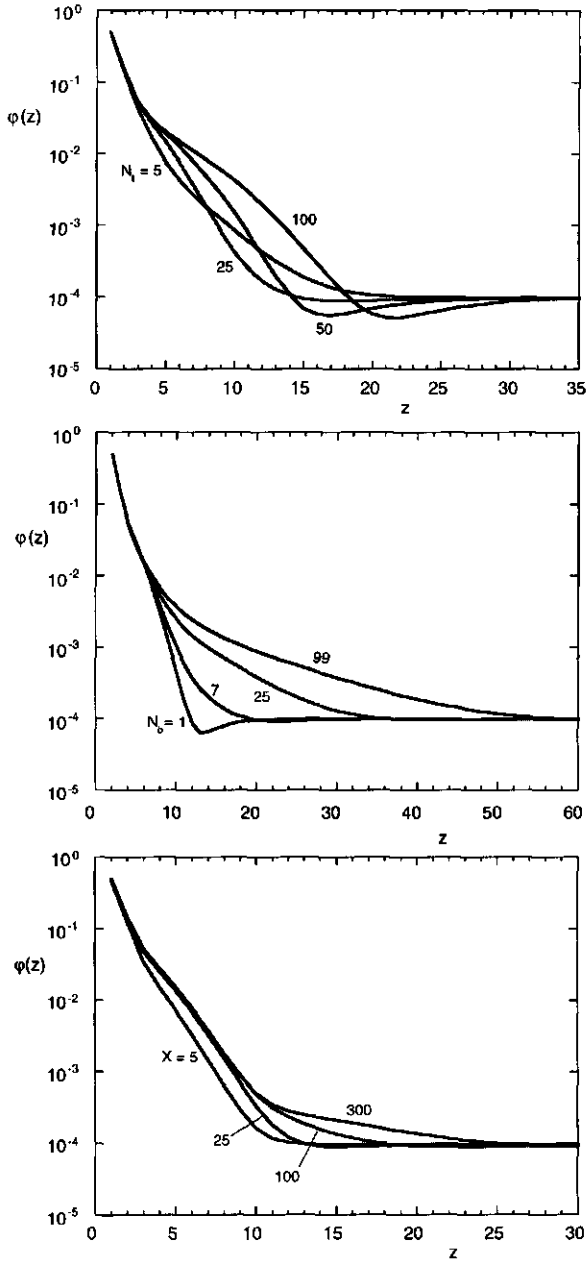

Figure 6. Volume fraction profiles for several comb polymers. Athermal solvent, bulk volume fraction 10^{-4}, adsorption energy = 1 kT. Top diagram: $N_{b1} = N_b = 5$, X = 50, N_t as indicated. Middle diagram: $N_t = 25$, X = 50, $N_{b1} = N_b$ as indicated. Bottom: $N_{b1} = N_b = 50$, $N_t = 25$, X as indicated.

If we increase the spacing between branches in the backbone (middle diagram of Fig. 6), we see that the polymer behaves more and more like a linear homopolymer: the characteristic steep decay and the depletion dip disappear. Indeed, the difference between the volume fraction profile of the polymer with N_b = 99 and the corresponding linear polymer with N = 6255 is negligible.

The effect of increasing the polymerisation index X is shown in the bottom diagram of Fig. 7. For high values of X, an extra shoulder appears in the volume fraction profiles at high z. Here, the outer parts of the backbone behave as tails and are lifted from the surface.

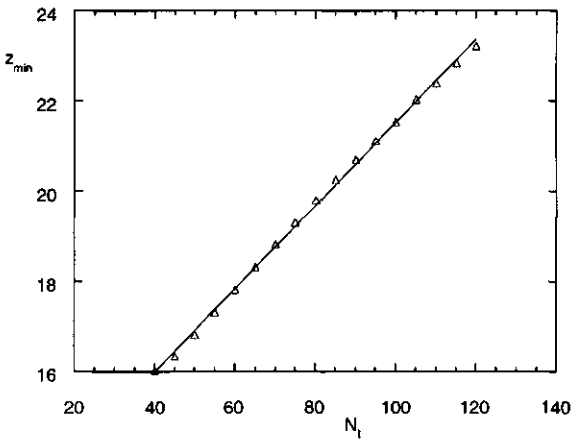

Figure 7. Position of the minimum in the volume fraction profile of Fig. 6a as a function of the tooth length N_t.

critical adsorption energy

A linear, flexible polymer adsorbing from solution onto a solid surface loses conformational entropy as it cannot use the half-space occupied by the adsorbent. Therefore, a polymer will avoid the surface if the adsorption energy is not large enough to compensate this entropy loss. The minimum adsorption energy needed to give net adsorption is called the critical adsorption energy. In a cubic lattice, a polymer loses one out of six possibilities to place a segment, so that the critical adsorption energy equals kT ln (6/5), or 0.182 kT. This value is independent of the polymer chain length, as long as the polymer is not too short (say, a few hundred segments). The critical adsorption energy for a particular polymer is defined here as the adsorption energy where the excess amount vanishes. The

critical adsorption energy of a large variety of linear and comb molecules can be determined from Fig. 8.

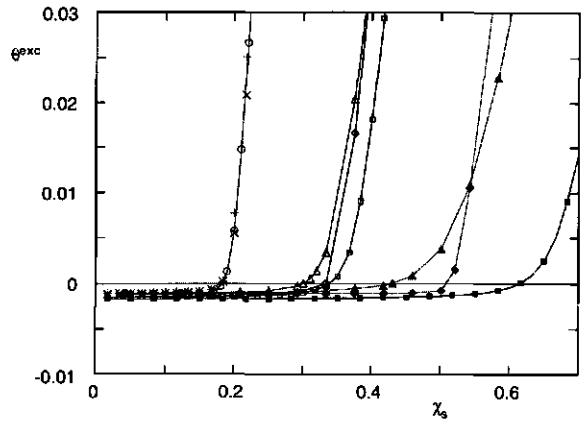

Figure 8. Critical adsorption energy for polymers varying in molecular architecture and adsorption energy. Open circles: linear polymer, N = 1555; pluses: $N_{b1} = N_b = 5$, $N_t = 25$, X = 50; crosses: $N_{b1} = 0$, $N_b = 5$, $N_t = 6$, X = 100. All segments have the same adsorption energy parameter χ_s, on the abscissa. Open triangles $N_{b1} = 0$, $N_b = 5$, $N_t = 6$, X = 100, tooth segments have the adsorption energy as indicated on the abscissa, backbone segments $\chi_s = 0$. Open diamonds: same as open triangles, but backbone segments have an adsorption energy, for all tooth segments $\chi_s = 0$. Open squares: multiblock copolymer, $(A_6B_6)_{100}$, A-block: $\chi_s = 1$, B block: $\chi_s = 0$. Filled triangles: $N_{b1} = N_b = 5$, $N_t = 25$, X = 50, outer 6 segments of teeth have an adsorption energy, for all other segments $\chi_s = 0$. Filled diamonds: $N_{b1} = N_b = 5$, $N_t = 25$, X = 50, backbone segments except b1 segments have an adsorption energy , for the tooth segments and b1 segments $\chi_s = 0$. Filled squares: multiblock copolymer $(A_6B_{25})_{50}$, A-block: $\chi_s = 1$, B block: $\chi_s = 0$. In all cases: athermal solvent, bulk volume fraction $\varphi^b = 10^{-4}$.

The open circles, pluses and crosses correspond to homopolymers: all segments have the same adsorption energy. The open circles represent the linear case, the crosses and pluses are for two different comb polymers. The molecular architecture turns out not to change the critical adsorption energy in the homopolymer case: for all molecules the critical value is 0.182 kT. This conclusion was also reached for the adsorption of ring polymers: the entropy difference per segment between rings and linear chains converges to zero in the limit of infinite chain length [2].

This situation changes drastically if copolymers are considered. Van Lent and Scheutjens [19] have shown that a random AB copolymer differing in adsorption energy adsorbing from an athermal solvent can be described by a homopolymer with effective adsorption energy:

$$\chi_s = \chi_{s,B} + \ln\left(\nu_B + \nu_A \exp\left(\chi_{s,A} - \chi_{s,B}\right)\right) \qquad (11)$$

with $\chi_{s,A}$ and $\chi_{s,B}$ the adsorption energy parameters of the A and B blocks, and ν_A or ν_B the fraction of A and B blocks, respectively. Using $\chi_{s,B} = 0$, $\nu_B = 1 - \nu_A$ and for χ_s the homopolymer critical adsorption energy In (6/5), we find for the critical adsorption energy for the A-blocks in a fully random copolymer:

$$\chi_{sc,A} = \ln\left(\frac{1+5\nu_A}{5\nu_A}\right) \qquad (12)$$

For a (long) diblock copolymer, the critical adsorption energy is almost equal to that of a homopolymer: at the point of desorption ($\theta^{exc} \approx 0$) the non-adsorbing block simply forms a long dangling tail that does not hinder the few adsorbed chains connected to the surface. If we divide up the adsorbing blocks so that we get a multiblock copolymer, the non-adsorbing blocks are always close to the adsorbing blocks. Hence, for the multiblock copolymer $(A_6B_6)_{100}$, shown in Fig. 8 in open squares, we find the value for the random copolymer with $\nu_A = 0.5$, namely 0.336. If we now imagine the non-adsorbing blocks of the multiblock as side chains on the adsorbing main chain we get the comb copolymer indicated with open diamonds, which turns out to have exactly the same threshold value. However, if the non-adsorbing blocks form the main chain and the tooth segments are adsorbing (open triangles), the critical adsorption energy is shifted towards a smaller value: a conformation with only a few (outer) tooth segments adsorbed leaves more entropy for the rest of the chain. Such a conformation is thus more favourable, and less energy is needed to get adsorption.
We can increase the length of the non-adsorbing block even further to 25 out of 31 segments in a repeating unit ($\nu_A = 0.19$), leading to the multiblock copolymer $(A_6B_{26})_{50}$, the filled squares in Fig. 8. The non-adsorbing spacings are so large here, that they can more easily move away from the surface as compared to a random copolymer, which leads to a lower value of the critical adsorption energy: about 0.61 instead of the random value 0.71. More interestingly, if we use the adsorbing blocks as the backbone for a comb copolymer and the long non-adsorbing block as the side chain (filled diamonds) the teeth can protrude into the solution, leading to an increase in entropy, and thus a lower critical adsorption energy. Lastly, it is even more

favourable to have only the last 6 segments of the long teeth able to adsorb (filled triangles).

comb copolymers

We have already discussed some aspects of comb copolymers in the last paragraph, around the desorption point. We concluded that it is more favourable to have adsorbing teeth, as this can lead to an extended conformation with only a few end segments on the surface and the rest of the molecule stretched out into the solution. In Fig. 9, we compare the volume fraction profiles of the same comb copolymers as in Fig. 8 at a higher adsorption energy of 1 kT for the adsorbing segments.

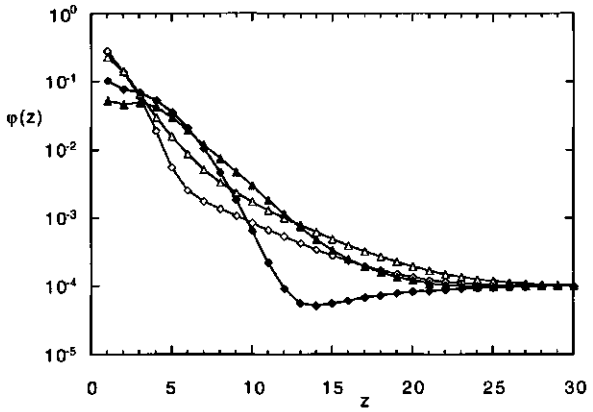

Figure 9: Volume fraction profiles for four of the polymers used in Figure 8 at χ_S = 1. Symbols as in Fig. 8.

The triangles correspond to adsorbing teeth, the diamonds to an adsorbing backbone, the open symbols to long polymers (X = 100) with short teeth (N_t = 6) and 600 adsorbing segments, the filled symbols to shorter chains (X = 50) with longer teeth (N_t = 25) and 300 adsorbing segments. It can be seen that more of the longer polymers is adsorbed: the ratio of adsorbing to non-adsorbing segments is more favourable. Also, longer teeth lead to thicker adsorbed layers. More interesting is the difference between an adsorbing backbone and adsorbing teeth: an adsorbing backbone (diamonds) leads to higher adsorbed amounts but thinner layers than adsorbing teeth. Basically, the non-adsorbing teeth only increase the typical "comb-behaviour" of backbone segments near the surface and the entropically favourable effect of having the teeth sticking out.

Conclusions

Upon increasing the number of end segments in polymer molecules by considering the series formed by ring polymers, linear polymers and comb polymers, we find that linear polymers are the most efficient in forming thick adsorbed layers. Ring polymers do not have any tails that can protrude into the solution, and comb polymers adsorb with the branch points preferentially on the surface. Comb polymers with long teeth and a small backbone spacing show a brush-like behaviour, with a depletion dip in the volume fraction profile immediately adjacent to the adsorbed layer. If the chemical species of the teeth and the backbone species differ, thicker layers are formed if the tooth segments have a higher adsorption energy than the backbone segments. However, the adsorbed amount is less in this case.

References

[1] J. M. H. M. Scheutjens, G. J. Fleer and M. A. Cohen Stuart, "End effects in polymer adsorption: a tale of tails" *Colloids Surf.* **21** (1986) 285.

[2] B. van Lent, J. M. H. M. Scheutjens and T. Cosgrove, "Self-consistent field theory for the adsorption of ring polymers from solution" *Macromolecules* **20** (1987) 366.

[3] IUPAC commission on macromolecular nomenclature, "Basic definitions of terms relating to polymers 1974" *Pure Appl. Chem.* **40** (1974) 479.

[4] P.-G. de Gennes, "Scaling concepts in polymer physics" (1979) Cornell University Press, Ithaca, N.Y.

[5] J. des Cloizeaux and G. Jannink, "Polymers in solution: their modelling and structure" (1990) Clarendon Press, Oxford.

[6] J. E. G. Lipson, "A Monte Carlo simulation study on long-chain combs" *Macromolecules* **24** (1991) 1327.

[7] A. Gauger and T. Pakula, "Static properties of noninteracting comb polymers in dense and dilute media. A Monte Carlo study" *Macromolecules* **28** (1995) 190.

[8] A. Shinozaki, D. Jasnow and A. C. Balazs, "Microphase separation in comb polymers" *Macromolecules* **27** (1994) 2496.

[9] D. Gersappe, P. K. Harm, D. Irvine and A. C. Balazs, "Contrasting the compatibilizing activity of comb and linear copolymers" *Macromolecules* **27** (1994) 720.

[10] R. Israëls, D. Foster and A. Balazs, "Designing optimal comb compatibilizers: AC and BC combs at an A/B interface" *Macromolecules* **28** (1995) 218.

[11] T. Pan and A. C. Balazs, "Interactions between linear polymers and amphiphilic combs in water: a molecular dynamics study" *Langmuir* **9** (1993) 3402.

[12] A. C. Balazs and C. P. Siemasko, "Contrasting the surface adsorption of comb and linear polymers" *J. Chem. Phys.* **95** (1991) 3798.

[13] M. Kawaguchi and A. Takahashi, "Ellipsometric study of the adsorption of comb-branched polystyrene onto a metal surface" *J. Polym. Sci., Polym. Phys. Ed.* **18** (1980) 943.

[14] J. M. H. M. Scheutjens and G. J. Fleer, "Statistical theory of the adsorption of interacting chain molecules. 1. Partition function, segment density distribution, and adsorption isotherms" *J. Phys. Chem.* **83** (1979) 1619.

[15] G. J. Fleer, M. A. Cohen Stuart, J. M. H. M. Scheutjens, T. Cosgrove and B. Vincent, "Polymers at interfaces" (1993) Chapman & Hall, London.
[16] F. A. M. Leermakers and J. M. H. M. Scheutjens, "Statistical thermodynamics of association colloids. I. Lipid bilayer membranes" *J. Chem. Phys.* **89** (1988) 3264.
[17] J. M. H. M. Scheutjens and G. J. Fleer, "Statistical theory of the adsorption of interacting chain molecules. 2. Train, loop, and tail size distribution" *J. Phys. Chem.* **84** (1980) 178.
[18] H. Hollenberg, "A tale of teeth." M.Sc. thesis, Wageningen Agricultural University (1994).
[19] B. van Lent and J. M. H. M. Scheutjens, "Adsorption of random copolymers from solution" *J. Phys. Chem.* **94** (1990) 5033.

CHAPTER V

Adsorption of polymers on heterogeneous surfaces

An extension of a self-consistent-field lattice theory is developed to study the adsorption of polymers on energetically heterogeneous surfaces. Surface heterogeneity is modelled by introducing distinguishable surface sites which differ in their interaction energy with polymer segments and solvent molecules. The probability for the polymer segments to meet a given kind of site depends on the distribution of the surface sites. In this chapter, the adsorption behaviour of polymers on a surface with adsorbing and non-adsorbing surface sites is studied. For homopolymers, we find that for high chain length and adsorption energy the adsorbed amount is higher on a surface with a random distribution of adsorbing surface sites as compared to a surface with a patchwise distribution, *i.e.*, where equal surface sites are grouped together. Block copolymers can segregate strongly on a patchwise distributed surface.

Introduction

In polymer adsorption theory, the surface is usually considered to be chemically homogeneous and smooth. However, in practice surface heterogeneity can play an important role in the adsorption characteristics. Therefore, efforts have been made to incorporate the effects of surface heterogeneity into existing polymer adsorption models. Two cases can be distinguished: physically heterogeneous (*i.e.*, rough) and chemically heterogeneous surfaces. Rough surfaces have been modelled as, *e.g.*, sinusoidal surfaces [1], fractal surfaces [2,3], and corrugated surfaces [4]. Chemical surface heterogeneity means that some types of surface site are preferred over others by (parts of) the adsorbing polymer. Odijk [5] and Andelman and Joanny [6] have modelled a chemically heterogeneous surface by taking the interaction between polymer and surface as a random variable. Recently, Joanny and Andelman have also considered the adsorption of polymers on soluble and insoluble surfactant monolayers, and on a periodically heterogeneous surface [7,8]. Balazs *et al.* [9,10] have used Monte Carlo techniques to investigate the influence of different distributions of adsorbing patches over the surface. Huang and Balazs [11] have used two-dimensional statistics to calculate volume fraction profiles of a block copolymer on a striped surface.

In this chapter we present a model that is, like the Huang and Balazs treatment, based on the self-consistent-field theory for polymer adsorption by Scheutjens and Fleer [12,13]. But in contrast to their approach we vary the average size of adsorbing patches on the surface by using neighbour probabilities for adjacent surface sites. In this way, it is possible to study the effects of site distribution on the adsorption behaviour of the polymer. Most of the calculations have been performed for homopolymers on a surface where only one out of two kinds of surface site has an attractive energetic interaction with the polymer segments. The model can be used analogously for block copolymers. One example of this type is given.

Theory

lattice

We introduce a simple cubic lattice with a characteristic length equal to the size of a solvent molecule. The surface is modelled as a flat wall divided into squares, the surface sites. This surface may contain different kinds of surface site, indicated by m, n, etc. The fraction of sites of type m is f_m, where $\sum_m f_m = 1$. Over the surface sites we place layers of cubes parallel to the surface, numbered 1 (at the surface) to M (in the bulk solution) (Fig. 1).

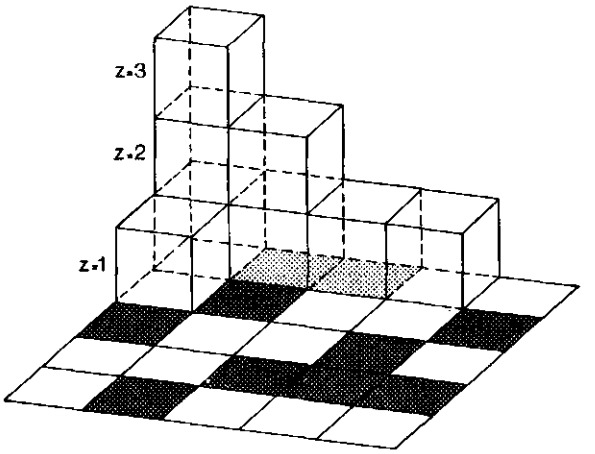

Figure 1. Schematic view of the surface and adjacent lattice. Two kinds of surface site are indicated by white and grey squares. A small number of lattice sites is drawn in the first three layers.

Each cube (lattice site) contains either a polymer segment or a solvent molecule. The volume fraction of a polymer i in layer z is denoted as $\varphi_i(z)$. If the polymer is a copolymer, $\varphi_i(z) = \sum_A \varphi_{Ai}(z)$ where $\varphi_{Ai}(z)$ is the contribution of segment type *A* to $\varphi_i(z)$. As surface heterogeneity can lead to an uneven distribution of polymer over the surface, we also need a separate volume fraction for every kind of site, $\varphi_A(z \mid m)$. The vertical bar is used because it is a conditional volume fraction: only the space above the m sites is considered. To fill the lattice, we need to have

$$\sum_A \varphi_A(z \mid m) = 1 \qquad (1)$$

for all z and m. In this summation the solvent is included.

surface

We define a neighbour probability M_{mn} as the probability that, coming from a site m, the next site on the surface is of type n. As this is a probability, we have

$$0 \le M_{mn} \le 1 \qquad (2)$$

and

$$\sum_n M_{mn} = 1 \tag{3}$$

The probability of finding first a site m and then a site n equals $f_m M_{mn}$. Summing over all sites m should give the *a priori* probability of finding a site n:

$$\sum_m f_m M_{mn} = f_n \tag{4}$$

Furthermore, the probability of finding a sequence mn should be equal to nm (inversion symmetry):

$$f_m M_{mn} = f_n M_{nm} \tag{5}$$

In the remainder of this section, we consider only two kinds of surface site. In this case, eq. (5) is not a new constraint, but it can be derived from eqs. (3) and (4).

To describe a surface with two kinds of surface site a cluster parameter C is defined:

$$C = M_{mm} - M_{nm} \tag{6}$$

With eq. (3) C can also be written as $1 - M_{mn} - M_{nm}$. With eq. 5 we find $C = 1 - (1 + f_n/f_m)M_{nm} = 1 - (1 + f_m/f_n)M_{mn}$. Since M_{nm} and M_{mn} are in between 0 and 1 we find for C the following constraints:

$$-\frac{f_m}{f_n} \le C \le 1 \qquad \text{and} \qquad -\frac{f_n}{f_m} \le C \le 1 \tag{7}$$

The minimum value of C, which only occurs if $f_n = f_m$, equals –1. In this case $M_{mm} = 0$ and $M_{nm} = M_{mn} = 1$, so that with every step we change from one type of surface site to the other. In other words, we have a *chequerboard* distribution (Fig. 2a). If C is close to unity, M_{mm} is much larger than M_{nm}, so equal surface types are grouped together (*patchwise* surface, Fig. 2c). For C = 0, we have $M_{mm} = M_{nm} = f_m$: there is no grouping nor avoiding of equal surface sites. We call this a *random* surface (Fig. 2b).

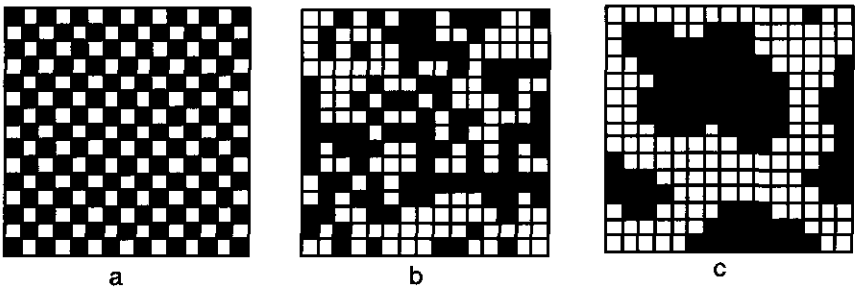

Figure 2. Schematic view of a surface with two kinds of site: (a) alternating surface (chequerboard): C = –1, (b) random surface (C = 0), (c) patchy surface (C positive).

polymer statistics

We define a free segment distribution function $G_A(z\,|\,m)$ which gives the relative preference of a free segment of type A to be in layer z above a site m with respect to the homogeneous bulk solution. This is a Boltzmann factor:

$$G_A(z\,|\,m) = \exp\left(-\frac{u_A(z\,|\,m)}{kT}\right) \tag{8}$$

where $u_A(z\,|\,m)$ is the potential of A in layer z above a site m, k is Boltzmann's constant, and T is the absolute temperature. The potential $u_A(z\,|\,m)$ is given by

$$u_A(z\,|\,m) = u'(z\,|\,m) + kT\sum_B \chi_{AB}\left(\langle\varphi_B(z\,|\,m)\rangle - \varphi_B^{bulk}\right) \tag{9}$$

Here, $u'(z\,|\,m)$ is the so-called "hard core potential", a Lagrange parameter ensuring that eq. (1) is satisfied. The second term on the right-hand-side accounts for all energetic interactions. It contains the Flory-Huggins interaction parameters χ_{AB} between segment types A and B. The expression between the angular brackets is the neighbour average of $\varphi_B(z\,|\,m)$, defined as:

$$\langle\varphi_B(z\,|\,m)\rangle = \frac{1}{6}\varphi_B(z-1\,|\,m) + \sum_n \frac{4}{6}M_{mn}\varphi_B(z\,|\,n) + \frac{1}{6}\varphi_B(z+1\,|\,m) \tag{10}$$

Note that the choice of a cubic lattice implies that contacts with segments on a different site can only occur within a layer z: segments in layers z–1 or z+1 are automatically situated above the same site. This simplifies the equations considerably. In the two-site case, the summation in eq. (10) contains only two terms: $\frac{4}{6}\{M_{mm}\varphi_B(z\,|\,m) + M_{mn}\varphi_B(z\,|\,n)\}$. For a homogeneous surface with

only sites of type m this middle term equals $\frac{4}{6}\varphi_B(z\,|\,m)$, and eq. (10) reduces to the standard Scheutjens and Fleer expression for the neighbour average. Adsorption energy is included in eq. (9) provided the surface sites m [with $\varphi_m(z\,|\,m) = 1$ for $z \leq 0$ and $\varphi_m(z\,|\,m) = 0$ for $z > 0$] are included in the summation over B. The adsorption energy contribution is only non-zero for z=1, and equals $\frac{1}{6}kT\chi_{Am}$.

Next, we define an end segment distribution function $G_{i,m}(z,s\,|\,1)$. This is the statistical weight of all walks of molecule i that start with segment 1 somewhere in the system and end after s–1 steps with segment s in layer z above a site m. For s =1 we get the monomer distribution function, which for monomers of type A reads:

$$G_{i,m}(z,1\,|\,1) = f_m G_A(z\,|\,m) \tag{11}$$

This expression just says that the probability for a monomer A to be in layer z above a site m is f_m times the probability to be in layer z for a homogeneous surface of only sites m (*i.e.*, when f_m=1). The distribution of all other segments in a chain molecule is obtained by taking into account the connectivity of the chain in a first order Markov approximation:

$$G_{i,m}(z,s\,|\,1) = G_i(z,s\,|\,m)\left(\begin{array}{l}\frac{1}{6}G_{i,m}(z-1,s-1\,|\,1)+\frac{1}{6}G_{i,m}(z+1,s-1\,|\,1)\\ +\sum_n \frac{4}{6}M_{nm}G_{i,n}(z,s-1\,|\,1)\end{array}\right) \tag{12}$$

where $G_i(z,s\,|\,m) = G_A(z\,|\,m)$ if segment s in molecule i is of type A. Starting at the other end of the chain, we obtain $G_{i,m}(z,s\,|\,N)$ in a similar way:

$$G_{i,m}(z,s\,|\,N) = G_i(z,s\,|\,m)\left(\begin{array}{l}\frac{1}{6}G_{i,m}(z-1,s+1\,|\,N)+\frac{1}{6}G_{i,m}(z+1,s+1\,|\,N)\\ +\sum_n \frac{4}{6}M_{nm}G_{i,n}(z,s+1\,|\,N)\end{array}\right) \tag{13}$$

with the starting condition: $G_{i,m}(z,N\,|\,N) = f_m G_A(z\,|\,m)$, analogous to eq. (11). Combining the two end segment distribution functions computed from eq. (12) and (13) and summing over all segments s, we find the volume fraction of polymer i in layer z that is above a site m:

$$\varphi_{i,m}(z) = C_i \sum_s \frac{G_{i,m}(z,s \mid 1) G_{i,m}(z,s \mid N)}{f_m G_i(z,s \mid m)} \qquad (14)$$

Dividing by $f_m G_i(z,s \mid m)$ is necessary to correct for double counting of segment s. The normalisation constant C_i can be found from the equilibrium volume fraction φ_i^{bulk} of molecules i in the bulk solution:

$$C_i = \frac{\varphi_i^{bulk}}{N_i} \qquad (15)$$

The adsorbed amount θ^a is calculated from the volume fraction profile by considering only the polymer chains that have at least one segment in the first layer. It is expressed in equivalent monolayers (= segments per site).

The free segment distribution functions $G_A(z \mid m)$ can be found from the volume fraction profiles using eqs (8) and (9). On the other hand, the volume fraction profiles are found from the free segment distribution functions by eqs (11)-(14). Also, eq. (1) (volume constraint) has to be fulfilled. An iterative procedure is used to find a self-consistent solution, where the number of iteration variables equals the number of free segment distribution functions. This number is the product of the number of layers, the number of types of site and the number of monomer types.

Results and discussion

homopolymers

In this section we show results of calculations for a homopolymer adsorbing on only one out of two or three kinds of surface site. The polymer segments are called A, the solvent is indicated by o. We use two solvency situations: an athermal solvent (Flory-Huggins parameter χ_{Ao}= 0) and a "Θ-solvent" (χ_{Ao}= 0.5). The parameter χ_{om} (where o denotes the solvent) is taken to be zero as only the difference $\chi_{Am} - \chi_{om}$ is important. To facilitate the comparison with standard homopolymer theories we use a Silberberg χ_s parameter for the adsorption energy. The χ_s parameter can be found from the Flory-Huggins parameter χ_{Am} by dividing by –6. Note that χ_s is positive if the adsorption energy is negative. The adsorption energies per site are then $\chi_{s,m}$ and $\chi_{s,n}$.

We start by taking only two kinds of surface site. The cluster parameter C represents the distribution of lattice sites over the surface. As can be seen from eq. (7), maximum variation of C is possible if we take f_m= f_n= 0.5. The

sites of type m are taken to be repelling, those of type n adsorbing, such that the average is 0 ($\sum_m \chi_{Am} = \sum_m f_m \chi_{Am} = 0$).

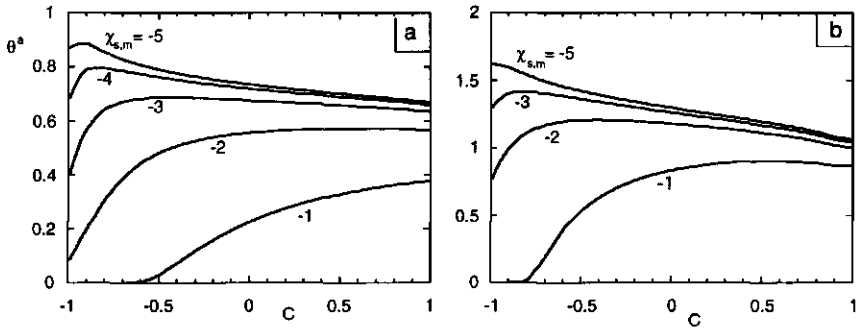

Figure 3. Adsorbed amount of a homopolymer with 1000 segments on a surface with two kinds of site as a function of the clustering parameter C. The fraction of adsorbing sites is 0.5, and the bulk volume fraction of polymer is 0.0001. The values of χ_s on non-adsorbing sites are indicated, and χ_s on the adsorbing sites equals $-\chi_s$ on the non-adsorbing sites. Diagram (a) is for an athermal solvent ($\chi_{Ao} = 0$), diagram (b) for a theta solvent ($\chi_{Ao} = 0.5$).

In Figure 3a the adsorbed amount is shown as a function of C in an athermal solvent. The polymer will try to adsorb on the adsorbing sites with as many segments as possible. On a chequered surface (C = −1) there is an unfavourable repelling site adjacent to each adsorbing site. For χ_s = +/− 1, the energetic interaction with the adsorbing sites is not high enough to compensate for the entropy loss that accompanies adsorption: the polymer is depleted from the wall. With increasing degree of clustering the polymer can adsorb on the favourable surface sites without having too many segments on the repelling sites, so that adsorption can occur. This effect leads to an increasing dependence of the adsorbed amount on C. For C close to unity the adsorbed amount is about half the value that is found for a homogeneous surface with an adsorption energy of 1 kT, because then the repelling sites hardly contribute to the adsorption behaviour. Thus, by only changing the distribution of sites we can change the surface from non-adsorbing to adsorbing.

For higher absolute values of the adsorption energies, adsorption even occurs on an alternating surface. Here, enough energy is gained on adsorbing sites to compensate for the segments that are on the repelling sites. If the degree of clustering increases the polymer avoids the repelling sites, so that

eventually, for C close to 1, only half the surface is used. This effect leads to a decreasing dependence of the adsorbed amount on C. For intermediate values of the adsorption energy these two compensating effects cause a maximum.

Figure 3b is similar as Fig. 3a but for theta-conditions (χ = 0.5). The non-adsorbing sites are now slightly less unfavourable than in the athermal case: in the first layer, the polymer has $\frac{1}{6}$ less possible unfavourable contacts with the solvent compared to the bulk solution. This causes the maximum to shift towards lower values of C. Adsorption on a heterogeneous surface without a net interaction has also been found by Odijk [5] and Andelman and Joanny [7,8].

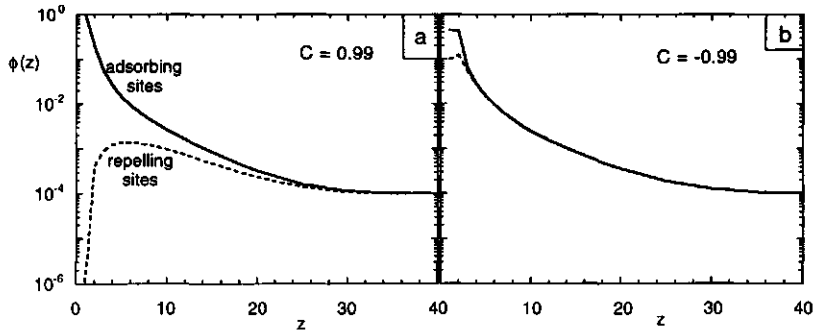

Figure 4. Volume fraction profiles taken from points in the curve in Fig. 3a where χ_s (adsorbing sites) = 4 for a patchy surface with C = 0.99 (a), and for a chequerboard surface with C = −0.99: (b).

The difference between adsorption on an alternating and a patchy surface can be seen clearly in Fig. 4, where the volume fraction profiles per kind of site are plotted for circumstances as in Fig. 3a (athermal solvent), for the curve with $\chi_{s,n} = -\chi_{s,m} = 4$ and two widely different values of C. Fig. 4a shows the volume fraction profiles on the adsorbing sites (full curve) and on the repelling sites (dotted curve) for a very "patchy" surface (C = 0.99). The adsorbing sites are almost completely filled with polymer ($\varphi(1) \approx 1$), whereas the repelling sites show a depletion in the first layer ($\varphi(1) < \varphi^{bulk}$). Fig. 4b shows the other extreme: C = −0.99 or a chequerboard surface. The adsorbed amount is almost the same as in Fig. 4a, but the profiles are completely different (note the different vertical scales): on the adsorbing sites the first layer is only half filled, but the most striking difference is the significant amount of polymer that is adsorbed on the repelling sites despite the unfavourable energetic interaction.

Odijk [5] and Andelman and Joanny [6] have studied the interaction of homopolymers with a random surface, where the interaction energy between polymer segments and surface sites is a random variable with zero mean and varying standard deviation. They both find that adsorption can take place although the average interaction is too low to justify net adsorption. According to Odijk the adsorption should decrease with increasing variance of the interaction energy whereas Andelman and Joanny find the opposite. To model this system in our scheme, we would need a very large number of types of surface site, which is not feasible. However, some insight can be obtained with three kinds of surface site, where the first and third site have an equal probability (*i.e.* $f_1 = f_3$) but an opposite sign of the adsorption energy ($\chi_{s,1} = -\chi_{s,3} = -1$). The remaining kind of site has a χ_s of 0, so that the average adsorption energy is exactly 0 kT. Using standard statistical theory, the variance is now defined as $\sigma^2 = \sum_m (\chi_{s,m})^2 f_m$, which in this simple case reduces to $2f_1$.

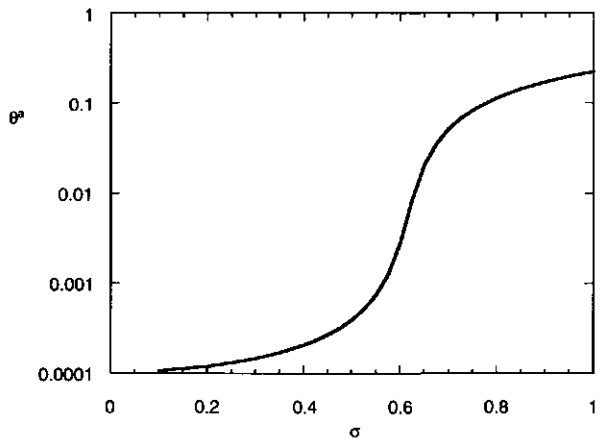

Figure 5. Adsorbed amount as a function of the width of the distribution. The surface was considered to consist of three kinds of site, with $\chi_s = -1$, 0 and 1, respectively, and an equal fraction of adsorbing and repelling sites. The width is plotted as the standard deviation σ. The solvent is athermal ($\chi_{As} = 0$). Other parameters as in Fig. 3.

By plotting the adsorbed amount as a function of σ (Fig. 5) we see that the adsorption increases with increasing standard deviation. If σ = 0 we have a homogeneous surface containing only sites with $\chi_s = 0$, so there can be no adsorption. By increasing σ, we create adsorbing sites. The higher σ is, the higher the adsorption energy of the adsorbing sites. If the adsorption energy of the adsorbing sites is high enough, the polymer will stick. This result agrees with that of Joanny and Andelman. Although it is a rather crude approximation

to model a Gaussian distribution using only three kinds of site, there is no reason to believe that the trends will change much if more kinds of site are taken into account.

In the remainder of this chapter, we restrict ourselves to only two kinds of site. In this case we can describe the distribution of surface sites by the cluster parameter C. The more extreme the ratio between the sites is, the smaller the possible range for C. However, any value for $0 \leq C \leq 1$ is always possible. We have taken two values for C: C = 0, a random surface and C = 0.95, a patchy surface. The results are compared with those for a homogeneous surface. A homogeneous surface is defined as a smooth surface with only one kind of surface site. The value of χ_s is taken as a weighted average of the adsorption energy on the surface sites in the heterogeneous case, *i.e.*, $\chi_s = \sum_m f_m \chi_{s,m}$.

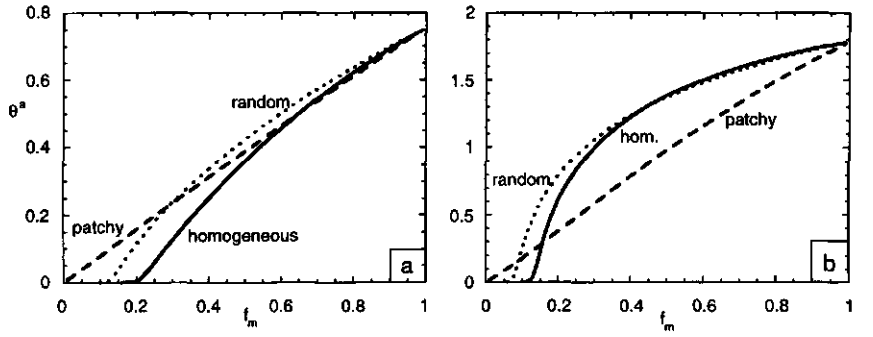

Figure 6. Adsorbed amount as a function of the fraction adsorbing sites on a random surface (dotted curve, C = 0) and on a patchy surface (dashed, C = 0.95). On adsorbing sites $\chi_s = 1$, on non-adsorbing sites $\chi_s = 0$. A curve for a homogeneous surface is also shown for comparison (full curve). In this curve, χ_s is taken as the independent variable and equals $f_m\chi_{s,m}$. Diagram (a) : athermal solvent ($\chi_{Ao} = 0$), (b): theta solvent ($\chi_{Ao} = 0.5$). The polymer has a chain length of 1000 and a bulk volume fraction of 10^{-4}.

Figure 6 shows the adsorbed amount as a function of the fraction of adsorbing sites f_m. We see that for a patchy surface the adsorption is almost proportional to the fraction of adsorbing sites (for C = 1 the plot would be linear). For a random surface there is no adsorption for small values of f_m. In this case the polymer is depleted for $f_m < 0.12$ because the entropy loss is greater than the energy gain upon adsorption. Note that, like in Figs. 3 and 5, adsorption can take place on a heterogeneous surface before the average adsorption energy exceeds the critical value, which is 0.182 kT for a cubic lattice [12]. For a Θ-solvent (Fig. 6b) the adsorption on a patchy surface is in

most cases even less than on a corresponding homogeneous surface. All other trends are the same as in the athermal case.

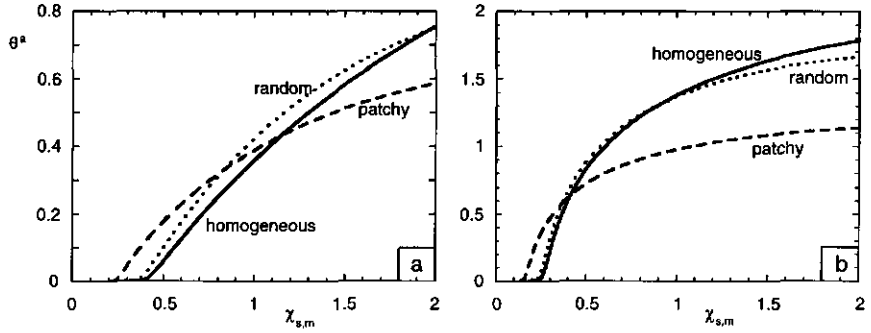

Figure 7. Adsorbed amount as a function of the adsorption energy of the adsorbing sites. The fraction of adsorbing sites is 0.5. The dotted curves are for a random surface (C = 0), the dashed curves for a patchy surface and the full curves apply to a homogeneous surface with $\chi_s = f_m\chi_{s,m}$. Other parameters as in Fig. 6.

Fig. 7 shows the dependence of the adsorbed amount on the adsorption energy χ_s for a good solvent (a) and a Θ solvent (b). It shows the same trend as in Fig. 6: adsorption occurs first on a patchy surface, because the polymer can use the adsorbing sites more effectively. With increasing adsorption energy, adsorption will also take place on a random surface as soon as the energy gained on the adsorbing sites is enough to compensate the entropy loss on the adsorbing as well as on the non-adsorbing sites. For high adsorption energies, there will be more polymer on a random surface because the non-adsorbing sites are occupied to a greater extent than on a patchy surface. For even higher values of χ_s, the curves for a random heterogeneous surface and a homogeneous surface intersect: less polymer is adsorbed on the heterogeneous surface because of the unfavourable interaction with non-adsorbing sites so that the first layer is less filled.
For chains of increasing length one could expect surface heterogeneity to be averaged out so that the curves for a random surface and a homogeneous surface would coincide for a long enough chains. However, for a homogeneous surface it has been shown [12] that for a chain length more than, say, 100, the occupation of the first layer does not increase any more. Any increase in the adsorbed amount is then purely due to the formation of longer loops and tails.

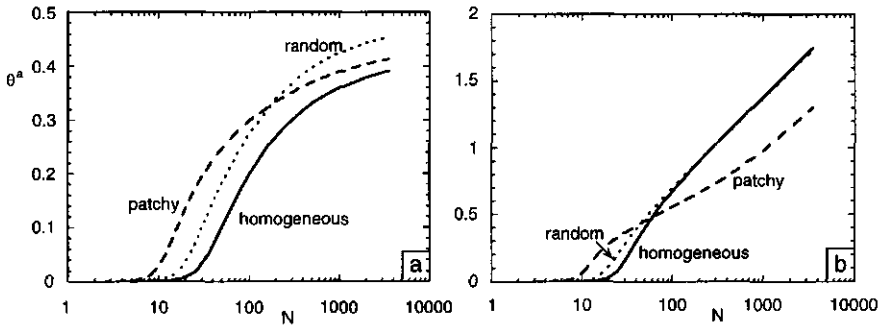

Figure 8. Adsorbed amount as a function of the chain length N of the polymer. The fraction of adsorbing sites is 0.5, the other parameters are the same as in Figure 6.

The chain length dependence is plotted in Fig. 8: for short chains we see that, like in the Figures 6 and 7, adsorption occurs first on a patchy surface, then on a random surface, and finally on a homogeneous surface. At high molecular weight the curve for a patchy and a random surface cross (both in Figs. 8a and 8b) because of the smaller useful surface area in the former case. Under the circumstances of Fig. 8a (good solvent) the curves for a random surface and for a homogeneous surface do not meet: the difference in adsorbed amount (about 0.06 monolayers for $N > 1000$) is situated in the layers closest to the wall, and this will not be altered with increasing chain length. However, for a Θ-solvent (Fig. 8b), where the occupation in the first layer is much higher, the influence of the surface is already smoothed out at relatively small chain length so that the curves coincide for longer chain lengths.

As a last example for homopolymer adsorption we calculate a displacement isotherm, like the ones calculated by Van der Beek *et al.* [14,15]. In a displacement isotherm, the polymer is dissolved in a binary mixture of solvent and displacer (a component which adsorbs more strongly than the polymer). If the displacer concentration is high enough, the polymer is desorbed from the surface. The point where the polymer is fully desorbed is called the critical displacer concentration or critical solvent strength. This concentration can be used to determine the difference in adsorption energy of a polymer segment and a solvent molecule, *i.e.*, χ_s. In the paper referred to above, the authors raise the question whether the method is justified in the case of surface heterogeneity. As can be seen from Fig. 9, the influence of surface heterogeneity is not very large: the shift in the critical displacer concentration is < 1 vol %, which is less than the experimental error. However, from this plot

we can conclude that the polymer is more weakly attached on a random surface than on a homogeneous surface (less displacer is needed to displace the polymer) but more strongly on a patchy surface. Hence, surface heterogeneity can give both a higher value than a homogeneous surface, as a lower one.

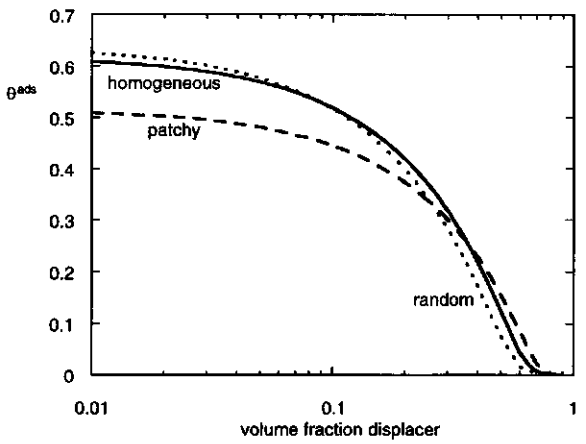

Figure 9. Displacement isotherm for a polymer on a random heterogeneous surface (C = 0, dotted curve), on a patchy surface (C = 0.95, dashed) and on a homogeneous surface full curve). The displacer d is monomeric ($N_d = 1$). The polymer has 100 segments, and the equilibrium volume fraction in the bulk $\varphi_A^b = 0.001$. The mixture is athermal ($\chi_{Ao} = \chi_{Ad} = \chi_{do} = 0$). The fraction of adsorbing sites is 0.5. The adsorption energies on adsorbing sites are 1.9 kT for the polymer and 1.88 kT for the displacer. On the non-adsorbing sites all adsorption energies are zero. For the homogeneous surface χ_s = 0.95 for the polymer and $\chi_s = 0.94$ for the displacer.

copolymers

For copolymers, the number of parameters increases drastically, which makes the choice for a representative system difficult. As an example, we first reproduce the results for one of the systems Huang and Balazs used in their paper in ref. [11] and then compare it with our model. As stated before, the Huang and Balazs model is two-dimensional: the sites are grouped in stripes on the surface, so that the volume fraction is now a function of position x on the surface as well as of the distance from the surface z. For x=1 to 4 we have sites m , for x=5 to 8 sites n. By placing a reflecting boundary between x=0 and 1 and between x=8 and 9 we only need to calculate 8 x-values for every layer z. For periodic boundaries 16 x-values would have been necessary. In this way, we model a system with stripes of 8 consecutive

lattice sites of the same kind: sites m for x=–3 to +4, sites n for x=5 to 12. In the y-direction a mean-field approximation is used.

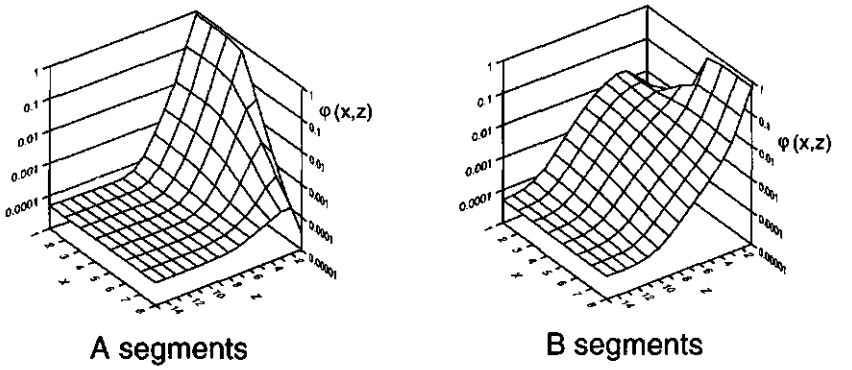

Figure 10. Volume fraction profiles calculated for a copolymer A_{25} B_{25}, $\varphi^b = 10^{-4}$ in solvent o with the Huang and Balazs method [11] using a two-dimensional striped surface. The left diagram gives the results for the A segments, the right one is for the B segments. The wall is located at z = 0. For x = 1-4 we have sites m, for x= 5-8 sites n. A reflecting boundary is placed between x=0 and x=1, and between x=8 and x=9. A mean field approximation is applied in the y-direction. Flory-Huggins parameters: $\chi_{AB} = \chi_{Ao} = 0.5$, $\chi_{Bo} = 0$, with the surface: $\chi_{Am} = \chi_{Bn} = -10$, $\chi_{An} = \chi_{Bm} = 0$.

In the system, we have an $A_{25}B_{25}$ copolymer in solvent o. The interaction parameters are $\chi_{AB} = 0.5$, $\chi_{Ao} = 0.5$ and $\chi_{Bo} = 0$. These values are too low to give micelles in solution. We took the bulk volume fraction of the polymer to be 10^{-4}. The A blocks adsorb on the sites m, the B's on the sites n : $\chi_{Am} = \chi_{Bn} = -10$, $\chi_{An} = \chi_{Bm} = 0$.

A view of the volume fraction profile distribution is shown in Fig. 10, where the A segments are plotted in Fig. 10a and the B segments in 10b. It can be seen that the volume fractions show a gradual transition at the boundary between the sites of type m or n (*i.e.* between x = 4 and x = 5). In Fig. 11 we compare the profiles in the middle of the stripes (*i.e.*, in layer 1 for the sites of type m and in layer 8 for the sites n, triangles), with our model for a patchy surface (C = 0.95, squares). The profiles on the sites m are shown in open symbols, those on the sites n in filled symbols. The two profiles for A segments on sites m coincide, but on the sites n our model tends to show less depletion. The profiles for the B segments are in good agreement with the two-dimensional model (note the logarithmic scale).

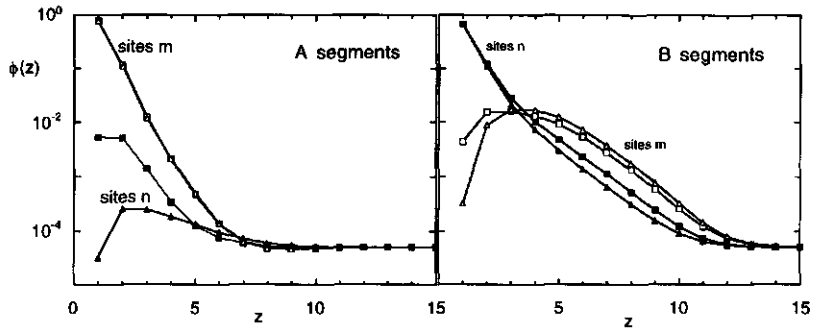

Figure 11. Comparison of volume fraction profiles calculated using the Huang and Balazs model (triangles) and our model (squares). The open triangles are for x = 1 (middle of the stripes with sites m), the closed triangles for x = 8 (middle of the stripes with sites n). For our model, we used the same interaction parameters as in Fig. 10, fraction m-sites 0.5, cluster parameter C = 0.95. Open squares: on sites m, closed squares: on sites n.

The advantage of the two-dimensional model is that information can be gained on the interface between the two kinds of site, which is impossible in our model. However, the geometry is limited: only stripes can be modelled (or, in a cylindrical lattice, circles), which does not seem very realistic on this scale. A random surface cannot be dealt with in this way. Furthermore, only small systems can be modelled as the number of iteration variables increases as the number of layers in the x-direction times the number of layers in the z-direction times the number of monomer types. Our model uses a separate mean-field potential for every kind of lattice site in every layer. This can be further reduced by taking only one mean field potential per layer for $z > z'$, where z' is not too large. As the potentials above different kinds of sites converge for much smaller z than the end segment distribution functions, this is not a severe approximation. The use of proper chain statistics ensures that the information about the surface structure is passed on into the solution. This leads to a significant reduction of the number of iteration variables, facilitating the calculation on longer chains or a broader distribution of surface sites.

Conclusions

It is possible to model chemical surface heterogeneity even using a mean-field approximation. Homopolymers can adsorb on a heterogeneous surface if the average energetic interaction with the surface is below the critical adsorption energy. This can happen more easily if the heterogeneity is distributed patchwise than when its distribution is more random. Long polymer

chains do not necessarily average out all surface heterogeneity. Adsorption is usually higher on a patchy surface than on a randomly distributed surface if the adsorption energy or chain length is low, but the opposite holds for high adsorption energy or chain length. For a patchy surface, adsorption is limited to the adsorbing patches. Displacement isotherms for homopolymers are not shifted dramatically by surface heterogeneity, regardless of distribution. The model can also be used for block copolymers on heterogeneous surfaces.

References

[1] D. Hone, H. Ji and P. A. Pincus, "Polymer adsorption on rough surfaces I: Ideal long chain" *Macromolecules* **20** (1987) 2548.

[2] M. Blunt, W. Barford and R. Ball, "Polymer adsorption and electron binding on rough and fractal surfaces" *Macromolecules* **22** (1989) 1458.

[3] J. F. Douglas, "How does surface roughness affect polymer-surface interactions?" *Macromolecules* **22** (1989) 2548.

[4] A. C. Balazs, K. Huang and C. W. Lantman, "Adsorption of triblock copolymers on rough surfaces" *Macromolecules* **23** (1990) 4641.

[5] T. Odijk, "Adsorption of a polymer to a randomly interacting surface" *Macromolecules* **23** (1990) 1875.

[6] D. Andelman and J.-F. Joanny, "On the adsorption of polymer solutions on random surfaces: the annealed case" *Macromolecules* **24** (1991) 6040.

[7] D. Andelman and J.-F. Joanny, "Polymer adsorption on surfactant monolayers and heterogeneous solid surfaces" *J. Phys. II (France)* **3** (1993) 121.

[8] J.-F. Joanny and D. Andelman, "Adsorption of polymer solutions on heterogeneous surfaces" *Makromol. Chem., Macromol. Symp.* **62** (1992) 35.

[9] A. C. Balazs, M. C. Gempe and Z. Zhou, "Polymer adsorption on chemically heterogeneous substrates" *Macromolecules* **24** (1991) 4918.

[10] A. C. Balazs, K. Huang, P. McElwain and J. E. Brady, "Polymer adsorption on laterally heterogeneous surfaces: a Monte Carlo computer model" *Macromolecules* **24** (1991) 714.

[11] K. Huang and A. C. Balazs, "Modelling copolymer adsorption on laterally heterogeneous surfaces" *Phys. Rev. Lett* **66** (1991) 620.

[12] J. M. H. M. Scheutjens and G. J. Fleer, "Statistical theory of the adsorption of interacting chain molecules. 1. Partition function, segment density distribution, and adsorption isotherms" *J. Phys. Chem.* **83** (1979) 1619.

[13] O. A. Evers, J. M. H. M. Scheutjens and G. J. Fleer, "Statistical thermodynamics of block copolymer adsorption. 1. Formulation of the model and results for the adsorbed layer structure" *Macromolecules* **23** (1990) 5221.

[14] M. A. Cohen Stuart, G. J. Fleer and J. M. H. M. Scheutjens, "Displacement of polymers. 1. Theory. Segmental adsorption energy from polymer desorption in binary solvents" *J. Colloid Interface Sci.* **97** (1984) 515.

[15] G. P. van der Beek, M. A. Cohen Stuart, G. J. Fleer and J. E. Hofman, "A chromatographic method for the determination of segmental adsorption energies of polymers. Polystyrene on silica" *Langmuir* **5** (1989) 1180.

SUMMARY

The work presented in this thesis is based on the theory for polymer adsorption by Scheutjens and Fleer (SF). Roughly, the thesis can be divided into two parts: the first two chapters consider the original theory from a new viewpoint, attempting to find universal laws and to establish connections with analytical theories. The last three chapters are devoted to extensions of the theory to more intricate systems.

In chapter 1 polymer adsorption from dilute solution is studied. We try to find the universal behaviour in the volume fraction profile as predicted by De Gennes from scaling arguments. In this analysis, three regimes are distinguished: close to the surface a *proximal regime*, which is dominated by the numerous contacts between polymer and surface, next to that a *central regime*, where the volume fraction profile decays as a power law which is independent of solution concentration and polymer chain length, and finally a *distal regime* with an exponential decay towards the bulk volume fraction. With the SF theory these regimes can indeed be found provided the polymer chains are sufficiently long (more than, say, 5000 segments). However, the exponent in the power law regime does depend on solution concentration and polymer chain length. Extrapolation to infinite chain length yields the proper mean-field exponent. Although in general mean-field theories (like the SF theory) can yield incorrect exponents, they tend to predict the proper trends, so that it can be expected that a chain length dependence is actually present. In Θ-solvents, where the mean-field treatment is thought to be exact because the second virial coefficient vanishes, an additional regime is found in between the central and distal regime. Its origin is, as yet, unclear.

The volume fraction profile is also the main topic in chapter 2, which discusses polymers adsorbing from a semi-dilute solution in a good solvent. In a semi-dilute solution the correlation length is independent of chain length, and it is found that this correlation length and the adsorption energy are the only parameters determining the volume fraction profile. Thus, in contrast to the case of dilute solutions in chapter 1, the profile for adsorption from semi-dilute solutions is independent of the polymer chain length. The free energy equation derived by SF is shown to be equivalent to that obtained in analytical mean-field theories if it is assumed that all segments of a polymer chain are distributed within the system in a similar way. Such

an assumption is called a ground-state approximation. This ground-state approximation can also be used to extract the adsorbed volume fraction profile (comprising only the polymer chains touching the surface) from the overall profile. This has been done by Johner *et al.* Their results compare well with SF calculations when the bulk concentration is high and the adsorption energy low, but the agreement is much less when this is not the case, possibly due to the larger influence of tails under these conditions. When a bidisperse polymer mixture adsorbs from a semi-dilute solution the overall profile is not affected, even though the individual components may show a very different profile.

In chapter 3 we leave the case of simple flexible homopolymers and consider the influence of partial rigidity within the chain. Rigid polymers possess less conformational entropy, and hence adsorb more easily than flexible polymers. Chain stiffness is modelled by excluding direct backfolding and defining an energy difference between a straight and a bent conformation of two consecutive bonds, where the straight conformation is more favourable. When all parts of the polymer are equally stiff, a persistence length can be defined, which increases with the energy difference. Using this persistence length, the radius of gyration of a stiff polymer in solution can be rescaled to a flexible one with a smaller number of segments. However, it turns out that this procedure does not work out well for adsorption from dilute solution: the scaling laws in the central regime as found in chapter 1 are altered. The critical adsorption energy decreases with increasing persistence length, in full agreement with an equation formulated by Birshtein, Zhulina and Skvortsov. The situation gets complicated when only part of the polymer is stiff. As the stiffer parts lose less entropy upon adsorption, they adsorb preferentially. This effect leads to copolymer adsorption behaviour, even when there is no difference in interaction energy between the stiff and the flexible moieties.

Entropic effects play a major role also in chapter 4, where the adsorption of comb polymers is considered. Comb polymers consist of a backbone and a (large) number of teeth, hence they have a large number of chain ends per molecule. These ends prefer to protrude into the solution to form dangling tails. As a result, combs tend to adsorb in a conformation where the backbone is preferentially on the surface and the teeth stick out. This leads to relatively thin adsorbed layers, and if the distance between the branch points of the comb is small compared to the tooth length a depletion zone develops adjacent to the adsorbed layer. For comb copolymers it is found

that if the teeth adsorb preferentially over the backbone segments the critical adsorption energy is lower than in the case where the backbone adsorbs, even though both types of molecules have the same number of adsorbing segments. At the point of desorption only a few segments are on the surface, and a polymer in which only the tooth segments adsorb loses less entropy than a polymer adsorbing with its backbone.

Finally, in chapter 5 we consider chemical surface heterogeneity by incorporating in the chain statistics a probability that a surface site has a particular adsorption energy. The surface can be constructed such that, on average, no energetic interaction between the polymer and the surface is present. Nevertheless, adsorption can take place on such a surface, provided "adsorbing sites" (sites with a favourable adsorption energy) are grouped together. The distribution of adsorbing sites determines largely the adsorption behaviour. If the driving force for adsorption is high, more polymer adsorbs on a surface with an equal distribution of adsorbing sites, as more of the available surface can be used. On the other hand, at low adsorption energy, it is more favourable to have the adsorbing sites group together, so that little of the non-adsorbing sites are in contact with the polymer.

In conclusion, universal behaviour is found only in the case of flexible, linear homopolymers adsorbing from a semi-dilute solution in a good solvent. In all other cases studied (dilute solutions, chain rigidity, chain branching and surface heterogeneity) the structure is more intricate. Although the mean-field character of the Scheutjens-Fleer theory is definitely a serious approximation, it does enable the modelling of a large variety of equilibrium systems, even at high concentrations, providing an abundance of detailed information. It is worthwhile to continue to check its assumptions and predictions with other theories and obviously with experiment. The volume fraction profile determines the properties of the system and is also very sensitive to the approximations used in the model. Therefore, precise and unambiguous measurements of the density profile remain of the utmost importance.

SAMENVATTING

Het woord "polymeer" is afgeleid uit het Grieks en betekent zoveel als: bestaande uit vele onderdelen. Polymeren worden gemaakt door hun onderdelen, de monomeren, onderling te laten reageren zodat grote, lange moleculen ontstaan. De chemische structuur van de monomeren bepaalt welk polymeer er gevormd wordt en dat is soms aan de naam te zien: polystyreen (PS, piepschuim) ontstaat uit styreen, polyetheen (PE, plastic tasjes) uit etheen. Bij andere polymeren is de naam wat minder duidelijk: polyetheentereftalaat (PET, frisdrankflessen) ontstaat uit ftaalzuur en glycol, rubber uit (bijvoorbeeld) isopreen, eiwitten uit aminozuren en zetmeel uit suikers. Als lange polymeermoleculen in een vloeistof opgelost worden, lijken ze nog het meest op gare spaghetti in kokend water: lange slierten die driftig bewegen. Voor de beschrijving van zo'n systeem blijkt het niet zoveel uit te maken welk polymeer we hebben, als het maar lang en flexibel is, geen zijtakken heeft en goed oplost. (Uitzonderingen hierop zijn biologisch aktieve eiwitten, die op een heel speciale manier opvouwen tot een compacte vorm. Die vorm is vaak belangrijk voor hun werking.) De specifieke eigenschappen van flexibele polymeren kunnen dan beschreven worden met slechts enkele parameters, zoals de kwaliteit van het oplosmiddel (hoe goed lost het polymeer op), de ketenlengte (hoe lang is het polymeer) en de concentratie (hoeveel polymeer per liter). Als de concentratie van het polymeer zo hoog wordt dat de slierten met elkaar verstrengeld raken spreken we van een semi-verdunde oplossing, en dan maakt het zelfs niet meer uit hoe lang de polymeerketens zijn. Dit noemen we universeel gedrag, en dat is waar we in de eerste twee hoofdstukken van dit proefschrift naar op zoek zijn. De laatste drie hoofdstukken zijn gewijd aan verschillende omstandigheden die voor speciale effecten zorgen. Al het werk is theoretisch van aard en gebaseerd op de theorie van Scheutjens en Fleer voor polymeeradsorptie, verder SF-theorie genoemd.

Adsorptie is ophoping aan een grensvlak en in dit proefschrift is het grensvlak altijd een vast oppervlak. Experimentele systemen die men zich hierbij kan voorstellen zijn bijvoorbeeld solen: systemen waarin vaste deeltjes fijn verdeeld zijn in een vloeistof, zoals latexverf. Aan dit soort systemen wordt vaak polymeer toegevoegd dat op de deeltjes gaat zitten. Dit noemen we adsorptie. Als de omstandigheden goed gekozen worden,

kan het toevoegen van polymeer voorkomen dat de deeltjes gaan klonteren en daardoor hetzij naar de bodem zakken, hetzij opromen, al naar gelang het verschil in dichtheid tussen de deeltjes en de vloeistof.
In het eerste hoofdstuk beschouwen we de adsorptie van polymeren uit een verdunde oplossing. In een verdunde oplossing is de concentratie polymeer zo laag, dat de individuele moleculen elkaar uit de weg gaan en geïsoleerde kluwens vormen. Als het polymeer een gunstige energetische wisselwerking met het oppervlak heeft, die groot genoeg is om het verlies aan vrijheid (entropie) in de oplossing te compenseren, dan ontstaat er een concentratiegradiënt van het polymeer loodrecht op het oppervlak: het volumefraktieprofiel. In het geval van adsorptie is het volumefractieprofiel een dalende functie van de afstand tot het oppervlak. (De energie die nodig is om nèt adsorptie te krijgen, heet de kritische adsorptie-energie. Dit begrip zullen we in latere hoofdstukken nog vaker tegenkomen.) Er is een theorie van De Gennes die zegt dat het volumefraktieprofiel te verdelen is in drie stukken. Vlak bij het oppervlak is de concentratie hoog. Het precieze verloop van de concentratie is daar sterk afhankelijk van het gebruikte polymeer, van het oppervlak, enzovoorts. Dit is het zogenaamde *proximale* gebied. Een stukje verderop verloopt de concentratie als een machtswet van de afstand tot het oppervlak. Dit is het *centrale* gebied, en hier voorspelt De Gennes universeel gedrag: de plaatselijke concentratie hangt niet af van de lengte van het polymeer of van de concentratie in de evenwichtsoplossing (de bulkconcentratie). In het laatste stuk, het *distale* gebied, valt het profiel exponentieel af naar de evenwichtsconcentratie die ver van het oppervlak heerst. Als we met de SF-theorie het volumefraktieprofiel uitrekenen voor lange polymeren, dan kunnen we precies de drie gebieden van De Gennes terugvinden, maar helaas blijkt de concentratie in het centrale gebied wel degelijk van de ketenlengte en van de bulkconcentratie af te hangen. Geen universeel gedrag dus. De SF-theorie gebruikt een zogenaamde gemiddeld-veld benadering, en het is bekend dat deze benadering nog wel eens leidt tot verkeerde exponenten in machtswetten. Aan de andere kant leveren gemiddeld-veld theorieën meestal wel de juiste trend op, en de afhankelijkheid van de ketenlengte is een duidelijke trend. De Gennes gebruikt in zijn afleidingen de limietwaarde voor oneindig lange polymeren. We kunnen de exponent in het centrale gebied op een slimme manier uitzetten tegen de ketenlengte, zodanig, dat we kunnen extrapoleren naar oneindige ketenlengte. Er komt dan precies de waarde uit die voor een gemiddeld-veld theorie verwacht mag worden, en die is wel onafhankelijk

van de bulkconcentratie. Dit alles doet vermoeden dat de theorie van De Gennes alleen geldig is voor oneindig lange polymeren en dat er in de praktijk geen sprake zal zijn van universeel gedrag.
In het tweede hoofdstuk bekijken we adsorptie vanuit een semi-verdunde oplossing. Zoals al eerder vermeld vertoont een semi-verdunde oplossing wèl universeel gedrag, en het blijkt dat dit ook opgaat voor het volumefraktieprofiel. We kunnen laten zien dat de vergelijking voor de vrije energie die in de (numerieke) SF-theorie gebruikt wordt veel overeenkomsten vertoont met een analytische vergelijking die o.a. door Johner en medewerkers gebruikt wordt. Hiervoor moeten we wèl aannemen dat alle segmenten (de onderdelen waaruit het polymeer is opgebouwd) op dezelfde manier verdeeld zijn. In het algemeen is dat niet zo, omdat de uiteinden van een polymeerketen de neiging hebben uit te steken in de oplossing. De segmenten in het midden van het polymeer zitten juist liever aan het oppervlak. Toch blijkt deze benadering goed te werken, want het SF-volumefraktieprofiel wordt uitstekend beschreven door een analytische vergelijking die met deze benadering afgeleid kan worden. Als de benadering nog eens gebruikt wordt om binnen het totale volumefraktie-profiel de geadsorbeerde ketens (dit zijn de moleculen die contact maken met het oppervlak) te onderscheiden, dan blijkt dat alleen goed te zijn als de evenwichtsconcentratie hoog is en de adsorptie-energie laag. Als dat niet het geval is werkt de benadering slecht, waarschijnlijk doordat de invloed van de staarten (de vrije uiteinden van geadsorbeerde moleculen) hier groot is. Als we een mengsel van polymeren met verschillende ketenlengten laten adsorberen uit een semi-verdunde oplossing, dan verandert het totale volumefraktieprofiel niet, hoewel elke afzonderlijke component een heel verschillend profiel kan hebben.
Vanaf hoofdstuk 3 worden de bestudeerde systemen ingewikkelder. Om te beginnen maken we de polymeerketen stijver. Een stijf molecuul heeft in oplossing minder bewegingsvrijheid, en die kan dan ook niet verloren gaan bij adsorptie. Tengevolge hiervan adsorbeert een stijf polymeer makkelijker dan een flexibel polymeer. Ketenstijfheid is eenvoudig te modelleren door een energetische "straf" op te leggen als twee opeenvolgende bindingen een hoek met elkaar maken. Daardoor wordt het gunstiger om bindingen in elkaars verlengde te leggen. We kunnen dan een persistentielengte definiëren, een maat voor het gemiddelde aantal bindingen dat een polymeer nodig heeft om weer op hetzelfde punt uit te komen. Hoe groter het energieverschil tussen rechte en haakse bindingsparen, des te groter de

persistentielengte. Met behulp van de persistentielengte kunnen we proberen een lange stijve keten te "herschalen" in een kortere keten waarvan de segmenten langer zijn. Voor de gemiddelde afmeting van een kluwen in een verdunde oplossing werkt dat goed, een resultaat dat al sinds de dertiger jaren bekend is. Helaas blijkt het voor een geadsorbeerde keten helemaal niet te werken. Hoe stijver het polymeer, hoe kleiner de kritische adsorptie-energie. De afhankelijkheid van de kritische adsorptie-energie van de persistentielengte is afgeleid door Birshtein, Zhulina en Skvortsov. Hun voorspelling blijkt precies te kloppen met de resultaten van de SF-theorie mits het polymeer (veel) langer is dan de persistentielengte. De situatie wordt nog veel gecompliceerder als niet het hele polymeer stijf is, maar bijvoorbeeld alleen de uiteinden. Het kan dan gebeuren dat die uiteinden bij voorkeur op het oppervlak gaan zitten, precies het tegenovergestelde van de situatie bij een flexibel polymeer. Het gedrag van een stijf-flexibel polymeer is vergelijkbaar met dat van een polymeer waarin de energetische wisselwerking tussen polymeersegmenten en oppervlak of tussen segmenten en oplosmiddel in verschillende stukken van de keten verschillend is.

In hoofdstuk 4 bekijken we polymeren die bestaan uit één hoofdketen met verschillende zijketens, de zogenaamde kampolymeren. Kampolymeren hebben veel uiteinden per molecuul, en zoals gezegd hebben uiteinden de neiging om uit te steken in de oplossing. De hoofdketen zit dus bij voorkeur op het oppervlak, en dat leidt tot relatief dunne polymeerlagen aan het oppervlak. Als de afstand tussen de tanden van de kam klein is in vergelijking met de lengte van de zijketens, dan ontstaat er net buiten die geadsorbeerde polymeerlaag zelfs een zone waarin de concentratie aan polymeer lager is dan die van de evenwichtsoplossing. De kritische adsorptie-energie van een polymeer waarvan de zijketen preferent adsorbeert boven de hoofdketen is lager dan andersom.

In het laatste hoofdstuk bekijken we de situatie dat er op het oppervlak plekjes voorkomen die een verschillende energetische wisselwerking hebben met het polymeer. Dit heet chemische oppervlakteheterogeniteit. We kunnen het oppervlak zelfs zo modelleren, dat de energetische wisselwerking met het polymeer gemiddeld precies nul is. Toch vindt er dan adsorptie plaats, als we er maar voor zorgen dat de gunstige plekjes in groepjes bij elkaar voorkomen. De verdeling van gunstige plekjes over het oppervlak bepaalt het adsorptiegedrag van het polymeer. Als de aantrekking door het oppervlak groot genoeg is, dan is het voordeliger om

de gunstige plekjes gelijkmatig te verdelen, omdat dan het gehele oppervlak gebruikt kan worden. Bij zwakke wisselwerking levert clustering van de gunstige plekjes voordeel op, omdat daarmee de ongunstige plekjes vermeden kunnen worden.

Samenvattend kunnen we stellen dat universeel gedrag alleen gevonden wordt bij flexibele, onvertakte polymeren die adsorberen vanuit een semi-verdunde oplossing. In alle andere gevallen (verdunde oplossingen, stijve polymeren, vertakte polymeren, oppervlakteheterogeniteit) is de struktuur ingewikkelder. Hoewel de gemiddeld-veld benadering die de SF-theorie gebruikt zeker tot grove fouten kan leiden, maakt het de modellering van een grote verscheidenheid aan systemen mogelijk. Daarbij komt een schat aan gedetailleerde informatie beschikbaar. Het blijft echter noodzakelijk om de veronderstellingen en voorspellingen te verifiëren met andere theorieën, en natuurlijk ook met experimenten. Het volumefraktieprofiel bepaalt de eigenschappen van het systeem en is zeer gevoelig voor de veronderstellingen die gemaakt worden in de theorie. Nauwkeurige en vooral ondubbelzinnige metingen blijven daarom van cruciaal belang.

LEVENSLOOP

Catharina Clasina van der Linden werd geboren op 19 december 1965 te Sittard. In 1984 behaalde zij het diploma gymnasium-β aan het Bisschoppelijk College "St. Jozef" te Sittard, waarna zij de studie aan de Landbouwuniversiteit (toen nog Landbouwhogeschool) te Wageningen begon, aanvankelijk Humane Voeding, later Moleculaire Wetenschappen. In 1990 studeerde zij (met lof) af. De doctoraalstudie omvatte de afstudeervakken Moleculaire Fysica, Wiskundige Analyse en Kolloïd- en Grensvlakchemie, alsmede een praktijktijd van zes maanden aan de School of Chemistry van de Universiteit van Bristol, Groot Brittannië. Van 1 september 1990 tot 15 november 1994 was zij als Onderzoeker in Opleiding werkzaam in dienst van NWO, gedetacheerd bij de vakgroep Fysische en Kolloïdchemie van de Landbouwuniversiteit. Hieruit is dit proefschrift voortgekomen. Vanaf 1 mei 1995 is zij werkzaam als postdoc bij het Max-Planck-Institut für Kolloid- und Grenzflächenforschung in Teltow, Duitsland.

NAWOORD

Het is nu alweer vijf jaar geleden dat Jan Scheutjens me een OIO-positie in polymeerfilms aanbood. Ik wist niet precies wat ik me moest voorstellen bij een polymeerfilm, maar met Jan als begeleider zou het wel goed komen, dacht ik.
Tijdens Jans afwezigheid (hij was op sabbatical in de VS), ontstond uit de dagelijkse, levendige diskussies met Frans Leermakers (algemene opzet: Frans kwam met een idee, en als ik echt geen argumenten meer kon verzinnen om het af te schieten, werd het voorlopig aangenomen. Alsnog mijn excuses aan alle kelderbewoners die ernstig onder de geluidsoverlast geleden moeten hebben) zowaar een artikel. Het vormt nu het grootste deel van hoofdstuk 1. Terwijl ik aan het schrijven was aan mijn geliefde "plekje" (hoofdstuk 5), in een poging het op Jans bureau te hebben liggen als hij van vakantie terugkwam, kwam het bericht dat Jan overleden was. Hij heeft dus helaas niets meer van dit proefschrift kunnen redden, en met die polymeerfilms is het al helemaal nooit meer goed gekomen. Dat er nu toch een proefschrift ligt, is te danken aan de theorie-groep, die op indrukwekkende wijze het verdriet verwerkte, en aan het feit dat Frans het op zich nam de promovendi, inclusief de fysisch niet relevante polymeer-mensen, verder te begeleiden. Die begeleiding ging bij één hoofdstuk zelfs zo ver, dat hij de plotjes uitrekende en ik er een verhaal bij schreef. Waar vind je nog zo'n co-promotor? Ik ben blij dat het, gezien recente uitlatingen, in ieder geval gelukt is om Frans enthousiast aan de polymeren te krijgen. Lieve Frans: je mag de stiften houden.
Gerard Fleer, mijn promotor, heeft altijd de indruk weten te wekken erg blij te zijn als ik hem weer werk kwam brengen. Zijn ongelofelijke snelheid en opmerkingsgave bij het nakijken van manuscripten (het record staat op 4 uur, met een gemiddelde opmerkingendichtheid van 25 per pagina), heeft ervoor gezorgd dat de vaart erin bleef èn dat er wat leesbare tekst tussen de formules staat.

Er zijn natuurlijk nog veel meer mensen die geholpen hebben met dit proefschrift. Om eens een paar wetenschappelijke bijdragen te noemen: dhr. Posthumus van de vakgroep Organische Chemie vond de Weinöl, Frans de Haas heeft gelukkig meer verstand van klassiek Grieks, Peter Barneveld heeft al mijn wis- & natuurkundeprobleempjes uit hoofdstuk 2 te verduren

gekregen, Heleen Hollenberg bracht een heel afstudeervak door met takketakken, waarna ik vrolijk de resultaten kon gebruiken voor hoofdstuk 4, en Boudewijn van Lent is ooit met de plekjes van hoofdstuk 5 aan komen zetten.
I would also like to thank Albert Johner from the Institut Charles Sadron at Strasbourg for all the help and discussions.
Verder heb ik vele ideeën opgedaan in discussies met mensen op de vakgroep, in het bijzonder met de theoriegroep (Klaas, Peter, Chris, Rafel), met het experimentele deel van de polymeergroep (Jaap, Nynke, Marcel, Henri, Martien), en buiten categorie met Martin T. en Marcel M..

Maar van alleen wetenschap draait het onderzoek niet. Gelukkig blijkt de vakgroep Fysische & Kolloïdchemie over prima randvoorwaarden te beschikken. Men heeft werkende computers, waarop je zelfs nog elegantere besturingssystemen mag installeren. En als de rekendoos onverhoopt weigert, lopen er Cassen of Peters rond die de zaak weer aan de praat krijgen. Er zijn experimentele, pluche, vierpotige en vijfvinnige kamergenoten, die ervoor zorgen dat je niet alle contact met de werkelijkheid verliest en die allerhande grote en minder grote crises opvangen. Er is een drukbezochte ruimte op de eerste verdieping die voorziet in enveloppen, papier, opbeurende woorden en wijze raad. Een grote verzameling medeaio's weet precies hoe je er aan toe bent: de mid-aio crisis, het terminale stadium.... En vrijdags om 6 uur vind je nog wel eens mensen die ook wel zin hebben in een potje bier.

Ik ben vast nog mensen of dingen vergeten. In ieder geval allemaal hartelijk bedankt, en keep up the good work!